B cells and the Antibody-Dependent Immune Response in Cancer and Infection

by

Jacquelyn Marie Lykken

Department of Immunology
Duke University

Date:_____

Approved:

_____
Thomas F. Tedder, Supervisor

_____
You-Wen He, Chair

_____ (Remote Participant) _____
Thomas Kepler

_____
Richard Lee Reinhardt

_____
Mari L. Shinohara

Dissertation submitted in partial fulfillment of
the requirements for the degree of Doctor of Philosophy
in the Department of Immunology in the Graduate School of Duke University

2015

ABSTRACT

B cells and the Antibody-Dependent Immune Response in Cancer and Infection

by

Jacquelyn Marie Lykken

Department of Immunology
Duke University

Date:_____

Approved:

_____
Thomas F. Tedder, Supervisor

_____
You-Wen He, Chair

____ (Remote Participant) ____
Thomas Kepler

_____
Richard Lee Reinhardt

_____
Mari L. Shinohara

An abstract of a dissertation submitted in partial fulfillment of
the requirements for the degree of Doctor of Philosophy
in the Department of Immunology in the Graduate School of Duke University

2015

Abstract

B cells and humoral immunity are critical components of an effective immune response. However, B cells are also a significant driver of a variety of autoimmune diseases and can also become malignant. Antibody-mediated B cell depletion is now regularly used in the clinic to treat both B cell-derived cancers and B-cell driven autoimmunity, and while depletion itself is effective in some patients, removal of B cells is not often curative for patients and may present additional, unforeseen risks. The overall goal of this dissertation was therefore to determine the impact of B cell depletion on T cell homeostasis and function during infection and to elucidate the genetic factors that determine the effectiveness of antibody-mediated therapy.

In Chapter 3 of this dissertation, the role of B cells in promoting T cell homeostasis was investigated by depleting mature B cells using CD20 monoclonal antibody (mAb). Acute B cell depletion in adult mice significantly reduced spleen and lymph node T cell numbers, including naïve, activated, and cytokine-producing cells, as well as $Foxp3^+$ regulatory T cells, whereas chronic B cell depletion in aged mice resulted in a profound decrease in activated and cytokine–producing T cell numbers. To determine the significance of this finding, B cell-depleted adult mice were infected with acute lymphocytic choriomeningitis virus (LCMV). Despite their expansion, activated and cytokine-producing T cell numbers were still significantly reduced one week later.

Moreover, viral peptide-specific T cell numbers and effector cell development were significantly reduced in mice lacking B cells, while LCMV titers were dramatically increased. Thus, B cells are required for optimal T cell homeostasis, activation, and effector development *in vivo*, particularly during acute viral infection.

In Chapter 4 of this dissertation, lymphoma genetic changes that conferred either sensitivity or resistance to CD20 mAb therapy were examined in a preclinical mouse lymphoma model. An examination of primary lymphomas and extensive lymphoma families demonstrated that sensitivity to CD20 mAb was not regulated by differences in CD20 expression, prior exposure to CD20 mAb, nor serial *in vivo* passage. An unbiased forward genetic screen of CD20 mAb-resistant and -sensitive lymphomas identified galectin-1 as a significant factor driving CD20 mAb therapy resistance. As some lymphomas acquired therapy resistance over time, galectin-1 expression also increased. Furthermore, inducing lymphoma galectin-1 expression within the tumor microenvironment ablated lymphoma sensitivity to CD20 mAb. Therefore, lymphoma acquisition of galectin-1 expression confers CD20 mAb therapy resistance.

In Chapter 5 of this dissertation, the distinct germline components that control the efficacy of host CD20 mAb-dependent B cell and lymphoma depletion were evaluated using genetically distinct lab mouse strains. Variations in B cell depletion by CD20 mAb among several lab mouse strains were observed, where 129 mice

had significantly impaired mAb-dependent depletion of endogenous B cells and primary lymphomas relative to B6 mice. An unbiased forward genetic screen of mice revealed that a 1.5 Mbp region of Chromosome 12 that contains *mycn* significantly altered CD20 mAb-dependent lymphoma depletion. Elevated mycn expression enhanced mAb-dependent B cell depletion and lymphoma phagocytosis and correlated with higher macrophage numbers. Thus, host genetic variations in mycn expression in macrophages alter the outcome of Ab-dependent depletion of endogenous and malignant cells.

These studies collectively demonstrate that B cells are required for effective cellular immune responses during infection and identified factors that alter the effectiveness of mAb-dependent B cell depletion. This research also established and validated an unbiased forward genetics approach to identify the totality of host and tumor-intrinsic factors that influence mAb therapy *in vivo*. The findings of these studies ultimately urge careful consideration in the clinical application of B cell depletion therapies.

Dedication

I would like to dedicate my dissertation to my family. My parents and sister, Jessie, have always pushed me to do great things and have supported me through any and all challenges I encountered. My husband, Erik, has been an unwavering source of encouragement, intellectual discourse, and happy distraction from the long days of lab work. Lastly, my four-legged best buddy, Molly, has been beside me through this entire journey and never hesitated to remind me to take a break and get some fresh air.

Contents

List of Figures

List of Abbreviations

Ab, antibody

ADCC, antibody-dependent cellular cytotoxicity

BCR, B cell receptor

BL, Burkitt's lymphoma

CD, cluster differentiation antigen

CLL, chronic lymphocytic leukemia

CpG, CpG oligodeoxynucleotide

DLBCL, diffuse large B cell lymphoma

FcR, Fc receptor

FcRn, neonatal Fc receptor

FcεR, Fc epsilon receptor

FcγR, Fc gamma receptor

FL, follicular lymphoma

Gal-1, galectin-1

GC, germinal center

Ig, immunoglobulin

IFN, interferon

HCL, hairy cell leukemia

IL, interleukin

ITAM, immunoreceptor tyrosine-based activation motif

LCMV, lymphocytic choriomeningitis virus

LPS, lipopolysaccharide

KLRG1, killer cell lectin-like receptor G1

mAb, monoclonal antibody

MCL, mantle cell lymphoma

MFI, mean fluorescence intensity

MHC-I, major histocompatibility complex class I

MHC-II, major histocompatibility complex class II

NHL, Non-Hodgkin lymphoma

PBS, phosphate-buffered saline

PCR, polymerase chain reaction

PFU, plaque-forming units

Poly(I:C), poly(I:C) oligodeoxynucleotide

qRT-PCR, quantitative real-time polymerase chain reaction

QTL, quantitative trait locus

RAG, recombination activating gene

SBP, streptavidin-binding peptide

SNP, single nucleotide polymorphism

TAA, tumor-associated antigen

TCR, T cell receptor

TEV, tobacco etch virus

TGF, transforming growth factor

TLR, toll-like receptor

TNF, tumor necrosis factor

TSA, tumor-specific antigen

Treg, regulatory T cell

Acknowledgements

I would first like to thank my mentor, Dr. Thomas Tedder, who has been an exceptionally loyal and patient mentor. Tom undertook the difficult task of molding a mathematician into a scientist, and I am very fortunate to have benefitted from his experience, time, and patience during my studies. I am confident that it was only in his lab that I could have been trained so thoroughly in the most important aspects of graduate school, namely basic science, technical expertise, communication, and professionalism.

Tom has a gift for assembling individuals with specific talents and expertise that are critical to the productivity of and dynamic within the laboratory. I have learned greatly from my experiences with my labmates, and I must especially thank former members Veronique Minard-Colin, Mayuka Horikawa, Yan Xiu, Jonathan Poe, David DiLillo, and Tomomitsu Miyagaki, as well as current members Kathleen Candando, Masahiro Kamata, Evgueni Kountikov, and Guglielmo Venturi. Working with these individuals has set the bar very high for my future labmates, and it was a great pleasure to train in this collaborative and engaging environment.

I would like to acknowledge my committee members, Drs. You-Wen He, Thomas Kepler, R. Lee Reinhardt, Mari Shinohara, and former member Shyam Unniraman, for their collaboration, guidance, and support during my graduate studies.

I would like to thank our many collaborators, including Doug Marchuk and Sehoon Keum of the Duke University Department of Molecular Genetics and Microbiology; Susanne Roser-Page of the Atlanta Department of Veterans Affairs Medical Center; Neale Weitzmann of the Emory University Division of Endocrinology, Metabolism, and Lipids; Mark Heise of the University of North Carolina at Chapel Hill Department of Genetics; and Jason Grayson of the Wake Forest University School of Medicine.

I would like to acknowledge the staff members of the core facilities at Duke that contributed greatly to my graduate studies, including Scott Langdon and Charles Bullard of the Duke Cancer Center DNA Analysis Facility; Mike Cook, Lynn Martinek, and Nancy Martin of the Duke Cancer Institute Flow Cytometry Facility; Holly Dressman, Laura-Leigh Rowlette, and Zhengzheng Wei of the Duke University Center for Genomic and Computational Biology; Hyuana Yang of the Duke University Department of Biostatistics and Bioinformatics; and the Duke University Genotyping Facility and the David H. Murdock Research Institute.

I would also like to thank my classmates and first friends in Durham, Ian Belle, Chaoran Li, Emily O'Koren, and Ashley Trama, for their friendship and many fond memories. I look forward to our continued friendships and your future successes.

Finally, I would like to thank my family, including my parents, sister Jessie, husband Erik, and dog Molly, without whose love and support I would not have been able to complete this tremendous undertaking.

1. Introduction

1.1. The Immune System

The immune system is chiefly responsible for protecting the host from pathogenic foreign microorganisms and malignancies. Its various cell populations are able to traverse physical tissue bounds throughout the body so that it may survey the entire organism and, when required, eliminate microscopic interlopers and cellular anomalies. The immune system is also uniquely tasked with balancing this clearance process with self-regulation to prevent aberrant tissue destruction. This internal defense mechanism is so critical to the survival of an organism that different facets of the immune system are conserved to some degree in almost all living organisms from archaea and plants through higher order species.

Some of the defining discoveries in the field of immunology derived from studies of transplant rejection and histocompatibility, which is the distinction of cells that derive from self versus a non-self entity. This distinction is mediated predominantly through immune cell-mediated recognition of the surface protein major histocompatibility complex class I (MHC-I) molecules, though many minor histocompatibility molecules exist. MHC-I is a codominantly expressed polygenic protein deriving from three main genes with a variety of polymorphisms, resulting in an exponential diversity for the potential MHC-I molecules expressed in the human population. Every nucleated cell of the body displays on its surface MHC-I, which binds peptide fragments generated

during protein degradation within the cell and thereby functions as a sort of encyclopedia for the processes ongoing within a given cell. Specific subsets of immune cells are able to "read" these molecules to determine whether foreign antigens, or molecular protein determinants, are present within the cell and can additionally discriminate between self and non-self molecules as well as gauge alterations in the levels of MHC-I expressed on the cell surface, forming the basis of histocompatibility.

The immune system is comprised of two distinct yet interactive arms: innate immunity which provides a rapid, general response, and adaptive immunity, which provides a specific response and is capable of immunologic memory. Cellular members of the innate immune system are characterized by the ability to rapidly identify and respond to a set of conserved molecular patterns on the surface of foreign organisms and are often referred to as the first line of defense against microorganisms. Innate immune cells predominantly operate at the onset of an immune response through consumption of the microbial insult and secretion of pro- or anti-inflammatory cytokines, or soluble signaling proteins. Though slower in initial responses, cells of the adaptive immune system can recognize a much wider diversity of molecules than cells of the innate immune system and are able to develop memory for those molecules to which there has been a previous exposure, allowing for more rapid subsequent responses. Adaptive immune cells principally function during an immune response by secreting cytotoxic effector molecules and antibodies (Ab), which are proteins specific for a wide diversity

of linear and conformational protein epitopes and are also referred to as immunoglobulins (Ig). An intricate balance exists between the innate and adaptive arms of the immune system, and the maintenance of this balance is integral to homeostasis and to protective immunity.

1.1.1. The Innate Immune System

The innate immune system functions as the immediate response to foreign pathogens and is made up of numerous different cell types (e.g., monocytes, macrophages, dendritic cells, basophils, eosinophils, and neutrophils) with origins and lineages that are still widely debated and undoubtedly intertwined. As an example, macrophages are a cell type comprised of many subpopulations, including resident (tissue) macrophages, which are of embryonic origin and are located in various tissues, and recruited (inflammatory) macrophages, which derive from monocytes following recruitment from the bone marrow into the blood. Depending on the cytokine milieu, monocytes can also develop into dendritic cells, whereas other dendritic cell populations derive from a common progenitor in the bone marrow and develop into either conventional dendritic cells or plasmacytoid dendritic cells. Despite these overlapping lineages, macrophages and dendritic cells are critical for different effector functions: macrophages are exceptional consumers through engulfment (phagocytosis) and are able to directly eliminate pathogens or dying cells, whereas dendritic cells, while also able to consume microorganisms, are essential for proper T cell activation. Thus, innate

immune cells sometimes share complicated origins and have overlapping functions yet also have unique effects on different aspects of the immune response.

While a central function of many innate cells is the phagocytosis of microorganisms, innate immune cells critically enable the activation and function of the adaptive immune system in a variety of ways downstream of phagocytosis, including the provision of co-stimulatory molecules necessary for the regulation of the primary immune response as well as inflammatory cytokine production. One of the most important functions of the innate immune system is antigen presentation through MHC-II molecules to instigate the cellular immune system, which is required for the primary and memory responses to pathogens. Unlike the ubiquitous expression of the MHC-I molecule, MHC-II molecules are only expressed by a select subset of innate and adaptive cells. Cells of the innate immune system present processed peptides via MHC-II after consuming microorganisms, cells, or debris through phagocytosis, which is instigated by receptor-dependent recognition of conserved microbial molecular patterns or immune effector proteins, including serum complement and Abs. Different innate cell populations express assorted subsets of these pattern recognition receptors, permitting selection of the appropriate innate cell types and fine tuning of the ultimate immune response. Recognition of conserved patterns is mediated by various surface and intracellular toll-like receptors (TLR) and other pattern recognition receptors that recognize molecules specific to microorganisms, such as lipopolysaccharide (LPS),

poly(I:C) oligodeoxynucleotide (poly(I:C)), or CpG oligodeoxynucleotide (CpG). Similarly, innate immune cells express specific receptors for activated serum complement proteins, including mannan-binding lectin, C1q, and C3b. Innate cells also express Fc receptors (FcRs) specific for different Ab isotypes that, when bound, instigate phagocytosis and Ab-dependent cellular cytotoxicity (ADCC) and further drive antigen presentation to the adaptive immune system.

The recognition of Ab-coated antigens, known as immune complexes, represents another important connection between the innate and adaptive immune systems. Gamma Ig (IgG), which comprises approximately 80% of the total serum Ab in adults, opsonizes microbes, can activate complement, and can be bound by high affinity isotype-specific FcRs (FcγR) expressed by innate cells, most notably macrophages, monocytes, and dendritic cells (*1*). Additionally, IgG diffuses to extravascular sites at significantly higher rates than other Ab isotypes, where it can activate tissue-resident innate immune cells via binding to FcγR (*2*). In mice, there are three extracellular activating FcγRs: FcγRI, which preferentially binds monomeric IgG2a/c with high affinity and also recognizes IgG1, IgG2b, IgG3; FcγRIII, which recognizes multimeric IgG1, IgG2a, and IgG2 with low affinity (*3*, *4*); and FcγRIV, which binds IgG2a and IgG2b with moderate affinity (*5*). Ligation of the inhibitory receptor, FcγRII, which recognizes multimeric IgG1, IgG2a, and IgG2b with low affinity, impedes innate cell activation (*6*, *7*). In humans, the extracellular activating FcγRI preferentially binds

monomeric IgG1, IgG3, and IgG4 with high affinity, whereas FcγRIIa binds multimeric IgG3, IgG1 with low affinity, and FcγRIIIa binds multimeric IgG1 and IgG3 with low affinity. The inhibitory FcγRIIb recognizes multimeric IgG3, IgG1, IgG4, and IgG2 with low affinity and, similar to mice, impairs innate cell activation when ligated (*6*, *7*). Further, IgG can be bound by neonatal Fc receptor (FcRn), which is thought to increase the longevity of IgG in the serum and to transport IgG within and across cells, as well as the intracellular FcR tripartite motif-containing protein 21 (TRIM21), which binds to internalized Ig. Thus, FcR expression by innate immune cells connects the specificity and memory of the adaptive immune response with the early rapid reaction of the innate immune system.

1.1.2. The Adaptive Immune system

The adaptive immune response permits immunological memory. The cells mediating adaptive immunity are known as lymphocytes and are classically subdivided into those functioning in the cellular or the humoral, or Ab-dependent, responses and are referred to as T cells and B cells, respectively. Both T and B cells express cell surface receptors that derive from a semi-random rearrangement of their respective receptor loci in a process dependent on recombination activating gene (RAG) expression followed by specific chain pairing and functional selection. This combinatorial gene rearrangement results in the expression of receptors that are unique to an individual cell and allow the lymphocyte population to recognize an exponential diversity of both self and foreign

antigens. During T cell development in the thymus and B cell development in the bone marrow, lymphocytes with receptors that react inappropriately to self-proteins are eliminated during negative selection. B cell receptors can be further modified after development in the bone marrow through both receptor editing and affinity maturation in peripheral lymphoid tissue, the latter of which leads to B cell receptors (BCRs) with enhanced affinity for antigen during an immune response. Once exposed during a primary immune response to an antigen, the adaptive immune system develops a pool of long-lasting memory T and B cells that can rapidly respond upon subsequent insult. During a primary cellular immune response, antigen-inexperienced naïve T cell activation requires both the recognition of MHC-peptide complex as well as costimulation of other receptors on the T cell surface, including CD28 and ICOS, by ligands expressed on antigen-presenting cells, including CD80 and ICOS-L. The requirement for costimulation and the preceding negative selection in the thymus prevents aberrant cellular immune activation during homeostasis. During a subsequent cellular immune response, memory T cells, which have expanded during a previous immune response, do not require costimulation. Similarly, B cells that react inappropriately with self- proteins can be eliminated through central tolerance mechanisms in the bone marrow as well as in the periphery through receptor editing and the induction of anergy or apoptosis through peripheral tolerance mechanisms. Thus, adaptive immune cells express a diverse cohort of antigens through specific

surface receptors and are normally prevented from inappropriately reacting against self through multiple tolerance checkpoints.

The cellular immune response can be further segmented into two subpopulations, $CD4^+$ and $CD8^+$ T cells. $CD4^+$ and $CD8^+$ T cells recognize and are activated upon recognition of linear antigenic epitopes displayed by either MHC-II or MHC-I, respectively, by their cell surface T cell receptor (TCR). During development in the thymus, T cells are positively selected for survival when the TCR recognizes self MHC, a process that occurs prior to negative selection of those T cells that react too strongly with self MHC. In the periphery during an immune response, professional antigen-presenting cells, namely macrophages, dendritic cells, and B cells, display phagocytosed, processed peptides as peptide:MHC-II complexes to $CD4^+$ T cells. $CD4^+$ T cells are then activated and differentiate into one of several semi-plastic subsets to produce a myriad of characteristic cytokines, which help to enhance, skew, or inhibit the immune responses of other adaptive and innate cells; this function has led to the common reference to $CD4^+$ T cells as T helper cells. Specifically, T helper type-1 $CD4^+$ T cells produce interferon-gamma (IFN-γ) and tumor necrosis factor-alpha (TNF-α), which activate innate cells and increase MHC-I and MHC-II expression, while T helper type-2 $CD4^+$ T cells produce interleukin-13 (IL-13), which skews immune cells toward an allergic inflammatory response. An ever-expanding list of other $CD4^+$ T helper subsets exist and are typically defined on the basis of their secretion of specific cytokines,

including T helper-17 cells, which secrete IL-17 to exacerbate inflammatory processes, and T follicular helper cells, which secrete IL-21 in lymphoid follicles to support humoral responses. In addition to pro-inflammatory $CD4^+$ T cell subsets, regulatory T cells (Tregs) produce immunosuppressive cytokines, including IL-10 and transforming growth factor-beta (TGF-β), to dampen local immune activation. In addition to the production of these cytokines, $CD4^+$ T cells can produce a number of additional cytokines depending on the inflammatory microenvironment they become activated in. In contrast to $CD4^+$ T cells, $CD8^+$ T cells can be activated by any nucleated cells in the body through the expression of peptide:MHC-I complexes. Following recognition of a peptide:MHC complex by the TCR and appropriate costimulation, typically by dendritic cells, $CD8^+$ T cells produce high amounts of cytotoxic molecules, including perforin, as well as cytokines, to directly lyse target cells; for this reason, $CD8^+$ T cells are often referred to as cytotoxic T cells. Therefore, the predominant role of $CD8^+$ T cells is to identify and eliminate cells that are either infected with foreign microorganisms or malignant, while $CD4^+$ T cells support and direct immune cells toward an appropriate effector response.

B cells are the origin of the humoral immune response, which refers to their classically defined role in producing Abs. Abs are important effector proteins, as they function as a natural barrier to infection by coating foreign pathogens or cells, often clearing unwanted microorganisms without eliciting significant inflammation or, when

necessary, instigating innate immune cell activation. Following B cell development in the bone marrow, immature B cells migrate into the periphery, where antigen exposure induces B cell activation and differentiation in secondary lymphoid follicles, particularly those of the spleen and lymph nodes. During a primary immune response, immature B cells can become activated by binding cognate antigen through the BCR and either receiving secondary stimulation from $CD4^+$ T cells following B cell presentation through peptide:MHC-II complexes or through co-ligation of other receptors, including TLRs, or multivalent BCR cross-linking. Once activated by an antigen, B cells can differentiate into short-lived plasma cells, which secrete antigen-specific IgM Abs, or proliferate in lymphoid follicles and migrate into the germinal center (GC) with follicular dendritic cells and $CD4^+$ T follicular helper cells. B cells cycle within the GC between proliferation and antigen engagement on the surface of follicular dendritic cells, while T follicular helper cells provide co-stimulatory signals and cytokines that induce BCR isotype switching and affinity maturation through mutation of the binding region of the BCR in a process termed somatic hypermutation (SHM). This process leads to the selection of higher affinity B cell clones that form the B cell memory compartment, which then generates isotype-switched plasma cells upon subsequent exposure to antigen. Of special note, in addition to plasma cells, a distinct subset of B cells in the peritoneal cavity that derives from the fetal liver produces significant amounts of serum T cell-

independent Ab (*8, 9*). Thus, a major function for B cells during homeostasis and in an ongoing immune response is Ab production.

While the role of B cells in an immune response is generally contextualized by their ability to produce Abs, B cells affect the immune response through many Ab-independent mechanisms. B cells are important for lymphoid tissue organogenesis and architecture, as mice congenitally deficient in B cells have smaller spleens (*10*), significant reductions in splenic dendritic cells, T cells, and macrophages (*11-13*), and impaired Peyer's patch and follicular dendritic cell network development (*13, 14*). B cells are also a critical source of immunomodulatory cytokines that influence innate cell and T cell activation and subset polarization (*8, 15*). For example, IL-10-producing B cells, known as B10 cells, profoundly impair bacterial clearance (*16*), Ab-dependent tumor depletion (*17*), and autoimmune disease (*18-22*) through IL-10-dependent inhibition of innate cell and T cell activation. As described earlier, B cells are one of the critical antigen presenting cell populations for T cells. In the absence of B cells, $CD4^+$ T cells are insufficiently activated (*23-27*) and consequently exhibit impaired anti-bacterial (*27*), anti-viral (*10, 28-33*), anti-tumor (*34*), and memory responses (*27, 30, 33, 35, 36*), and these effects are all independent of Ab production (*37, 38*). B cell Ab production and other effector functions are therefore critical for the overall homeostasis and function of the innate and adaptive immune systems.

1.2 Cancer and the Immune System

While the role of the immune system in combatting infection with foreign microorganisms has long been understood, the relationship between the immune system and cancer has been debated among medical experts. Paul Ehrlich first postulated in the early 1900s that the immune system could protect the host from cancer development, however histocompatibility studies in the 1950s indicated that the immune response against cancer only developed as a consequence of histocompatibility mismatches following allogeneic transfers between non-inbred mice. Later studies using syngeneic mice demonstrated that when tumors developed following chemical exposure or viral infection, an immune response formed against novel tumor-specific antigens that were distinct from host proteins (*39*, *40*). These findings provided the basis for the cancer immunosurveillance hypothesis put forth by Burnet and Thomas, which argues that in a healthy, long-lived organism, cells can develop mutations over time and consequently some become malignant and express mutant neo-antigens or tumor-specific antigens (TSAs) to which an immune response can form, eliminating the malignancy before it becomes clinically apparent (*41-43*). This theory was widely disregarded in subsequent decades due to a series of experiments that demonstrated that nude mice (*44*), which have little to no thymus tissue and were therefore presumed to lack any functional T cells, developed tumors at rates equal to those of immunocompetent mice. However, it was not appreciated until much later that nude mice do contain functional $CD8^+$ and

$CD4^+$ T cells (*45, 46*), indicating that nude mice likely retain some degree of cellular surveillance for malignant cells. A series of studies in the 1990s reinvigorated the cancer immunosurveillance hypothesis by demonstrating that mice deficient in key immune cell-derived cytotoxic molecules, including IFN-y and perforin, and lymphocytes, due to RAG deficiency, were more likely to develop both spontaneous and chemically-induced tumors than wild-type mice. Later studies demonstrated that perturbations in specific immune cell populations, including various T cell and innate cell subsets, also increase cancer development, indicating that multiple immune cell populations conduct cancer immunosurveillance (*47, 48*). Immune cells therefore normally protect the host from overt cancer development by constant immunosurveillance and destruction of malignant cells.

Despite immunosurveillance mechanisms, cancer can develop in the presence of an intact immune system, though these tumors are notably different from those that develop in immunodeficient hosts. A number of studies have demonstrated that, as compared to tumors deriving from immunocompetent mice, tumors that develop in the absence of an intact immune system are more frequently rejected upon transplant into immunocompetent hosts. These studies indicate that the immune system can drive the selection of tumor variants with lower immunogenicity. These so-called tumor escape variants can develop due to the inherent genetic instability of malignant cells, which exist as a heterogeneous pool able to undergo immune-mediated Darwinian selection in

a process referred to as cancer immunoediting. Cancer immunoediting has been suggested to occur in a progressive three-part process: elimination of malignant cells due to adequate cancer immunosurveillance; equilibrium established between immune cell control of cancer growth and immune selection of tumor escape variants; and escape of the immunoedited tumor variants whose growth outpaces the capacity of the immune system (*47*, *48*). Adequate cancer immunosurveillance (i.e., the elimination phase of cancer immunoediting) can be maintained for the life of the organism. However, once an equilibrium develops between the immune system and malignant cells, where immune cells control but do not fully eradicate the cancerous growth, tumor escape variants are more likely to lead to the development resistant tumors. Indeed, selection for a lack of immunogenicity is just one of many ways in which tumors escape immune control. There are several mechanisms through which tumors can directly dampen the immune response, including the downregulation of MHC-I and TSAs, modulation of the expression of pro-apoptotic (e.g. p53, pten) or anti-apoptotic proteins (e.g. c-myc, Bcl2), or through surface expression of apoptosis-inducing molecules (e.g. FasL, PDL1) to eliminate anti-tumor immune cells. Further, tumors can secrete immunosuppressive cytokines (e.g. IL-10, TGF-β) and chemoattractants (e.g. VEGF) to recruit regulatory innate and lymphocyte populations, including Tregs and B10 cells. Lastly, the outgrowth of a tumor that is fully resistant to immune-mediated suppression leads to clinically apparent symptoms and without intervention, death of the organism (*47*, *48*).

Thus, the immune system eliminates malignant cells normally through cancer immunosurveillance but can select for tumor escape variants during cancer immunoediting, which can lead to unrestrained cancer development.

1.2.1. B cell leukemias and lymphomas

The immune system predominantly serves to protect the body from microorganisms and malignant growth, but like any other dividing cell in the body, immune cells can also become malignant and develop into cancer. Malignant immune cells develop into either single cell blood cancers (leukemias) or solid lymphoid tissue cancers (lymphomas) based on the developmental stage at which malignant transformation occurred. Non-Hodgkin lymphoma (NHL) is the most common hematologic malignancy and one of the most common cancers overall, accounting for approximately 4% of all adult cancers in the United States (*49*). The vast majority (80-95%) of NHLs derive from B cells (*50*), and there are several sub-types that largely derive from GC or post-GC B cells, including Burkitt's (BL), diffuse large B cell (DLBCL), follicular (FL), and mantle cell lymphomas (MCL). Of these lymphomas, DLBCL and FL account for more than half of all B cell lymphoma diagnoses. B cell NHLs can be further partitioned based on cell surface phenotype, cytology, and either indolent or aggressive growth characteristics. In addition to NHL, B cells can transform to become Hodgkin lymphoma, which also derive from GC B cells but differ from NHLs by pathology and disease course, as well as hairy cell leukemia (HCL), chronic lymphocytic leukemia

(CLL), and plasma cell-derived multiple myeloma and plasmacytoma (*8*, *51*). Most B cell malignancies therefore derive from GC B cells and become NHLs.

A common feature of many NHLs is the chromosomal translocation of transcription factors that ubiquitously regulate cell cycle or survival into Ig loci in addition to further mutations in other so-called tumor suppressor genes that regulate cell cycle and apoptosis (*51*). This malignant transformation then leads to the unregulated proliferation and survival of B cells. In particular, BL and DLBCL are often associated with the translocation of the c-myc transcription factor, which regulates cell cycle progression and apoptosis, into the Ig locus. Other aberrant genetic events common in NHL include Bcl-6 and Bcl-2 translocations into the Ig locus and p35 and Fas mutations. That most B cell lymphomas derive from GC B cells is thought to occur due to the expression of factors that induce mutations and double strand breaks, both of which are necessary for effective SHM and isotype switching during a GC reaction but also can lead to chromosomal translocations and off-target gene mutation. Certain viruses have also been implicated in driving the genetic anomalies observed in B cell lymphomas. Epstein-Barr virus in particular has received a lot of attention, as it is found in virtually all endemic BL cases and to a lesser extent in other B cell NHLs (*51*). While B cell NHLs vary by the transformative event and growth pattern, most express surface BCR, and greater than 90% of human B cell NHLs express cell surface CD19 and CD20

(*50*), making these markers attractive tumor-associated antigens (TAAs) for lymphoma therapy.

1.2.2. CD20 Immunotherapy

Due to the prevalence of diseases that originate from B cells, including most Non-Hodgkin lymphomas, as well as conditions that are worsened by B cell effector functions, such as excessive or inappropriate Ab and cytokine production, specific B cell depletion has become an attractive therapy for many of these clinical needs. A small subset of cell surface glycoproteins are restricted in expression to B cells, including CD19 and CD20. The specificity of CD19 and CD20 expression among B cells alone makes them ideal candidates for Ab immunotherapy targets to specifically deplete endogenous and malignant B cells *in vivo*.

1.2.2.1. The Role of CD20 in B cell Development and Function

CD20 is cell surface phosphoprotein first expressed during the transition from pre-B to immature B cell and continues through maturation until plasma cell differentiation (*52-55*). Formerly known as B1 antigen, it is encoded by the *ms4a1* gene and is located within the MS4A gene family, which also includes the high-affinity receptor for the Fc portion of the IgE Ab (FcεR) complex. Similar to other MS4a genes, CD20 has four helical membrane-spanning domains and three cytoplasmic domains, which contain the N- and C-terminal regions, and also lacks a signal sequence (*56-58*). Upon mitogenic stimulation of resting B cells, the serine- and threonine-rich cytoplasmic

domains of CD20 are extensively phosphorylated, leading to three different protein forms ranging from 33 to 37 kDa in size (*59-61*). *Ms4a1* is located on the long arm of Chromosome 11 in humans (*62*) and in an evolutionarily conserved region on Chromosome 19 in mice (*57*), with 75% overall amino acid sequence conservation in CD20 between mouse and human and 90% conservation in the transmembrane regions.

CD20 plays a role in B cell activation, proliferation, and calcium transport by regulating transmembrane calcium conductance and subsequent cell cycle progression following activation (*61, 63*). Transfection of CD20 into human and mouse cell lines leads to enhanced steady-state calcium levels and transmembrane calcium conductance resulting from enhanced plasma membrane permeability. Ligation of CD20 with monoclonal Ab similarly enhances transmembrane calcium conductance. However, CD20 Ab binding does not appear to induce release of intracellular calcium stores (*61*), indicating that CD20 forms a calcium channel. Direct ligation of CD20 with most monoclonal Abs (mAb) leads to CD20 phosphorylation mediated by ubiquitous kinases, including protein kinase C, casein kinase II, and calcium/calmodulin-dependent kinase II, which phosphorylate CD20 at different residues and lead to distinct functional outcomes (*64-66*). In addition to inducing CD20 phosphorylation, direct ligation of CD20 with mAbs induces c-myc and B-myb expression as well as serine, threonine, and tyrosine phosphorylation of cellular proteins and increases CD18, CD58, and MHC-II expression. CD20 ligation also enhances B cell homotypic adhesion(*67*) and inhibits B

cell differentiation and cell cycle progression from the G1 to S/G2/M stages following mitogenic stimulation (*63, 68-70*), likely because cell cycle progression from G1 to S is dependent on decreased calcium. Intriguingly, mice that are deficient in CD20 are largely normal and do not display overt anatomical, morphological, or reproductive abnormalities nor increased susceptibility to infection. CD20-deficient mice do have significantly decreased B cell surface IgM expression in addition to fewer peritoneal B1a cells yet have comparable serum IgM to wild-type mice (*71*). CD20 is therefore not explicitly required for B cell development or tissue localization.

1.2.2.2. CD20 as a Tumor-Associated Target for Immunotherapy

The specificity of CD20 expression on B cell subsets makes it an ideal target for the treatment of diseases driven by malignant B cells, including those that development into leukemias and lymphomas. Rituximab, the chimeric IgG1 anti-human CD20 mAb, was the first Ab-based therapy approved to treat human disease, with initial approval for the treatment of indolent non-Hodgkin's lymphoma (*72*). Other chimeric and radiolabeled CD20 mAbs are also available and are used to treat non-Hodgkin's lymphoma (*73-78*) as well as rheumatoid arthritis, systemic lupus erythematosus, idiopathic thrombocytopenic purpura, hemolytic anemia, and other autoimmune conditions (*79-82*). CD20 is expressed on more than 90% of human B cell lymphomas and on approximately 50% of B cell leukemias (*50*). As described earlier, CD20 is expressed on the surface of circulating B cells and is thus not an effective treatment

option for malignancies deriving from pre-B cells nor plasma cells. For the treatment of non-Hodgkin's lymphoma deriving from mature B cell subsets, the initial effectiveness of Rituximab varies widely amongst patients and typically wanes over time, despite sustained CD20 expression by malignant cells among the vast majority of relapsing patients (*83, 84*). Though Rituximab is widely used, the precise mechanisms by which humans develop resistance to CD20 mAb immunotherapy are not established (*85*).

In humans, there are many pathways through which CD20 mAb has been proposed to deplete malignant B cells. As CD20 is known to regulate calcium transport across the B cell membrane, CD20 mAb binding itself may alter cell cycle progression and induce apoptosis (*61, 86, 87*). In select patients, decreased CD20 expression density may account for ineffective CD20 mAb therapy of malignant B cells (*88*). It has also been suggested that CD20 mAb depletion occurs through innate immune system activation by inducing complement- or Ab-dependent cytotoxicity or phagocytosis (*72, 87, 89-91*). Some studies have shown that Rituximab treatment of recently isolated lymphoma cells or immortalized B cell lines drives classical pathway complement activation and complement-dependent cytotoxicity (*89, 92-94*). Further, Rituximab has been observed to activate complement in some patients (*95*). However, other studies have found that neither the observed complement-mediated lysis nor lymphoma expression of complement inhibitors (e.g., CD46, CD55, CD59) predict therapeutic outcome (*96*). Indeed, while complement deletion had no effect on mAb treatment of human

melanoma or carcinoma in nude mice, inhibition of macrophage effector function eliminated mAb-dependent tumor depletion (*97*). Polymorphisms in the activating FcγRIIa and FcγRIII proteins have been correlated with the efficiency of B cell and tumor depletion during CD20 mAb therapy in some lymphoma patients (*98-100*). FcγRIIa and FcγRIII are both expressed by cells of the myeloid lineage, including macrophages, neutrophils, dendritic cells, and NK cells, indicating that some or all of these cell populations are critical for mAb-dependent cell depletion in humans (*7*). Deletion of the inhibitory FcγRIIb exacerbates cell-mediated cytotoxicity of humanized mAbs, including Rituximab, toward human lymphoma cells in nude mice *in vivo* (*90*), though no relationship has been found between FcγRIIb protein density and patient prognosis (*101*). It is important to note when considering the mAb-dependent effector mechanisms driving malignant B cell depletion that most human studies focus on evaluating blood B cells, which account for less than 2% of total B cells in a healthy adult (*102*) and may therefore neglect the impact of B cells in various lymphoid tissues. Further, as many patients see little therapeutic benefit from CD20 mAb treatment and many more individuals become unresponsive to treatment, consideration of differences in B cell depletion across different tissues and the likely existence of malignant B cell reservoirs becomes critically important.

Much of what is known about the kinetics and mechanisms by which endogenous and malignant B cells are depleted by CD20 mAb treatment has been

established in mice. As in humans, CD20 mAb treatment depletes mature B cells from the circulation and lymphoid tissues and does not affect serum Ab levels nor bone marrow pre B cells or plasma cell numbers in wild-type mice, in accordance with the known expression pattern of CD20 through B cell differentiation (*103-105*). Mouse anti-mouse CD20 mAbs react uniformly with primary B cells *in vitro* and reach saturating staining levels as observed by flow cytometry between 1-10 μg/mL (*71*). The efficiency of B cell depletion by these CD20 mAbs correlates with mAb isotype as follows: IgG2a/c > IgG1 > IgG2b > IgG3, though IgG3 Abs do not deplete B cells effectively (*71, 104, 106*). A single 250 μg dose of the CD20 mAb MB20-11 (IgG2c) depletes more than 95% of mature B cells from the blood, bone marrow, spleen, and lymph nodes within one week, with B cell numbers beginning to recover seven to eight weeks later (*71, 103*); for reference, this dosage is approximately 10-fold lower per kg than the dosage of Rituximab given to humans (*7, 75*). The serum half-life is 4.6 days in wild-type mice and 4.4 days in humans (*103, 107*). Mature B cells are depleted from the circulation and bone marrow within the first hour of CD20 mAb treatment, whereas spleen and peritoneal cavity B cells are coated with CD20 mAb in this time frame but are not largely depleted until two days post-treatment. B cells in the lymph nodes have 10-fold lower levels of CD20 mAb binding within one hour of CD20 mAb treatment, but are mostly depleted within two days (*103*). CD20 mAb therapy thus rapidly eliminates most endogenous mature B cells and also effectively depletes malignant B cells in the preclinical *Eu-cmyc* transgenic

mouse lymphoma model (*17, 108*). Treatment with CD20 mAb also alleviates allograft-specific Abs following skin or kidney transplant, though treatment does not prevent allograft rejection in these models (*109*).

The residual B cells found in lymphoid tissues one week after CD20 mAb treatment are phenotypically immature or plasma cell-like and are typically found in small lymphoid clusters with T cells. The remaining immature cells are thus likely recent emigrants from the bone marrow, whereas plasma cells do not express CD20 and are therefore not depleted by CD20 mAb (*103-105*). These residual B cells can have functional consequences for CD20 mAb therapy; residual regulatory IL-10-producing B (B10) cells are known to inhibit CD20 mAb therapy for malignant B cell depletion (*17*). Further, peritoneal B1 and B2 cells are more resistant to CD20 mAb-dependent depletion than B cells in other tissues. In addition to the protection conferred by the physical isolation of the peritoneum from most effector cells, B1 cells are also intrinsically more resistant to CD20 mAb-mediated depletion (*103*). This defect in peritoneal B cell depletion by CD20 mAb as well as the delayed deletion of B cells residing in the spleen and lymph nodes occurs despite comparable opsonization by CD20 mAb of the B cell surface. Importantly, these data indicate that CD20 mAb binding alone does not induce B cell-intrinsic changes or apoptosis, but that CD20 mAb treatment requires effector cells for efficient B cell depletion. Also, the differential depletion of B cells across tissues likely has important consequences for mAb treatment of human disease, as malignant B

cells in peripheral lymphoid tissues and the peritoneal cavity are not depleted as quickly as circulating B cells and could serve as an important reservoir for recrudescent tumors.

Macrophages are the key mediators of mAb-dependent B cell depletion *in vivo*. Mice that have reduced tissue macrophage numbers following clodronate injection, which predominantly depletes macrophages in the spleen and liver, clear far fewer endogenous and malignant B cells than wild-type mice following CD20 mAb treatment (*17*, *106*, *108*). Indeed, Kupffer macrophages in the liver have been directly observed to clear endogenous and malignant B cells following mAb therapy through Ab-dependent phagocytosis independent of reactive oxygen and nitrogen species production (*110, 111*). The mAb-dependent depletion of endogenous and malignant B cells by macrophages can be augmented by activating macrophage pattern recognition receptors with poly(I:C) (TLR3/TRIF agonist), LPS (TLR4 agonist), and CpG (TLR9 agonist) (*17*). However, stimulation with poly(I:C) is preferential to other TLR agonists, because poly(I:C) specifically enhances macrophage phagocytosis without expanding or inducing immunosuppressive B10 cells. Stimulation of macrophages, but not neutrophils or NK cells, with poly(I:C) specifically enhances surface FcγR expression. The amount and type of FcγR expressed by macrophages is critical, as FcγRI, FcγRIII, and FcγRIV cooperate to mediate mAb-dependent B cell depletion and can compensate for deficiencies in any one of these receptors (*17*, *104*, *106*, *108*). The inhibitory FcγRIIb, however, inhibits malignant B cell depletion by CD20 mAb (*104*, *108*). Further,

polymorphisms in FcγRs among different mouse strains alter the efficacy of CD20 mAb. NOD mice, which have a truncated FcγRI and polymorphisms in FcγRIII and FcγRIV relative to C57/BL6 (B6) mice, deplete fewer B cells following CD20 mAb treatment (*112*). While complement activation has been suggested as a mechanism by which human B cells are depleted following CD20 mAb therapy, mice deficient in C1q, C3, or C4 clear B cells following CD20 mAb treatment at rates similar to wild-type mice. Further, deficiencies in T cells, perforin, neutrophils, or functional NK cells do not impact CD20 mAb-dependent depletion of endogenous or malignant B cells (*17*, *106*, *108*). Thus, macrophages deplete endogenous and malignant B cells following CD20 mAb therapy predominantly through Ab-dependent cell phagocytosis mechanisms.

1.2.3. CD19 Immunotherapy

In addition to CD20, CD19 is also uniquely expressed by B cells, making it another potential target for therapeutic B cell depletion. In contrast to CD20, however, CD19 is critical for B cell development and is expressed earlier in B cell development than CD20.

1.2.3.1. The Role of CD19 in B cell Development and Function

CD19, which was previously referred to as B4, is a B cell-specific surface protein with low expression during pre-B cell development that then increases throughout B cell development, most notably from the transition from immature to mature B cells, until plasma cell differentiation (*113*). Peritoneal B1 cells express the highest levels of CD19,

displaying on average 2-3 fold more surface CD19 than B2 cells (*114*). This 95 kDa glycoprotein is a member of the Ig superfamily and contains two extracellular C2-type Ig-like domains in addition to a membrane-spanning domain and a large, highly charged cytoplasmic tail that is largely conserved between mouse and human (*115*). The cytoplasmic tail of CD19 has nine conserved tyrosine residues that allow CD19 to act like a membrane-bound adapter molecule for Src homology-2 (SH2) domain-containing signaling molecules, including protein tyrosine kinases Lyn, Fyn, Vav, Grb2, phosphatidylinositol 3-kinase (PI3K), phospholipase Cy2 (PLCγ2), and c-Abl (*116*). CD19 is a component of the multimeric cell surface signal transduction complex on mature B cells that includes CD21 (CR2, C3dR, EBVR), CD81 (TAPA-1), and CD225 (IFITM1, Leu-13) (*116-120*).

CD19 is a costimulatory molecule that regulates B cell signaling thresholds during negative selection and clonal expansion as well as B cell development (*114, 120-124*). Surface CD19 engagement increases free intracellular calcium levels, activates phospholipase C and protein tyrosine kinases, and induces B cell homotypic adhesion via LFA-1 and ICAM-1 (*67, 117, 125, 126*). The role of CD19 in B cell development and function has been extensively evaluated *in vivo* using mice that either lack CD19 or overexpress the human CD19 (huCD19) transgene, the latter of which enables the *in vivo* prediction of human therapeutic efficacy. CD19-deficient mice have no impairments in B cell generation in the bone marrow but have significant reductions in peripheral B cells,

most notably in B1 cells (75-90%), and 80% reductions in serum Ig, particularly IgM, IgG1, and IgG2a. Further, B cells lacking CD19 express more surface IgM but proliferate less in response to mitogen and have weaker T cell-dependent immune responses. CD19-deficient B cells are hyporesponsive to BCR and CD40 ligation and have reduced phosphorylation of signaling molecules following BCR ligation, despite comparable expression levels of signaling molecules (*122, 123, 127*). CD19 deficiency thus critically dampens the human immune system. Reciprocally, mice that overexpress human CD19 have normal B cell maturation, though mature B cell numbers are significantly reduced in the periphery (*121, 122, 124*), likely due to enhanced negative selection in the bone marrow. These mice also have increased peritoneal B1 cell numbers and elevated serum Ig, including serum autoAbs (*114*). B cells overexpressing human CD19 have low surface IgM and augmented proliferation following mitogenic stimulation as well as elevated T-dependent Ab production. CD19-transgenic B cells are hyperresponsive to BCR and CD40 ligation, displaying exaggerated phosphorylation of signaling molecules relative to wild-type mice (*121, 123*). Despite altering B cell receptor signaling thresholds, CD19 likely functions independently of B cell receptor engagement, as alterations in CD19 expression affects all B cell subsets equally (*121, 122*). In addition to functioning as a scaffold for the "processive" amplification of Src family kinase activity, predominantly Lyn kinase, CD19 engagement augments calcium responses at least in part by sequestering Lyn from CD22, a negative regulator of B cell signaling (*116, 128*). CD19 is

therefore a critical universal regulator of signaling thresholds during B cell development and function.

1.2.3.2. CD19 as a Tumor-Associated Target for Immunotherapy

CD19 is expressed on the surface of most B cell populations and is critical for B cell function, making it an ideal target for immunotherapy of malignant B cells. Indeed, CD19 is expressed on more than 90% of leukemias and lymphomas of B cell origin (*50, 129*) and was one of the first target molecules for mAb-linked immunotoxin therapies (*130-133*). Several studies have demonstrated therapeutic efficacy of CD19 mAbs in xenotransplant models using human leukemias (*134*) and lymphomas (*135-137*). In particular, the CD19 mAb XmAb5574 is a humanized anti-hCD19 mAb that has been optimized for enhanced FcγR binding affinity and efficiently depletes most circulating B cells and lymphoid tissue B cells in a mouse xenograft model, though it did not affect serum Ab levels in a monkey xenograft model (*138, 139*). Another CD19 mAb, HB12, which has been humanized and optimized to increase affinity for human FcγRs, depletes most circulating and lymphoid tissue B cells in huCD19 transgenic mice; this process is dependent on macrophages and independent of complement (*67, 140, 141*).

The mechanisms by which endogenous and malignant B cells are depleted following CD19 mAb treatment have been studied extensively in wild-type and huCD19 transgenic mice. A single dose of CD19 mAb (IgG2a) depletes more than 90% of B cells from the blood, spleen, and lymph nodes within a week of CD19 mAb treatment, and B

cell numbers begin to recover in the circulation fifteen weeks after treatment. The peritoneal cavity again serves as a protective barrier for B cells during CD19 mAb treatment such that peritoneal B cells are only reduced by 60-70%, with B1a cells showing a particular resilience to depletion. Unlike CD20 mAbs, CD19 mAb treatment has significant effects on the humoral immune responses. CD19 mAb depletes both short-lived plasmablasts and some long-lived plasma cells as well as serum IgM, IgG, and IgA during homeostasis. Further, CD19 mAb treatment impairs primary and secondary Ab responses to T cell-independent and -dependent antigens and ablates autoAb development in huCD19 transgenic mice (*109, 140*). Further, CD19 mAb therapy prevents chronic renal allograft rejection by ablating allograft-reactive IgG development, which leads to renal injury and complement deposition, and also inhibits graft-specific Ab production following acute heart transplant (*109*). Additionally, unlike CD20 mAb, the efficacy of different CD19 mAbs is comparable among different isotypes, likely owing to the relatively elevated expression of CD19 on the B cell surface. CD19 mAbs of the IgG2, IgG2a, and IgG2b isotypes have similar rates of B cell depletion, though CD19 IgA mAbs do not deplete B cells *in vivo* (*140*). Macrophages and FcγR expression are both key components for CD19 mAb-dependent B cell depletion *in vivo* in a mechanism very similar to CD20 mAb. As such, mice depleted of macrophages following clodronate injection do not efficiently deplete endogenous or malignant B cells (*17, 140*). Similarly, mice treated with poly(I:C), which enhances macrophage FcγR expression, have

enhanced malignant B cell depletion (*17*), and mice with FcγR deficiencies do not deplete endogenous B cells following CD19 mAb treatment (*140*). CD19 mAb thus depletes endogenous and malignant B cells through mAb-dependent cell phagocytosis by macrophages.

CD19 and CD20 immunotherapies are effective tools for the treatment of human conditions that derive from or are enhanced by B cells and their effector products. Both mAbs effectively deplete circulating immature and mature B cells, while CD19 mAb treatment also reduces pre-B, plasmablast, and plasma cell populations. That CD19 mAb depletes pre-B cells indicates that this mAb may have a more durable therapeutic effect for some diseases versus CD20 mAb. Further, the role of the humoral immune response in different conditions would have to be carefully considered, as Ab-secreting cells are significantly reduced by CD19 mAb therapy. As both CD19 and CD20 mAbs deplete B cells through a mAb-dependent cell phagocytosis mechanism that requires macrophages, treatments that augment macrophage phagocytosis are a potential means to augment the efficacy of these immunotherapies. Intriguingly, the combination of low doses of both CD19 and CD20 mAb depletes more B cells in the spleen and lymph nodes than either mAb alone (*140*), indicating that these mAbs have additive effects that may prove important for clinical treatment regimens. B cell depletion by CD19 and CD20 mAbs is therefore a powerful clinical option with potential avenues for improving therapeutic efficacy.

2. Materials and Methods

2.1. Study Design

These studies are comprised of controlled laboratory experiments using mice and publicly available human data. All data, including outliers, were included in the presented experiments. Unless otherwise noted, all experiments were performed at least twice with multiple samples to ensure reproducibility.

2.2. Mice

B6 mice were from the National Cancer Institute-Frederick Laboratory (Frederick, MD). P14 mice with the lymphocytic choriomeningitis virus (LCMV) gp33-H-2Db–specific TCR [B6.Cg-Tcratm1Mom Tg(TcrLCMV)327Sdz] (*142*) were from Taconic Farms (Hudson, NY). PWK/PhJ (PWK), A/J, WSB/EiJ (WSB), NZO/H1LtJ (NZO), 129S1/SvImJ (129), NOD/ShiLtJ (NOD), and B6129SF1/J (B6 x 129 F1, F1), and B6.Cg-Tg(IghMyc)22Bri/J (*Eμ-cMyc* transgenic) hemizygous mice were obtained from The Jackson Laboratory (Bar Harbor, ME). Mice with selective mycn-deficient macrophages were generated by crossing mice expressing Cre recombinase under the lysozyme 2 gene promoter (B6.129P2-Lyzstm1 (cre)Ifo/J, $Lysm^{Cre/+}$) to mice with floxed mycn alleles (B6.129-$Mycn^{tm1Psk}$/J, $Mycn^{F/F}$) to generate experimental mycn-deficient mice ($Lysm^{Cre/+}Mycn^{F/F}$). $Lysm^{Cre/+}$ had been backcrossed onto the B6 background for more than six generations and were provided by M.D. Gunn (Department of Medicine, Duke University, Durham, NC, USA). $Mycn^{F/F}$ mice had been backcrossed onto the B6

background for seven generations and were provided by A. Balmain (Helen Diller Family Comprehensive Cancer Center, University of California San Francisco, San Francisco, CA, USA). Consomic mice were generated by serially back-crossing mice with the F1 genotype from 11.5 to 13 Mbp on Chromosome 12 to B6 mice. Consomic mice were identified by sequencing (Duke Cancer Center DNA Analysis Facility) informative single nucleotide polymorphisms (SNPs) between B6 and 129 mice using genomic DNA primers specific for species-specific SNPs identified by the Mouse Genome Browser (Ensembl, ensembl.org/Mus_musculus/Info/Index) and the Mouse Genomes Project (Wellcome Sanger, www.sanger.ac.uk/cgi-bin/modelorgs/mousegenomes/snps.pl). Mice that had the B6 genotype on Chromosome 12 at the N4, N5, and N6 generations were used as wild-type controls.

All mice were housed in a specific pathogen-free barrier facility and were used at 8-10 weeks of age unless otherwise specified. Mice used in LCMV studies were housed in isolator cages. All studies were approved by the Animal Care and Use Committees of Duke University Medical Center, Emory University, and the Atlanta VA Medical Center and performed in accordance with the recommendations in the Guide for the Care and Use of Laboratory Animals of the National Institutes of Health.

2.3. Immunotherapy

To induce *in vivo* B cell and lymphoma depletion, sterile and endotoxin-free CD20 mAb (MB20-11, IgG2c; 250 μg, unless otherwise noted) or isotype-matched control

mAb were injected in 200 ml phosphate-buffered saline (PBS) through lateral tail veins or intraperitoneally (*106*). For acute B cell-depletion studies, mice were injected once with control or CD20 mAb two weeks before analysis. For chronic B cell–depletion studies, mice aged six months were depleted of B cells by repeated injections with control or CD20 mAb once a month for six months and analyzed two weeks following the final injection. For migration studies, 10^7 B cell–depleted splenocytes labeled with CellTracker Orange CMRA (Invitrogen Life Technologies, Carlsbad, CA) were injected through the lateral tail veins of mice that had received either control or CD20 mAb one week prior; mice were then analyzed two days following cell transfer.

2.4. LCMV Infection

Mice were infected with 2×10^5 plaque-forming units (PFU) LCMV Armstrong 53b prepared as described (*143*) through intraperitoneal injection. Mice were infected with LCMV one week after treatment with control or CD20 mAb and then analyzed one week post-infection. For LCMV-specific $CD8^+$ T cell studies, P14 $CD8^+$ T cells (1×10^5) were transferred through lateral tail veins 6 days after treatment with control or CD20 mAb. Mice were then infected with LCMV one day later and evaluated one week post-infection. To quantify LCMV-specific T cell responses, T cells were stimulated with $GP_{33–41}$ ($CD8^+$ T cells) and $GP_{61–80}$ ($CD4^+$ T cells) peptides (10 mg/ml; AnaSpec, Fremont, CA) in the presence of brefeldin A for five hours before cell surface and intracellular cytokine staining.

2.5. Lymphoma Culture and Adoptive Transfer

Spontaneous monoclonal lymphomas isolated from the lymph nodes of individual *Eμ-cMyc* transgenic mice were cultured in complete medium [RPMI 1640 (Cellgro, Herndon, VA), 15% FBS (Sigma-Aldrich), 100 U/ml penicillin, 100 μg/ml streptomycin, 2 mM L-glutamine (Cellgro), and 55 μM 2-mercaptoethanol (Invitrogen, Carlsbad, CA)] for up to one week before freezing in aliquots. Viable cells were quantified by trypan blue staining using a hemocytometer. Thawed lymphoma cells were cultured for 24-48 hours in complete medium prior to injection of 1×10^5 viable cells in 250 μl PBS under the dorsal skin of recipient wild-type mice. Mice were injected one day later with 250 μg purified MB20-11 or unreactive mouse control IgG2c mAbs in 200 μl through lateral tail veins to induce *in vivo* lymphoma depletion.

Mice were monitored daily for behavioral and morphologic changes. Tumor size was measured weekly with a calibrated micrometer, and tumor volumes were calculated as follows: tumor volume = [(greatest transverse diameter)^2 x greatest longitudinal diameter] / 2 (*108*). Mice exhibiting distress or with lymphoma volumes that exceeded 2.0 cm^3 were euthanized, with the date recorded as death from disease. For tumor studies, the primary endpoint for survival following tumor transfer was defined as 60 days, as most mice that developed lymphomas succumbed to disease by day 60, while other mice had normal lifespans without obvious symptoms or disease and were considered lymphoma-free (*108*).

Lymphoma sensitivity to CD20 immunotherapy was determined by calculating the increase in the area under the curve (AUC) from 60-d Kaplan-Meier survival plots as follows: sensitivity = [(AUC for CD20 mAb-treated mice) - (AUC for control mAb)] / (AUC for control mAb) X 100. Lymphomas obtained from mice used to determine the sensitivity of primary lymphomas to CD20 immunotherapy were collected and referred to as secondary lymphomas, which were then evaluated for sensitivity to CD20 immunotherapy in the same manner as primary lymphoma cells. This process was repeated for several generations to generate lymphoma families derived from single primary lymphomas.

2.6. Genome-Wide Linkage Analysis

Tail DNA was collected from 235 N1 mice that had been injected with the spontaneous primary B cell lymphoma BL3750 and CD20 mAb the next day as described above (*108*). Mice were then monitored for survival until day 60. Tail DNA was isolated and sequenced using the Illumina (San Diego, California) GoldenGate genotyping assay for the 377 genome-wide Mouse LD Linkage Panel (Duke University Genotyping Facility and David H. Murdock Research Institute). Genetic map positions were identified using the NCBI SNP database (build 37.1). Mouse genotypes at each locus were then correlated with the number of days each mouse survived and analyzed for the presence of a significant relationship using J/QTL software from The Jackson Laboratory (Bar Harbor, ME, USA, http://churchill.jax.org/software/jqtl.shtml). The phenotypes of all

four sequence datasets were not normally distributed. Thus, data were fit to a non-parametric phenotype distribution. Data analysis parameters were as follows: genotype probability calculated step-wise by 2.0 cM; genotyping error rate of 0.001; Haldane mapping function; and fixed step-width type. Significance thresholds for the number of days of survival were established using 100,000 permutations with separate permutations for Chromosome X using all informative markers. The degree of variability in survival attributed to the identified QTL was determined using the Fit QTL function. LOD scores and plots were generated using J/QTL. For high-resolution mapping of mice with genotype cross-overs, informative SNPs for B6 and 129 mice were identified and sequenced as described earlier to determine the genotype of each mouse at a given locus.

2.7. Retroviral Construct Generation and Infection

BL3750^{Ctrl} and BL3750^{Gal1} lymphomas were generated by retroviral transfection of primary BL3750 lymphoma cells with the pMX-IRES-GFP plasmid (*144*) with or without mouse *Lgals1* cDNA inserted. Briefly, mouse *Lgals1* cDNA was amplified from primary splenic CD19^{+} B cell RNA by polymerase chain reaction (PCR) and was introduced to the pMX-IRES-GFP plasmid downstream of the 5′ long terminal repeat sequence using BamHI and NotI sites, leaving eGFP downstream of the internal ribosome entry site. Phoenix-Eco cells (ATCC, Rockville, MD) were then transduced with either control GFP or Gal1-GFP expression plasmids, and virus was collected 3 days later for retroviral

infection of BL3750 cells. GFP^+ BL3750 cells were sorted by FACS four times to ensure homogeneity and the stability of plasmid expression between the $BL3750^{Ctrl}$ and $BL3750^{Gal1}$ cells. Mice were given $BL3750^{Ctrl}$ or $BL3750^{Gal1}$ lymphoma cells (1×10^5) in 250 µl PBS under the dorsal skin and were injected one day later with 250 µg MB20-11 or unreactive mouse control IgG2c mAbs in 200 µl through lateral tail veins. Serum was obtained at day 45 for Gal-1 measurements, and lymphoma size was measured weekly.

2.8. Macrophage Phagocytosis Assay

Peritoneal macrophages were collected by lavage four days after intraperitoneal thioglycollate injection and were allowed to adhere to tissue culture dishes overnight. $BL3750^{Ctrl}$ and $BL3750^{Gal1}$ tumors were labeled with CellTrace Violet (Invitrogen-Molecular Probes) according to the manufacturer's protocol and were coated with control isotype, MB20-11, or MB19-18 (IgG2c) mAb for 20 min on ice. Tumors were then added to macrophage cultures at a 1:1 ratio for a final concentration of 2×10^6 cells per mL, and cultures were incubated for 3, 6, or 24 hours. Control co-cultures were incubated at 4 ^oC for the duration of the experiment. Non-adherent cells were collected, and adherent cells were then removed using trypsin-EDTA and were stained for immunofluorescence analysis.

2.9. Cell Isolation and Immunofluorescence Analysis

Single-cell suspensions were generated by gentle dissection of spleen, peripheral lymph nodes (axial, brachial, and inguinal), or lymphoma, and erythrocytes were

hypotonically lysed. Viable single-cell suspensions (1 x 10^6 per sample) were first stained with Fc block (Clone 93, Biolegend, San Diego, CA), and LIVE/DEAD Fixable Dead Cell Stain Kit (Invitrogen Life Technologies) in PBS according to the manufacturer's protocols. For cell surface staining, cell suspensions were stained using predetermined optimal concentrations of mAb in FACS buffer (2% FCS in PBS) on ice for 30 minutes or with MHC-II tetramers for 2 hours at 37 ˚C. Treg visualization was carried out using the Foxp3/Transcription Factor Staining Buffer Set (eBioscience, San Diego, CA) according to the manufacturer's instructions. Intracellular cytokine staining was performed using the Cytofix/Cytoperm kit (BD Biosciences) according to the manufacturer's instructions. Cells were washed between all staining steps in FACS buffer and were resuspended in PBS containing 1.5% paraformaldehyde after staining and kept in the dark at 4 ˚C until analysis.

Immunofluorescence staining of single live unstained cells was analyzed using a FACSCanto II flow cytometer (BD Biosciences, San Jose, CA), with background staining levels determined using isotype- and fluorochrome-matched control mAbs. Dead cells were excluded from data analysis by staining with LIVE/DEAD Fixable Dead Cell Stain Kit, and cells with the forward and side light scatter properties of leukocytes, including lymphocytes and macrophages, or tumors were analyzed. Background staining was assessed using nonreactive, isotype-matched control mAbs and was subtracted from shown mean fluorescence intensity (MFI) values.

For intracellular T cell cytokine staining, spleen lymphocytes were isolated and depleted of B cells using CD19 mAb-coated magnetic beads (Invitrogen Life Technologies). The remaining non–B cells were cultured *in vitro* with plate-bound functional-grade CD3ε (145-2C11, 1 mg/ml, Ebioscience) and CD28 (37.51, 10 mg/ml, Ebioscience) mAbs for 3.5 hours in the presence of the secretion inhibitor brefeldin A (5 mg/ml; BD Biosciences) to identify T cells that were actively producing cytokines *in vivo*.

CD20 expression was visualized using the CD20 mAb MB20-11 conjugated to Pacific Blue by succinimidyl ester (Invitrogen, Carlsbad, CA). Other mAbs conjugated to FITC, PE, PE-Cy5, PE-Cy7, APC, or biotin included in these studies are as follows: L-selectin (CD62L; clone LAM1-116) mAb was as described (*145*); CD19 (6D5), CD21/35 (7E9), B220 (RA3-6B2), CD25 (PC61), CD127 (A7R34), killer cell lectin-like receptor G1 (KLRG1, MAFA, 2F1), F4/80 (BM8), streptavidin, and isotype control mAbs from Biolegend; CD5 (53-7.3), CD23 (B3B4), IgM (II/41), and Foxp3 (FJK-16s) mAbs from Ebioscience (San Diego, CA); CD24 (M1/69) CD4 (H129.19), CD8 (53-6.7), CD44 (IM7), IFN-γ (XMG1.2), Ly6C (AL-21), PSGL1 (2PH1), and TNF- α (MP6-XT22) from BD Pharmingen (San Jose, CA); and IgD (11-26C) from Southern Biotechnology Associates (Birmingham, AL). The MHC-I tetramers, $D^bGP_{33–41}$ (GP33), used to identify LCMV-specific $CD8^+$ T cells were generated as described (*146*). The MHC-II tetramer $I\text{-}A^bGP_{66–77}$ (GP66; National Institutes of Health Tetramer Facility) was used to identify LCMV-specific $CD4^+$ T cells.

2.10. Transcript Expression Measurement

Quantitative and relative transcript levels were measured following total RNA extraction using TRIzol (Invitrogen-Molecular Probes) from either purified spleen lymphocytes to determine viral RNA levels, lymphomas to determine *lgals1* expression, or peritoneal resident or Thioglycollate-elicited macrophages for *mycn* expression. Relative transcript levels were quantified by GeneChip analysis (Affymetrix Mouse Genome 430 2.0 GeneChips; Affymetrix, Santa Clara, CA). All quality parameters for the arrays were confirmed to be in the range recommended by the manufacturer. Relative transcript data are shown as *Lgals1* transcript levels relative to internal housekeeping transcripts.

Quantitative transcript levels were determined using cDNA generated from 250 μg RNA and a mixed-priming strategy with random hexamer primers (Promega, Madison, WI) and Oligo dT(12-18) primers (Invitrogen). Transcripts were measured by quantitative real-time (qRT)-PCR amplification of triplicate samples using the SYBR Green detection reagent and the iCycler iQ system (Bio-Rad, Hercules, CA). Transcripts were amplified using *gapdh* primers (*147*), LCMV glycoprotein-specific primers (*148*), *Lgals1* primers (forward, CGCCAGCAACCTGAATC; reverse, GTCCCATCTTCCTTGGTGTTA), or *mycn* primers (forward, CTCCGGAGAGGATACCTTGA; reverse, ACGCACAGTGATCGTGAAAG). Cycle conditions were as follows: one denaturation cycle of 95°C for 2 min followed by forty

cycles of 95˚C for 30 s, 60˚C for 30 s, and 72˚C for 30 s. The specificity of qRT-PCR products was confirmed by melting curve analyses and by sequencing (Duke Cancer Center DNA Analysis Facility) cloned cDNA PCR products using the StrataClone PCR Cloning Kit (Agilent Technologies, Santa Clara California). Quantitative transcript data for LCMV virus RNA and *mycn* expression are shown as threshold values ($2^{-\Delta\Delta Ct}$) determined by normalizing RNA transcript levels to *gapdh* expression within both sample groups and then normalizing to the indicated control group. Quantitative transcript data for lymphoma studies are shown as *Lgals1* transcript levels relative to *gapdh*.

2.11. Enzyme-linked Immunosorbent Assay

Gal-1 protein secretion by individual lymphomas was measured in triplicate after culture at 1 x 10^6 cells/mL for 24 hours. Quantification of gal-1 in the culture supernatant fluid was performed using the Mouse Galectin-1 DuoSet ELISA kit (R&D Systems, Minneapolis, MN).

2.12. Bioinformatics Analysis

Human *LGALS1* microarray data were from GEO Accession GSE2350. Control non-malignant human B cell subpopulations were obtained from routine tonsillectomies. Leukemia and lymphoma samples were obtained as follows: BL, lymph node biopsies; CLL, peripheral blood cells (1) or peripheral blood $CD19^+$ cells DLBCL lymph node biopsies (1) or lymph node biopsy $CD19^+$ cells (2); FL, lymph node biopsies;

HCL, bone marrow biopsies or peripheral blood cells; MCL, lymph node biopsy $CD19^+$ cells.

FcγRI, FcγRIII, and FcγRIV sequences were as published for B6 and NOD mice (*112*). FcγRI sequence for 129 mice were as published (GenBank Accession number AAD34940.1). 129 homology to B6 and NOD mouse FcγRIII and FcγRIV were determined by identifying SNPs in coding sequence using the Mouse Genomes Project (Wellcome Sanger). Protein domains were identified using Uniprot (www.uniprot.org). Identity-by-descent plot was generated using the Mouse Phylogeny Viewer (msub.csbio.unc.edu). Homology between human and mouse *mycn* sequence was identified using Vista Browser (http://pipeline.lbl.gov/). Human *mycn* polymorphisms were identified using data from the International HapMap Project (http://hapmap.ncbi.nlm.nih.gov/) and 1000 Genomes Project (http://www.1000genomes.org/).

2.13. Statistical Analysis

Data are shown as individual data points or as mean (± SEM). Significant differences in mouse survival were calculated using the log-rank test. The F-test was used to measure the equality of variances between two samples, and significant differences in sample means were determined using the unpaired two-tailed Student's *t* test with Welch's correction for unequal variances where appropriate. Correlations between lymphoma sensitivity and CD20, *Lgals1*, or Gal-1 expression were determined

by calculating Spearman's correlation coefficient (ϱ), with statistically significant linear regressions indicated by regression lines where appropriate and *P* values calculated by a Gaussian approximation. Comparative statistical analysis and the generation of Kaplan-Meier cumulative survival plots were performed with Prism software (version 5; GraphPad Software, San Diego, CA). Human microarray data were analyzed using the Kruskal-Wallis one-way ANOVA with Dunn's Multiple Comparison test for performing *post hoc* multiple pair-wise comparisons.

3. The role of B cells in the Homeostasis and Effector Response of the Cellular Immune System

The following text was modestly adapted from its original manuscript, "Acute and Chronic B Cell Depletion Disrupts $CD4^+$ and $CD8^+$ T Cell Homeostasis and Expansion During Acute Viral Infection in Mice," published in *The Journal of Immunology* (193: 746-756) in 2014 (*149*).

3.1. Introduction

B cells have many functions during homeostasis and immune responses, including Ab production, organizing lymphoid tissue organogenesis, antigen presentation, and cytokine production, all of which can modulate cellular and innate immune responses (*8*). The Ab-independent role of B cells during cellular immune responses has received recent attention due to the clinical demonstration that therapeutic B cell depletion results in disease remission in select autoimmune diseases. Even though patients undergoing B cell depletion therapies frequently remain B cell insufficient for 8-18 months, their autoAb titers may not decrease after treatment (*150*). Thus, B cells must contribute to autoimmune pathogenesis via mechanisms in addition to autoAb production, but the cellular effects of acute or chronic B cell depletion on the human or

mouse immune systems remain inadequately characterized, particularly during cellular immune responses.

The effect of short-term and chronic B cell depletion on T cell homeostasis and immune responses to LCMV infection was assessed in this study using naïve mice with intact immune systems and a potent mAb specific for mouse CD20 (*71, 106*). As CD20 is downregulated early during plasma cell differentiation, long-lived plasma cells are not depleted by CD20 mAb, and serum Ig levels remain stable after CD20 mAb-induced B cell depletion (*105*), allowing for the dissection of the relationship between B and T cells at homeostasis and during viral infection independent of Ab production.

3.2. Results

3.2.1. Acute B cell depletion by CD20 mAb reduces T cell numbers

Studies examining the effects of CD20 mAb-induced B cell depletion on T cell numbers and function have generated variable findings (*18, 27, 34, 106, 151-153*). Therefore, the effect of short-term B cell depletion on spleen and lymph node T cell frequencies and numbers was compared in littermate groups of 2-month-old and 4-month-old fully mature mice where B and T cell numbers are stable. Tissue lymphocyte subsets were analyzed two weeks after a single dose of control or CD20 mAb treatment to optimally evaluate the effect of B cell

depletion on T cell homeostasis. In all mice, spleen and lymph node $B220^+$ B cell numbers were reduced by >99% in littermates given CD20 mAb relative to control mAb (Fig. 1A). Consequently, the frequencies of $CD4^+$ and $CD8^+$ T cells among lymphocytes were increased. However, total spleen and lymph node $CD4^+$ and $CD8^+$ T cell numbers in 2-month-old B cell-depleted mice were overlapping with control mAb-treated mice, but mean values were decreased by 44-53% (Fig. 1B-C), although variability was observed between individual mice and groups of littermate mice in four independent experiments. Mean $CD4^+$ and $CD8^+$ T cell numbers in 4-month-old mice given CD20 mAb were similarly reduced by 35-40% and 54-62% in the spleen and lymph nodes, respectively, with a range of variability between mice and littermate groups between different experiments. Treg cell frequencies within spleens and lymph nodes did not change following B cell depletion, although total Treg cell numbers were significantly reduced (2-month-old, 55-57%; 4-month-old, 47-61%; Fig. 1D). The migration of adoptively transferred $CD4^+$ and $CD8^+$ T cells into blood, the spleen, and lymph nodes was not significantly affected by the absence of B cells, as transferred dye-labeled cells migrated normally into tissues (P>0.05, Fig. 1E-F). However, when endogenous T cell numbers were reduced in CD20 mAb-treated mice, transferred T cell numbers were reduced similarly. Thus, B cell depletion

significantly reduced overall $CD4^+$ and $CD8^+$ T cell and Treg cell homeostasis in 2- and 4-month-old naïve mice relative to control mAb-treated littermates.

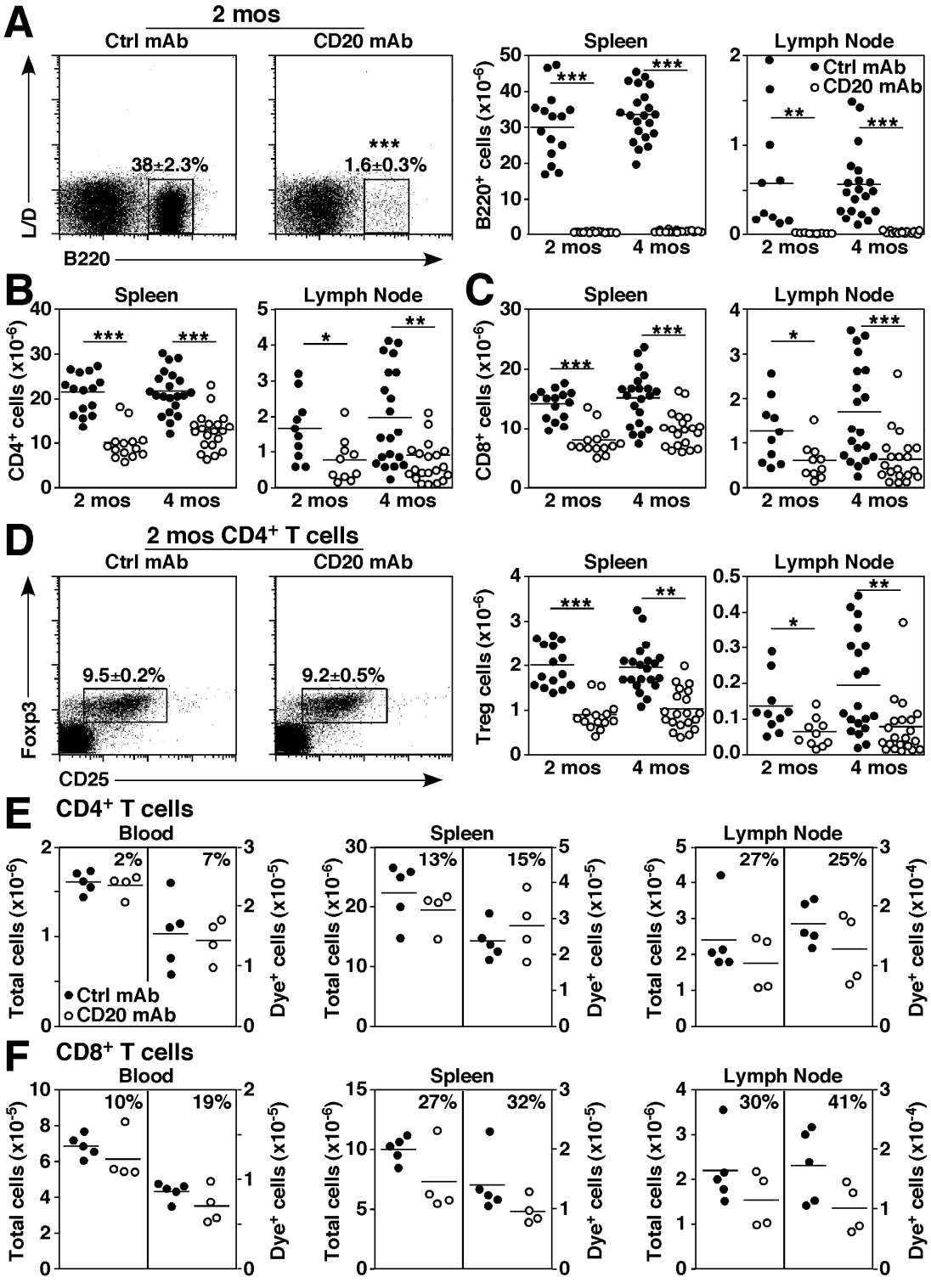

Figure 1. B cell depletion alters T cell homeostasis.

Figure 1. B cell depletion alters T cell homeostasis. (A-D) Naïve 2- or 4-month-old mice were treated with control (closed circles) or CD20 (open circles) mAb, with viable single spleen and lymph node lymphocytes assessed 14 days later by immunofluorescence staining with flow cytometry analysis. Representative panels show (A) $B220^+$ vs. LIVE/DEAD (L/D) spleen B cell staining (left panels) and absolute B cell numbers (right panels), (B) $CD4^+$ T cell numbers, (C) $CD8^+$ T cell numbers, and (D) CD25 vs. intracellular Foxp3 staining for $CD4^+$ T cells (left panels) and $Foxp3^+CD25^+CD4^+$ Treg cell numbers (right panels) following B cell depletion. Pooled results from 4 independent experiments are indicated in graphs (n = 10-21 mice per group with means indicated by horizontal bars). (E-F) $CD4^+$ and $CD8^+$ T cell migration is not profoundly impacted by B cell depletion. Dye-labeled B cell-depleted splenocytes were adoptively transferred into naïve 2-month-old mice given control or CD20 mAb 7 days earlier. Absolute numbers of total endogenous and adoptively transferred dye+ (E) $CD4^+$ and (F) $CD8^+$ T cells within the blood, spleen, and lymph nodes were assessed 2 days later by immunofluorescence staining with flow cytometry analysis. Percentage differences in T cell numbers for CD20 mAb-treated relative to control mAb-treated mice are shown, where graphs show results from individual mice (n = 5 mice per group with means indicated by horizontal bars). (A-F) Mean cell frequencies (± SEM) within the indicated dot plot gates are shown. Significant differences between sample means are indicated: *, $P < 0.05$; **, $P < 0.01$; ***, $P < 0.001$.

3.2.2. Acute B cell depletion reduces both naïve and activated T cell numbers

The effect of B cell depletion on spleen T cell subsets with naïve $CD44^{lo}CD62L^{hi}$ and activated $CD44^{hi}CD62L^{lo}$ phenotypes was quantified relative to all $CD4^+$ or $CD8^+$ lymphocytes. The frequencies of activated $CD4^+$ and $CD8^+$ T cells were reduced by 30-38% in 2-month-old mice treated with CD20 mAb in comparison with control mAb-treated littermates (Fig. 2A-B). The numbers of activated $CD4^+$ and $CD8^+$ T cells were reduced by 52-68% and 47-66% in 2- and 4-month-old mice, respectively. B cell depletion reduced total naïve $CD4^+$ and $CD8^+$ T cell numbers by 40-50% in 2-month-old mice and by 35-37% in 4-month-old mice. Thus, mean numbers of naïve and activated $CD4^+$ and $CD8^+$ T cells were decreased in CD20 mAb-treated mice relative to littermate controls.

As cytokine production is an integral component of the effector T cell immune response, the effects of B cell depletion on T cell cytokine production were quantified. IFN-γ- and TNF-α-expressing $CD4^+$ and $CD8^+$ T cell frequencies were not profoundly altered in either 2- or 4-month-old mice after CD20 mAb treatment for two weeks (Fig. 2C-D). However, mean IFN-γ- and TNF-α-expressing $CD4^+$ T cell numbers were reduced by 58-61% and 51-54%, respectively, in B cell-depleted 2- and 4-month-old mice, while mean IFN-γ- and

TNF- α -expressing $CD8^+$ T cell numbers were reduced by 51-59% and 36-49%, respectively. Thus, B cell depletion significantly reduced the total numbers of cytokine-producing $CD4^+$ and $CD8^+$ T cells relative to control mAb-treated littermates.

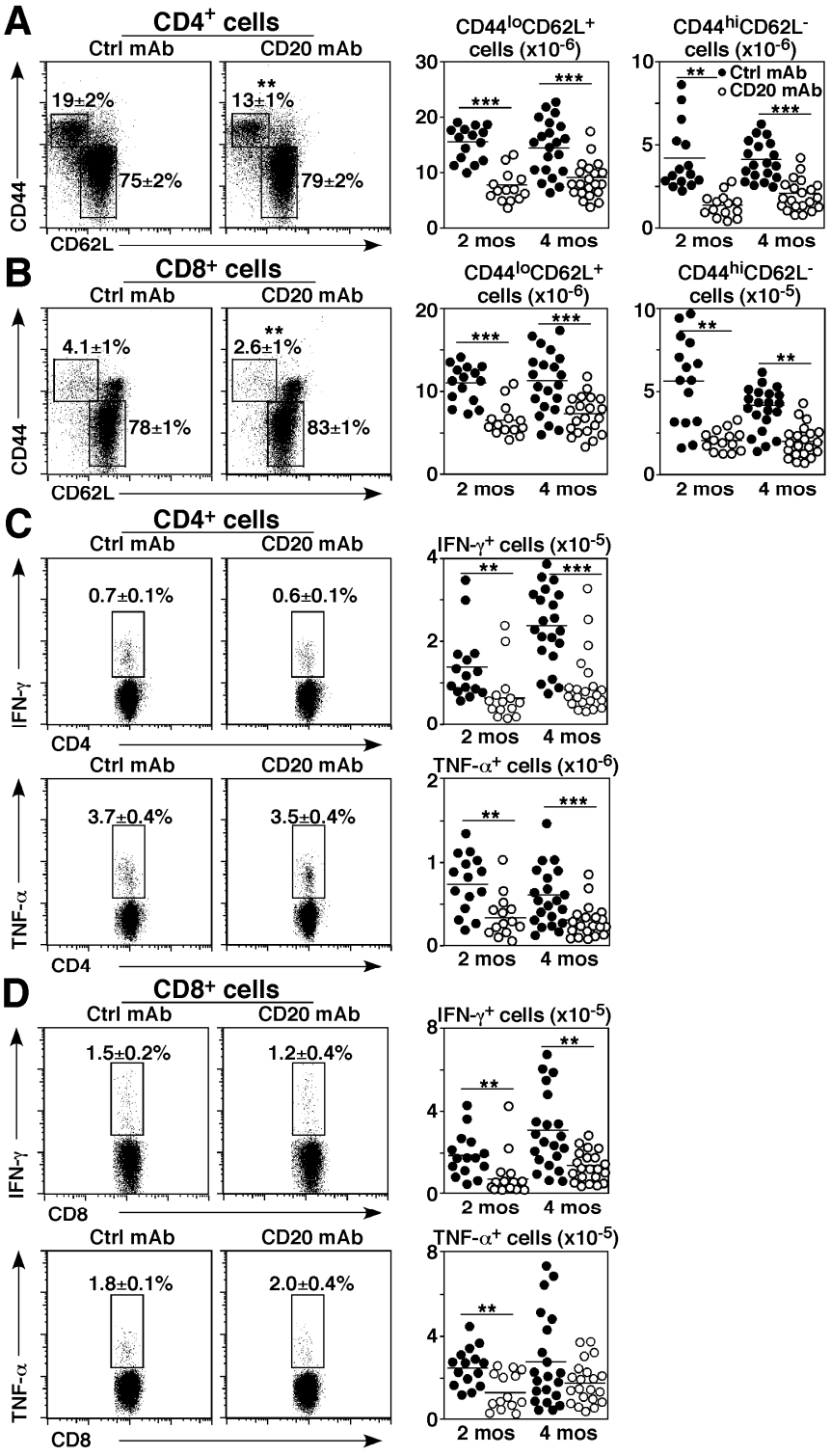

Figure 2. B cell depletion alters naïve and memory T cell homeostasis.

Figure 2. B cell depletion alters naïve and memory T cell homeostasis. Naïve 2- or 4-month-old mice were treated with control (closed circles) or CD20 mAb (open circles). Viable, single spleen lymphocytes were isolated 14 days later (A-D) and depleted of B cells using CD19 mAb-coated magnetic beads (C-D). The remaining non-B cells were cultured for 3.5 hours with plate-bound CD3/CD28 mAbs before cell surface CD4/CD8 labeling and intracellular cytokine staining with flow cytometry analysis. Representative panels show CD44 vs. CD62L staining (left panels) and cell numbers (right panels) for (A) $CD4^+$ and (B) $CD8^+$ T cells. Representative panels show IFN-γ and TNF-α expression (left panels) and cell numbers (right panels) for (C) $CD4^+$ and (D) $CD8^+$ T cells. (A-D) Mean cell frequencies (± SEM) within the indicated dot plot gates are shown. Graphs show results from individual mice pooled from 3-4 independent experiments (n = 15-21 mice per group) with means indicated by horizontal bars. Significant differences between sample means are indicated: **, $P < 0.01$; ***, $P < 0.001$.

3.2.3. Chronic B cell depletion reduces activated CD4$^+$ T cell numbers

Whether the effects of B cell depletion on T cell homeostasis observed in young mice were age-associated was assessed using naïve 6-month-old mice with fully-mature immune systems that were then treated monthly with CD20 mAb for six months. Spleen and lymph node B220$^+$ B cell numbers were decreased by more than 98% after chronic B cell depletion (Fig. 3A). Spleen CD4$^+$ T cell numbers were decreased by 51% in CD20 mAb-treated mice, including a 56% decrease in Treg cell numbers. Mean lymph node CD4$^+$ T cell and Treg cell numbers were reduced by 48% and 63%, respectively. Spleen and lymph node CD8$^+$ T cell numbers were affected less by chronic B cell depletion.

Chronic B cell depletion significantly reduced activated CD44^{hi}CD62L^{lo} CD4$^+$ and CD8$^+$ T cell frequencies by 40% and 48%, respectively (Fig. 3B). Activated CD4$^+$ and CD8$^+$ T cell numbers were also decreased by 70% and 44%, respectively, while total CD8$^+$ and naïve CD44^{lo}CD62L^{hi} CD4$^+$ T cell numbers did not change significantly with chronic B cell depletion. Consistent with these changes, mean IFN-γ-producing CD4$^+$ T cell frequencies were decreased by 50% in B cell-depleted mice, but mean TNF-α-producing CD4$^+$ T cell and IFN-γ- and TNF-α-producing CD8+ T cell frequencies were not changed significantly (Fig. 3C-D). Additionally, the numbers of IFN-γ- and TNF-α-producing CD4$^+$ T cells

were reduced by 70% and 40%, respectively, following B cell depletion, while the numbers of IFN-γ^+ and TNF-α^+ $CD8^+$ T cells were unaffected. Thus, as occurred with acute B cell depletion, chronic B cell depletion in older mice significantly reduced the proportion and number of activated $CD4^+$ and $CD8^+$ T cells, and only reduced cytokine-producing $CD4^+$ T cell numbers relative to their control mAb-treated littermates.

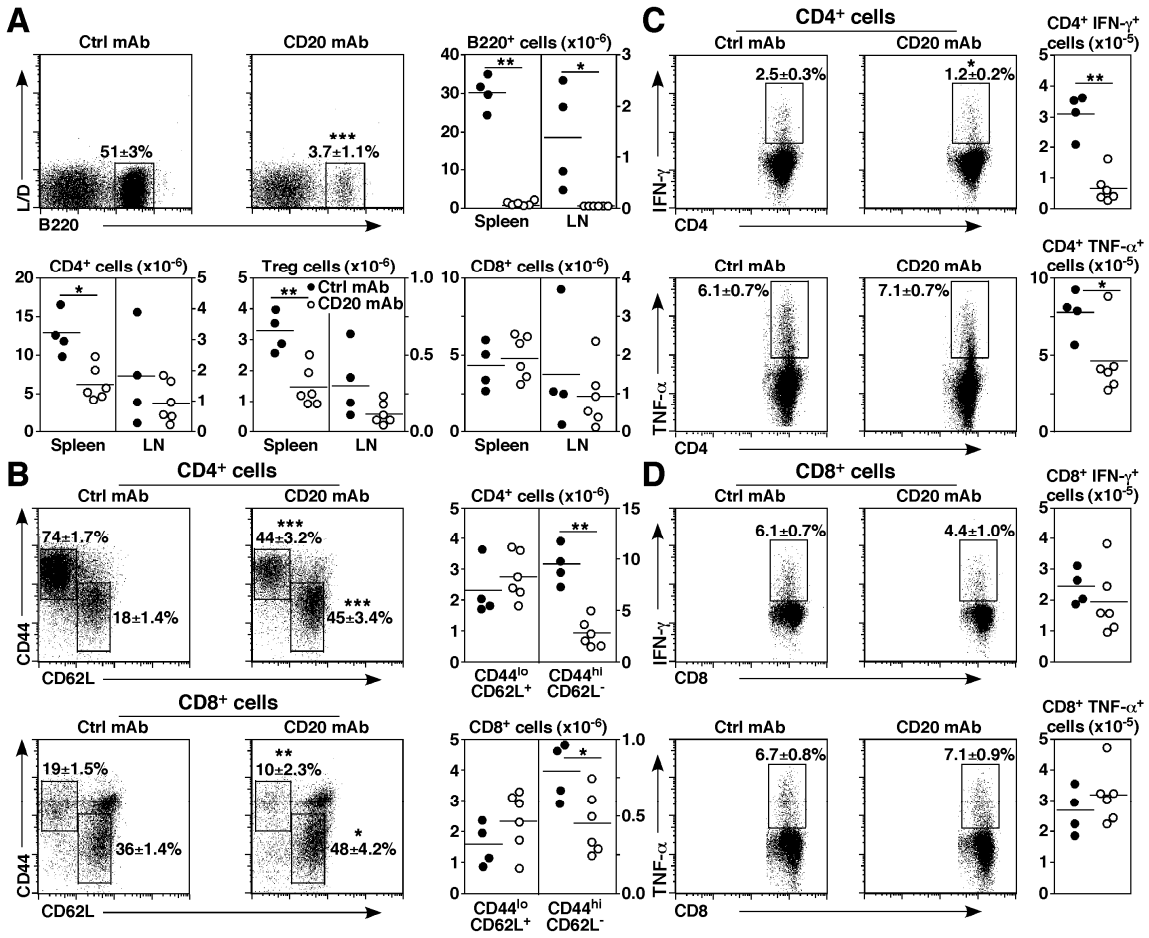

Figure 3. Chronic B cell depletion alters T cell homeostasis and cytokine production.

Figure 3. Chronic B cell depletion alters T cell homeostasis and cytokine production. Naïve 6-month-old mice (*n* = 4-6 mice per group) were treated with control (closed circles) or CD20 mAb (open circles) monthly for 6 months before spleen and lymph node (LN) lymphocyte isolation and analysis as in Fig. 1-2. (A) Chronic B cell depletion reduces $CD4^+$ T cell and Treg cell numbers. Representative $B220^+$ B cell depletion vs. LIVE/DEAD (L/D) cell staining, as well as B cell, $CD4^+$ and $CD8^+$ T cell, and Treg cell numbers are shown. (B) Chronic B cell depletion reduces $CD4^+$ and $CD8^+$ T cell activation. Representative panels show CD44 vs. CD62L staining (left panels) for $CD4^+$ and $CD8^+$ T cells and cell numbers (right panels). (C-D) Chronic B cell depletion impairs IFN-γ and TNF-α expression by $CD4^+$ and $CD8^+$ T cells. Representative panels show IFN-γ and TNF-α expression (left panels) and cell numbers (right panels) for (C) $CD4^+$ and (D) $CD8^+$ T cells. (A-D) Mean cell frequencies (± SEM) within the indicated dot plot gates are shown. Graphs show results from individual mice (*n* = 4-6 mice per group) with means indicated by horizontal bars. Significant differences between sample means are indicated: *, $P < 0.05$; **, $P < 0.01$; ***, $P < 0.001$.

3.2.4. B cell depletion impairs virus clearance in LCMV-infected mice

To understand whether reduced $CD4^+$ and $CD8^+$ T cell homeostasis in B cell-depleted mice affected cellular immune responses, 4-month-old mice were given CD20 or control mAb one week before infection with LCMV Armstrong. Spleen $CD4^+$ and $CD8^+$ T cell numbers were assessed one week after infection. In control mAb-treated mice, LCMV infection reduced mean $CD4^+$ T cell numbers by 33% relative to uninfected mice (Fig. 4A). Prior CD20 mAb treatment significantly reduced $CD4^+$ T cell numbers in virus-infected mice relative to infected control mAb-treated mice (23%). Treg cell numbers were comparably reduced during LCMV infection in B cell depleted mice (30%, Fig. 4B). In contrast to $CD4^+$ T cells, LCMV infection induced a ~3-fold expansion in $CD8^+$ T cell numbers following control mAb treatment relative to naïve mice. However, virus-induced $CD8^+$ T cell expansion was profoundly inhibited following B cell depletion (42% decrease, Fig. 4A). Thus, B cell depletion reduced total $CD8^+$ T cell numbers generated in response to acute virus infection.

The effect of reduced T cell numbers in B cell-depleted mice on *in vivo* viral clearance was assessed by quantifying relative LCMV RNA levels as described (*148*). Spleen viral RNA levels were 48-fold higher in B cell-depleted mice relative to control mAb-treated mice one week after infection (Fig. 4C).

Accordingly, the numbers of activated $CD44^{hi}CD62L^{-}$ $CD4^{+}$ T cells were reduced by 54-60% in the spleen and lymph nodes, while naïve $CD4^{+}$ T cell numbers were less affected by B cell depletion following viral infection (Fig. 4D). Similarly, $CD4^{+}$ effector ($Ly6C^{+}PSGL1^{+}$), pre-memory ($Ly6C^{-}PSGL1^{+}$), and T follicular helper ($Ly6C^{-}PSGL1^{-}$) cell numbers were reduced by 69%-84% in the spleen, with comparable reductions in the numbers of pre-memory (62%) and T follicular helper (68%) $CD4^{+}$ T cells within the lymph nodes of B cell-depleted mice infected with LCMV (Fig. 4E, (*154*). While naïve $CD8^{+}$ T cell numbers were normal following virus infection in B cell-depleted mice, the numbers of activated $CD44^{hi}CD62L^{-}$ spleen and lymph node $CD8^{+}$ T cells were reduced by 51-52%, (Fig. 4F). $CD8^{+}$ $KLRG1^{+}$ effector T cell numbers were also reduced by 64-74% in the spleen and lymph nodes of B cell-depleted mice that were infected with LCMV (Fig. 4G, (*155*)). Thus, B cells were needed for the optimal generation of $CD4^{+}$ and $CD8^{+}$ T cells with an activated phenotype and the expansion of effector cell subsets following infection.

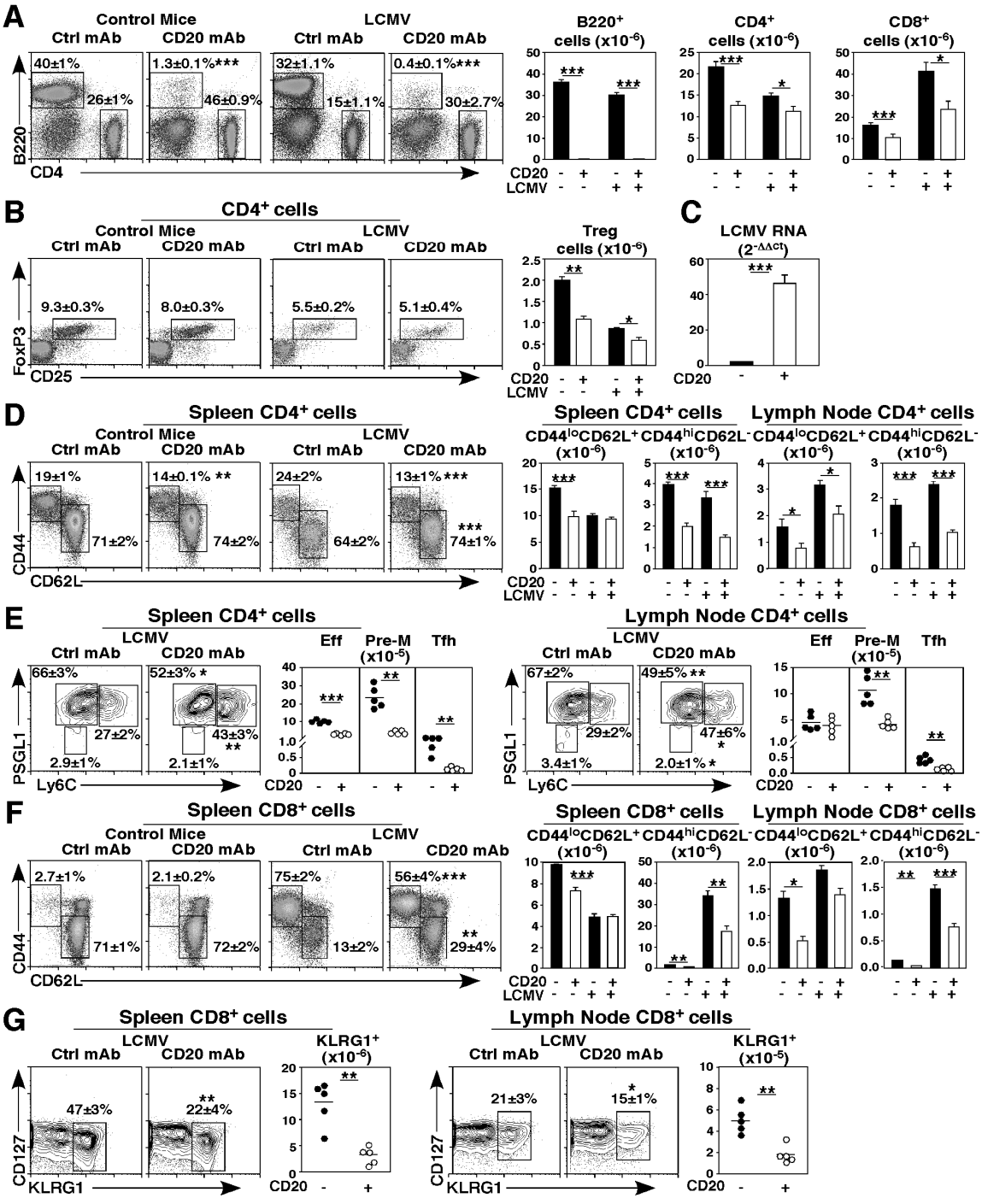

Figure 4. B cell depletion impairs T cell expansion, memory conversion, and virus clearance during LCMV infection.

Figure 4. B cell depletion impairs T cell expansion, memory conversion, and virus clearance during LCMV infection. Naïve 4- month-old mice were given control (closed bars) or CD20 mAb (open bars) 7 days prior to treatment with PBS or infection with LCMV. Splenocytes harvested 7 days later were assessed by immunofluorescence staining with flow cytometry analysis of viable, single lymphocytes. Representative panels show (A) B220 vs. CD4 staining (left panels) and B cell, $CD4^+$, and $CD8^+$ T cell numbers (right panels) and (B) CD25 vs. intracellular Foxp3 staining for $CD4^+$ T cells (left panels) and Treg cell numbers (right panels). (C) B cell depletion reduces LCMV viral clearance. Spleens from control and CD20 mAb-treated mice infected with LCMV were harvested 7 days post-infection, with viral RNA levels quantified by RT-PCR. Bar graph values represent mean (± SEM) relative LCMV RNA expression levels shown pooled from 3 independent experiments (n = 12 mice per group). (D-G) B cell depletion impairs LCMV-driven T cell activation and effector subset conversion. Representative panels show CD44 vs. CD62L staining (left panels) for spleen (D) $CD4^+$ and (F) $CD8^+$ T cells, with cell numbers for the spleen and lymph nodes shown (right panels). (E) Representative panels show PSGL1 vs. Ly6C staining (left panels) for spleen and lymph node $CD4^+$ cells, with activated $CD4^+$ T cell conversion to effector (Eff, $Ly6C^+PSGL1^+$), pre-memory (Pre-M, $Ly6C^-PSGL1^+$),

and T follicular helper (Tfh, Ly6C$^-$PSGL1$^-$) numbers shown (right panels). (G) Representative dot plots show CD127 vs. KLRG1 staining (left panels) for spleen and lymph node CD8$^+$ T cells, with KLRG1$^+$ effector cell numbers shown (right panels). (A, B, D, F) Graphs show mean (± SEM) numbers of the indicated cell types from mice treated with control or CD20 mAb pooled from 4-5 independent experiments (n = 21-26 mice per group). (E, G) Graphs show results from individual mice (n = 5 mice per group), with means indicated by horizontal bars. (A-G) Mean (± SEM) cell frequencies within the indicated dot plot gates are shown. Significant differences between sample means are indicated: *, $P < 0.05$; **, $P < 0.01$; ***, $P < 0.001$.

3.2.5. B cell depletion impairs T cell cytokine responses to LCMV infection

B cell-depletion significantly reduced the frequencies (47-50%) and the numbers (51-53%) of spleen IFN-γ- and TNF- α -expressing $CD4^+$ T cells in infected mice (Fig. 5A). While the relative frequencies of IFN-γ- and TNF- α -expressing $CD8^+$ T cells were not altered in B cell-depleted and infected mice, IFN-γ- and TNF- α -expressing $CD8^+$ T cell numbers were reduced by 35% and 44%, respectively (Fig. 5B). Thus, B cell depletion impaired $CD4^+$ T cell cytokine production during immune responses to LCMV, but did not reduce the relative frequencies of $CD8^+$ T cells producing cytokines despite their overall reduced numbers in B cell-depleted mice.

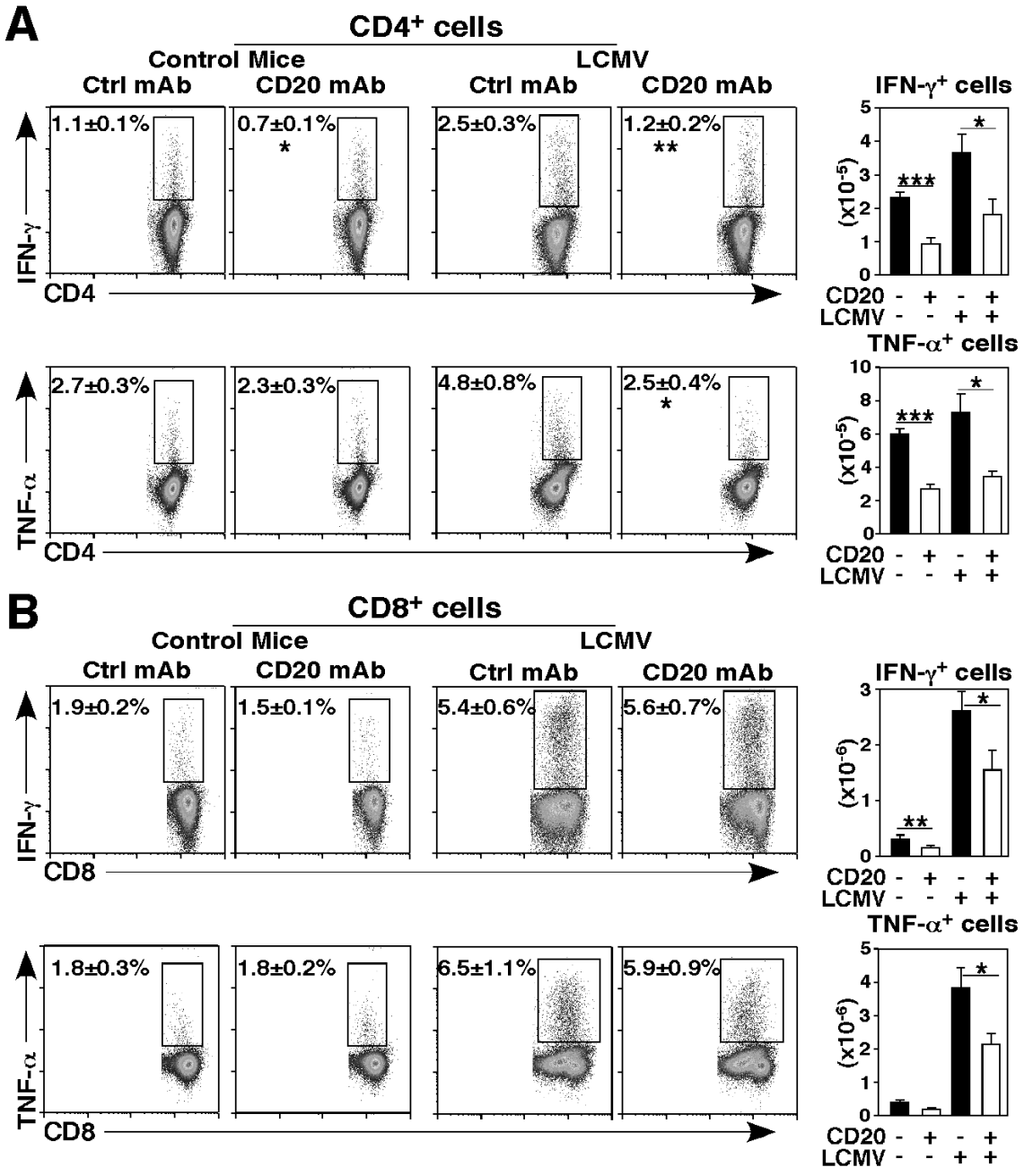

Figure 5. B cell depletion impairs T cell cytokine production during LCMV infection.

Figure 5. B cell depletion impairs T cell cytokine production during LCMV infection. Naïve 4-month-old mice (were given control (closed bars) or CD20 mAb (open bars) 7 days before infection with LCMV or treatment with PBS as in Fig. 4. Seven days post-infection, spleen lymphocytes were harvested, depleted of B cells with CD19 magnetic beads, and stimulated using plate-bound CD3 and CD28 mAbs as in Fig. 2. Intracellular cytokine production was assessed by immunofluorescence staining with flow cytometry analysis and is shown pooled from 4-5 independent experiments (n = 21-26 mice per group). Flow cytometry dot plots show representative (A) $CD4^+$ or (B) $CD8^+$ T cell cytokine staining (left panels), with mean (± SEM) cell frequencies shown for the indicated gates. Bar graphs represent mean (± SEM) numbers of the indicated cell types (right panels). Significant differences between sample means are indicated: *, $P < 0.05$; **, $P < 0.01$; ***, $P < 0.001$.

3.2.6. B cell depletion impairs antigen-specific T cell responses

Consistent with reduced T cell numbers in B cell-depleted mice after LCMV infection, CD20 mAb treatment reduced mean spleen LCMV peptide-specific $CD4^+$ ($GP66^+$) and $CD8^+$ ($GP33^+$) T cell numbers by 67% (Fig. 6A). B cell-depletion significantly reduced the numbers of activated GP66-specific $CD44^{hi}CD62L^-$ $CD4^+$ T cells (87-91%) and the numbers of effector (58-71%), pre-memory (90-94%), and T follicular helper (84-91%) $CD4^+$ T cell subsets in the spleen and lymph nodes following LCMV infection (Fig. 6B). Virus-specific $CD4^+$ and $CD8^+$ T cell cytokine production was therefore assessed using B cell-depleted splenocytes from LCMV-infected mice that were restimulated with LCMV peptides *in vitro* for 5 hours. B cell depletion reduced both virus-specific IFN-γ^+ and TNF-α^+ $CD4^+$ T cell frequencies (56-62%) and numbers (72-75%) in infected mice (Fig. 6C). By contrast, the frequencies of GP33-specific IFN-γ^+ and TNF-α^+ $CD8^+$ T cells were not changed, but mean numbers of GP33-specific $CD8^+$ T cells expressing IFN-γ^+ and TNF-α^+ were reduced (52-63%) in B cell-depleted LCMV-infected mice (Fig. 6D). Thus, B cell depletion reduced the numbers of antigen-specific $CD4^+$ and $CD8^+$ T cells responding to viral infection.

Impaired LCMV clearance following B cell depletion may occur as a direct consequence of reduced T cell numbers or may result from reduced $CD8^+$ T cell

function. To address this, naïve TCR transgenic $CD8^+$ T cells that recognize the dominant LCMV epitope GP33-41 (*154*) were adoptively transferred into control or B-cell depleted mice prior to infection. B cells were not required for antigen-driven $CD8^+$ T cell expansion, activation, or cytokine production in the spleen (Fig. 6E). However, effector $KLRG1^+$ $CD8^+$ T cell generation was reduced by 50% in the absence of B cells. In lymph nodes, B cell depletion significantly inhibited $GP33^+$ $CD8^+$ T cell expansion (63%), activation (67%), and $KLRG1^+$ effector cell development (68%). Thus, B cell depletion impaired the induction of antigen-specific $CD4^+$ and $CD8^+$ T cells following viral infection predominantly by reducing total antigen-specific T cell numbers, although $KLRG1^+$ effector cell generation was impaired.

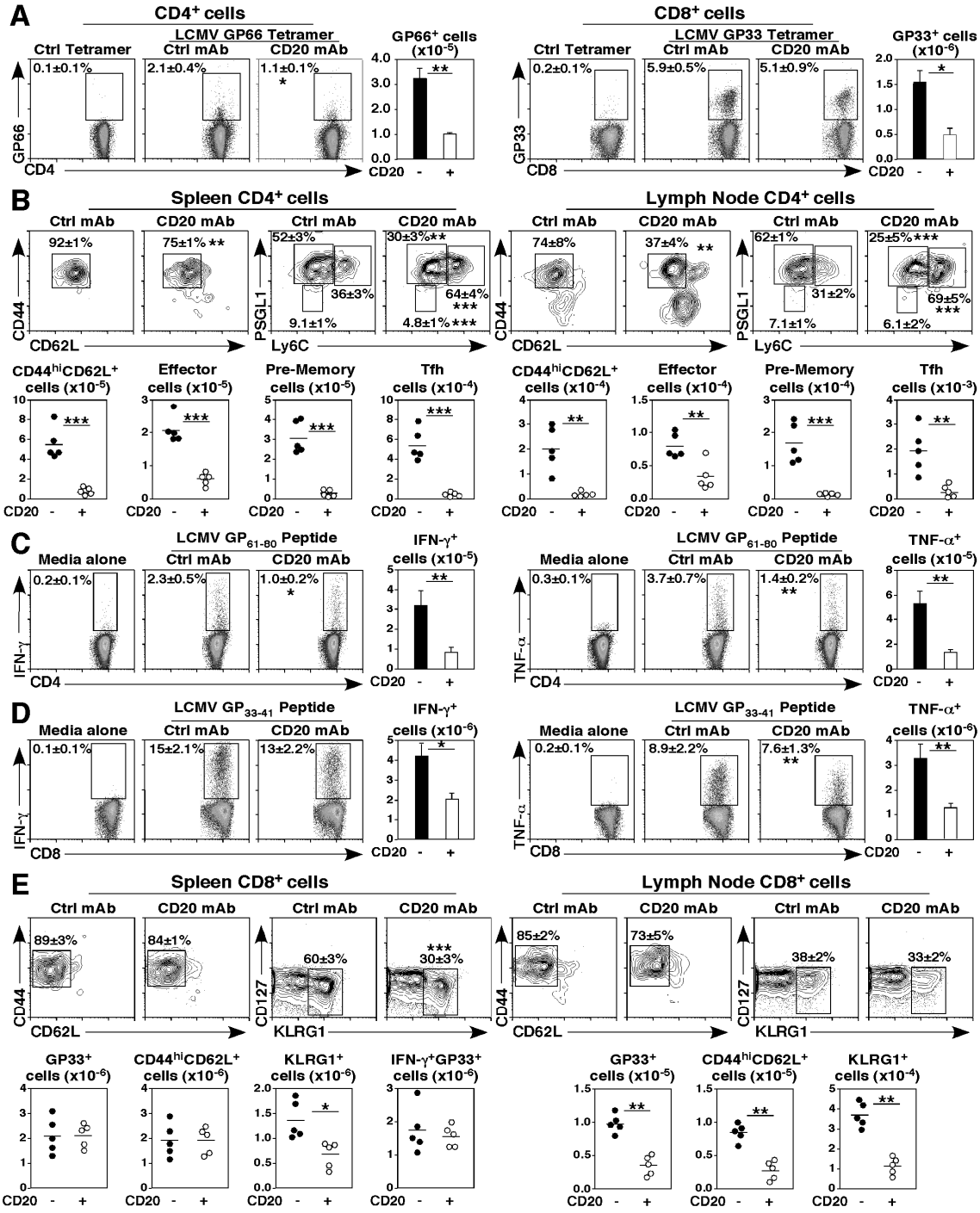

Figure 6. B cell depletion impairs antigen-specific T cell function.

Figure 6. B cell depletion impairs antigen-specific T cell function. (A-D) B cell depletion impairs virus peptide-specific $CD4^+$ and $CD8^+$ T cell function. Naïve 4-month-old mice were given control (closed bars) or CD20 mAb (open bars) 7 days before infection with LCMV or treatment with PBS as in Fig. 4-5. Spleen and lymph node lymphocytes were harvested 7 days post-infection. (A) B cell depletion reduces LCMV GP66 tetramer$^+$ $CD4^+$ T cell and GP33 tetramer$^+$ $CD8^+$ T cell numbers. Representative panels LCMV-specific tetramer staining (left panels) and cell numbers (right panels). (B) Representative panels show CD44 vs. CD62L and PSGL1 vs. Ly6C staining (top panels) for LCMV-specific $GP66^+$ $CD4^+$ T cells from the spleen and lymph nodes, with activated ($CD44^{hi}CD62L^{lo}$), effector ($Ly6C^+PSGL1^+$), pre-memory ($Ly6C^-PSGL1^+$), and T follicular helper (Tfh, $Ly6C^-PSGL1^-$) $GP66^+$ $CD4^+$ T cell numbers shown (bottom panels). (C-D) B cell depletion reduces the frequencies and numbers of cytokine expressing LCMV-specific $CD4^+$ (C) and $CD8^+$ (D) T cells. Following B cell depletion using CD19 magnetic beads, T cells were stimulated with LCMV Armstrong GP_{61-80} or GP_{33-41} viral peptides for 5 hours, with intracellular IFN-γ or TNF-α expression quantified by immunofluorescence staining. Flow cytometry dot plots show representative CD4 or CD8 expression vs. cytokine staining. (E) B cell depletion impairs virus-specific $CD8^+$ T cell effector development. Naïve 4-month-old mice

were given control (closed bars) or CD20 mAb (open bars) 6 days before the adoptive transfer of naïve TCR transgenic $CD8^+$ T cells that recognize GP_{33-41}. Mice were infected with LCMV 1 day later and evaluated 7 days after infection as in Fig. 4-5. Representative panels show CD44 vs. CD62L and CD127 vs. KLRG1 staining (top panels) for transferred LCMV-specific $GP33^+$ $CD8^+$ T cells from the spleen and lymph nodes, with numbers for total ($GP33^+$), activated ($CD44^{hi}CD62L^+$), effector ($KLRG1^+$), and IFN-γ^+ cells shown (bottom panels). (A, C, D) Graphs show mean (± SEM) numbers of the indicated cell types from mice treated with control or CD20 mAb pooled from 4-5 independent experiments (n = 21-26 mice per group). (B, E) Graphs show results from individual mice (n = 5 mice per group), with means indicated by horizontal bars. (A-E) Mean (± SEM) cell frequencies within the indicated dot plot gates are shown. Significant differences between sample means are indicated: *, $P < 0.05$; **, $P < 0.01$, ***, $P < 0.001$.

3.3. Conclusions

These collective studies demonstrate that B cells are necessary for T cell homeostasis and optimal anti-viral responses during acute LCMV infection. Acute depletion of mature B cells depletion in 2- and 4-month-old adult mice significantly reduced $CD4^+$, $CD8^+$, and Treg cell numbers in the spleen and lymph nodes (Fig. 1B-D). These reductions were likely a result of perturbed T cell homeostasis after B cell depletion, as no changes were observed in T cell migration (Fig. 1E-F). Activated $CD4^+$ and $CD8^+$ T cell numbers in adult mice were more significantly affected by B cell depletion than naïve $CD4^+$ and $CD8^+$ T cell numbers (Fig. 2A-B). The observed T cell reduction in B cell-depleted mice resulted in reductions the numbers of effector $CD4^+$ and $CD8^+$ T cells producing IFN-γ and TNF-α (Fig. 2C-D). Total, activated, and cytokine-producing $CD4^+$ T cells were more dramatically affected by chronic B cell depletion in aged mice than $CD8^+$ T cells, though activated $CD8^+$ T cells were also significantly reduced (Fig. 3). Importantly, B cell depletion during acute LCMV infection impaired $CD4^+$ and $CD8^+$ T cell expansion and the generation of activated and effector T cells and $CD4^+$ cytokine-producing cells (Figs. 4-5). LCMV-specific $CD4^+$ and $CD8^+$ T cell numbers and effector cell expansion and $CD4^+$ T cell activation and cytokine production were profoundly reduced in B cell-depleted mice (Fig. 6)

with concomitant elevated LCMV titers in the spleen (Fig. 4C). Thus, B cells are critical for $CD4^+$ and $CD8^+$ T cell homeostasis and optimal effector responses during viral infection.

4. Lymphoma-intrinsic mechanisms that drive resistance to CD20 Immunotherapy

The following text was modestly adapted from its original manuscript, "Galectin-1 Expression Confers Lymphoma Resistance to CD20 Immunotherapy," which is currently in submission.

4.1. Introduction

Non-Hodgkin lymphoma (NHL) is the most commonly diagnosed hematologic cancer of adults in the United States, with close to 70,000 people diagnosed in 2013 alone (*49*). NHL encompasses a wide variety of heterogeneous malignancies, of which 80-90% derive from B lymphocytes that express cell surface CD20 (*50*). The CD20 mAb Rituximab was the first biologic approved for treatment of indolent NHL (*72*). CD20 mAbs are now used to treat a variety of human cancers, but there is wide variation in therapeutic efficacy between individual patients and among different tumor types (*84*). Similarly, the initial effectiveness of Rituximab varies widely amongst patients with the same tumors and typically wanes over time, despite sustained CD20 expression by malignant cells among the vast majority of relapsing patients (*83, 84*). Though Rituximab is widely used, the molecular mechanisms by which human NHLs gain resistance to CD20 mAb immunotherapy are unknown (*85*). A limited number of patient

studies have searched for the molecular basis of tumor resistance to CD20 immunotherapy (*85, 98-100, 156*). However, heterogeneity between tumors, the predominant use of CD20 mAb in combination with other drugs, the inherent difficulty in quantifying therapeutic efficacy, and variable disease staging among patients in combination with their intrinsic genetic diversity makes these studies a daunting task. Because most NHL patients eventually succumb to their disease despite CD20 immunotherapy, understanding the molecular basis for tumor resistance to therapy could lead to alternative and more effective treatment strategies.

Therefore, the following study examined the molecular mechanisms responsible for lymphoma resistance to CD20 immunotherapy in a homologous mouse preclinical model of lymphoma. In this model, CD20 mAb therapeutic efficacy can be measured precisely under conditions where the host genetic background and timing of tumor initiation are identical. Primary malignant cells of spontaneous lymphomas isolated from *Eμ-cMyc* transgenic mice were transferred into wild-type inbred mice that were then treated with mouse anti-mouse CD20 mAb as a monotherapy (*71, 108*). This model allowed for the unbiased identification of lymphoma genetic changes that conferred either sensitivity or resistance to CD20 immunotherapy initially and over time through

the serial propagation of lymphomas, mimicking the genetic changes that occur during disease progression.

4.2. Results

4.2.1. Primary B cell lymphomas express varying levels of surface CD20

Spontaneous B cell lymphomas were obtained from *Eμ-cMyc* transgenic mice, which typically develop aggressive monoclonal Burkitt's-like B cell lymphomas by six months of age (*157, 158*). Twenty-two primary B cell lymphomas were isolated, with cell surface CD20 expression visualized by immunofluorescence staining (*71*). CD20 expression varied between individual lymphomas, but all maintained measurable CD20 *ex vivo* (Fig. 7A) and generally shared a $CD19^{+}IgM^{+}IgD^{+}B220^{+}CD5^{lo}CD21/35^{+}CD23^{lo}CD24^{+}$ cell surface phenotype (Fig. 7B).

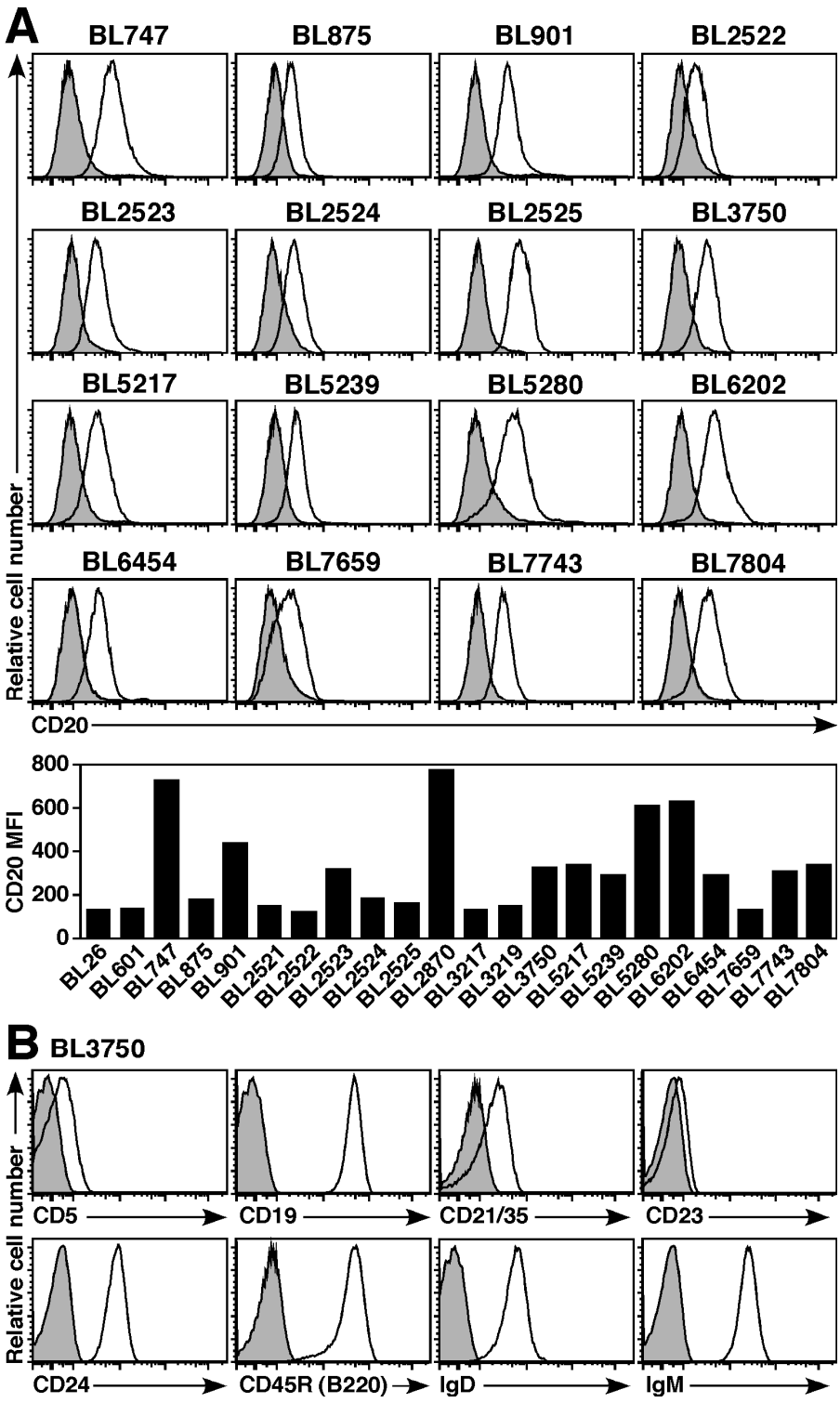

Figure 7. CD20 expression by mouse B cell lymphomas.

Figure 7. CD20 expression by mouse B cell lymphomas. (A) Representative CD20 expression by primary B cell lymphomas isolated from Eμ-cMyc transgenic mice. Cell surface CD20 (open histograms) and isotype-matched control (shaded histograms) immunofluorescence staining were quantified by flow cytometry after brief periods of culture for 24-48 hours. The bar graph shows CD20 mean linear fluorescence staining intensities (MFI) with isotype-matched control values subtracted. (B) Representative cell surface phenotype of the BL3750 lymphoma. Histograms show cell surface molecule staining (open histograms) versus isotype-matched control mAb staining (shaded histograms).

4.2.2. Lymphoma response to CD20 immunotherapy does not correlate with CD20 expression levels

The sensitivity of each lymphoma to CD20 immunotherapy was measured *in vivo* after tumor cells were adoptively transferred into recipient syngeneic wild-type mice (*108*). Mice given lymphoma cells were treated one day later with either CD20 or control mAb. All mice that developed lymphomas succumbed to disease by day 60, while all other mice had normal lifespans without obvious symptoms or disease and were considered lymphoma-free. Therefore, only 60-day survival curves are shown (Fig. 8A). CD20 mAb sensitivity was measured as the increase in the area under the survival curves for CD20 versus control mAb-treated mice, and ranged between 0% to ~65% among primary lymphomas (Fig. 8B). The BL26, BL2525, BL3217, BL3750, BL5217, BL6454, and BL7659 primary lymphomas were sensitive to CD20 immunotherapy, though most primary lymphomas (68%, n = 15 of 22) were CD20 mAb-resistant under these conditions. Notably, the level of CD20 expression by primary lymphomas showed no correlation with their sensitivity to CD20 immunotherapy (ϱ = -0.12; Fig. 8C).

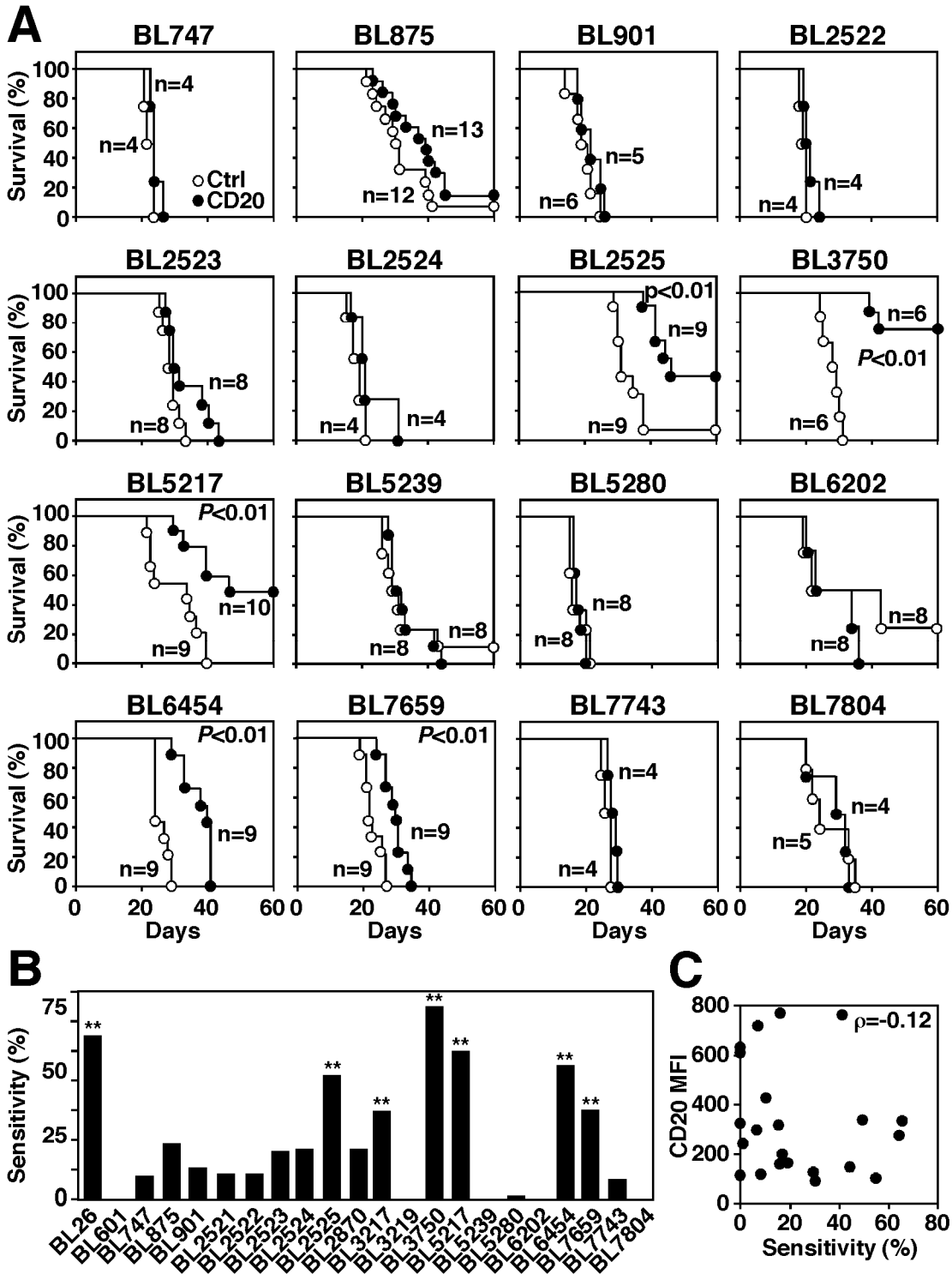

Figure 8. Lymphoma *in vivo* sensitivity to CD20 mAb.

Figure 8. Lymphoma *in vivo* sensitivity to CD20 mAb. Mice given 1 x 10^5 primary lymphoma cells were treated with either CD20 (closed circles) or control (open circles) mAb one day later. (A) Kaplan-Meier survival plots of mice given the indicated tumor cells and CD20 or control mAb. Pooled results represent 1-3 independent experiments (n = 4-13 total mice per group) with significant cumulative survival differences between groups treated with CD20 versus control mAb indicated. (B) Primary lymphoma sensitivity to CD20 immunotherapy. Significant differences between sample means are indicated: **, $P < 0.01$. (C) CD20 expression (Fig. 7A) and lymphoma sensitivity to CD20 immunotherapy (Fig. 7B) are not correlated.

4.2.3. CD20 immunotherapy does not select for treatment-resistant lymphomas

Following primary BL3750 lymphoma cell transfer and treatment with control or CD20 mAb (Fig. 8), fourteen lymphomas that developed in recipient syngeneic mice were collected and evaluated for CD20 expression and subsequent responsiveness to CD20 immunotherapy (Fig. 9A). Secondary BL3750 lymphomas had varying levels of CD20 expression, which did not correspond with their prior exposure to CD20 or control mAb *in vivo* (Fig. 9B). Most secondary lymphomas (64%, $n = 9$ of 14) were sensitive to CD20 immunotherapy, but prior exposure to CD20 or control mAb *in vivo* had no influence on their subsequent sensitivity to mAb treatment (Fig. 9C-D). Similarly, the levels of CD20 expression of secondary lymphomas showed no correlation with CD20 mAb sensitivity ($\rho = -0.03$; Fig. 9E). Thus, neither CD20 cell surface density nor *in vivo* selection during prior CD20 mAb therapy correlated with the outcome of secondary lymphoma treatment.

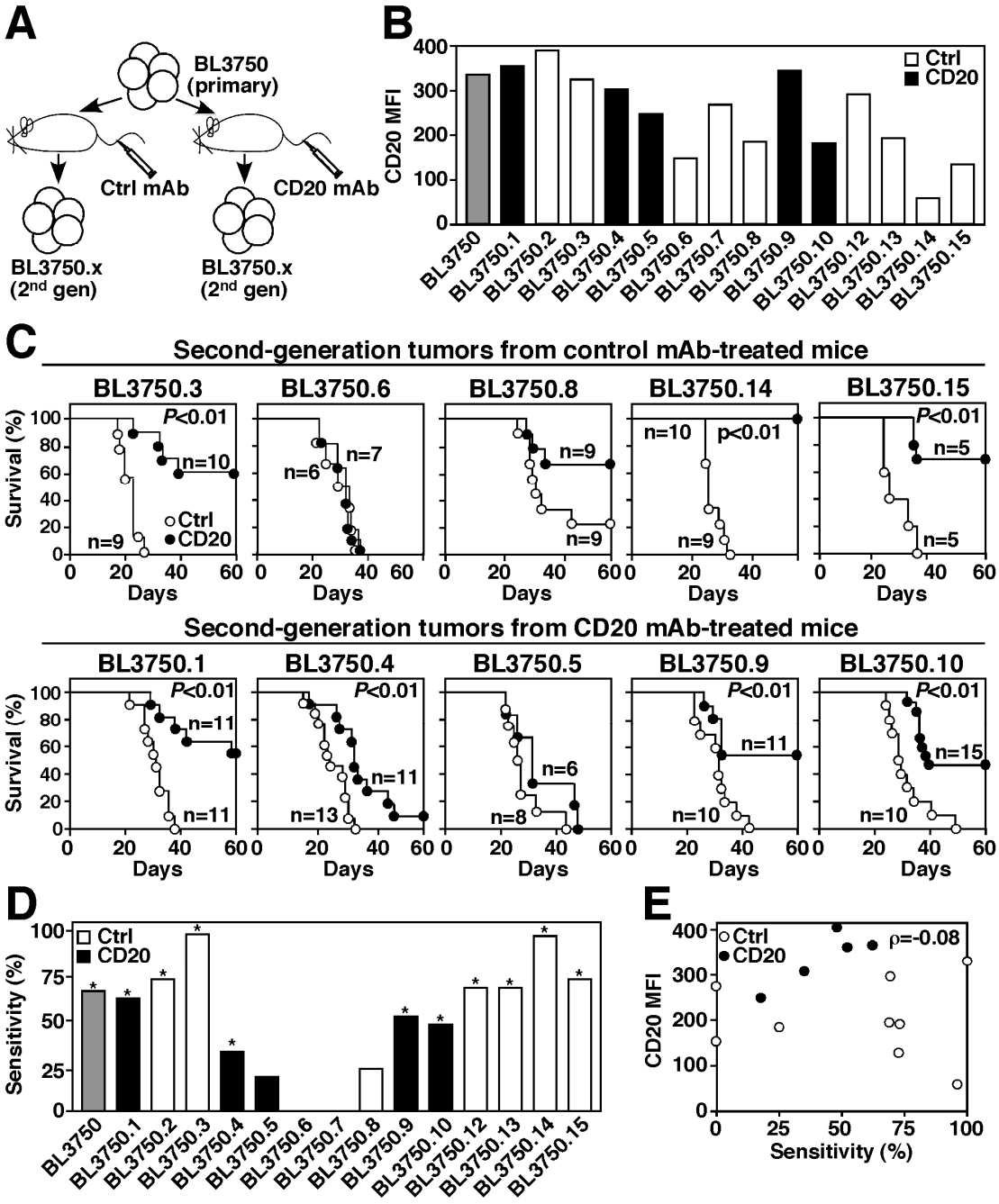

Figure 9. Second-generation lymphoma sensitivity to CD20 mAb.

Figure 9. Second-generation lymphoma sensitivity to CD20 mAb. (A) Method for isolating second-generation BL3750 lymphomas from mice given primary cells described in Fig. 7. (B) CD20 expression by second-generation lymphomas with control mAb values subtracted. The gray bar indicates primary BL3750 cells; black bars are second-generation lymphomas from CD20 mAb-treated mice; white bars are second-generation lymphomas from control mAb-treated mice. (C) Second-generation lymphoma resistance to CD20 mAb is not driven by CD20 mAb selection *in vivo*. Mice were given second-generation lymphoma cells isolated from mice previously treated with either control (top panels) or CD20 (bottom panels) mAbs as indicated. One day later, littermates were given either CD20 (closed circles) or control (open circles) mAb. Survival plots represent pooled results for 1-3 independent experiments (n = 5-15 mice per group) with significant differences between groups indicated. (D) Secondary lymphoma sensitivity to CD20 mAb as in Fig. 8, with prior control or CD20 mAb exposure indicated. Significant differences between sample means are indicated: **, $P < 0.01$. (E) Second-generation lymphoma survival does not correlate with CD20 expression. Scatter plot comparing the percent sensitivity of secondary lymphoma cells to immunotherapy versus CD20 MFI.

4.2.4. Lymphoma duration *in vivo* does not select for treatment-resistance

The effects of repeated *in vivo* passage and CD20 immunotherapy on lymphoma sensitivity to therapy was also evaluated serially over three to seven generations within lymphoma families derived from single primary lymphomas (Fig. 10A). In some instances, primary lymphomas that were initially sensitive to CD20 immunotherapy, such as BL3750 and BL6454, acquired resistance to CD20 immunotherapy during subsequent generations (Fig. 10B). By contrast, other lymphomas from the same BL3750 family remained sensitive to CD20 immunotherapy over six generations (Fig. 10B-C). However, lymphomas that were initially resistant, such as BL5239, or lymphomas that became resistant to CD20 immunotherapy during repeated *in vivo* passages never reverted to a CD20 mAb-sensitive phenotype. Importantly, changes in CD20 expression levels had no correlation with the development of resistance to CD20 immunotherapy (Fig. 10C). Thus, resistance to CD20 immunotherapy appears to reflect lymphoma-intrinsic phenotypic changes that do not correlate with altered CD20 expression during *in vivo* progression.

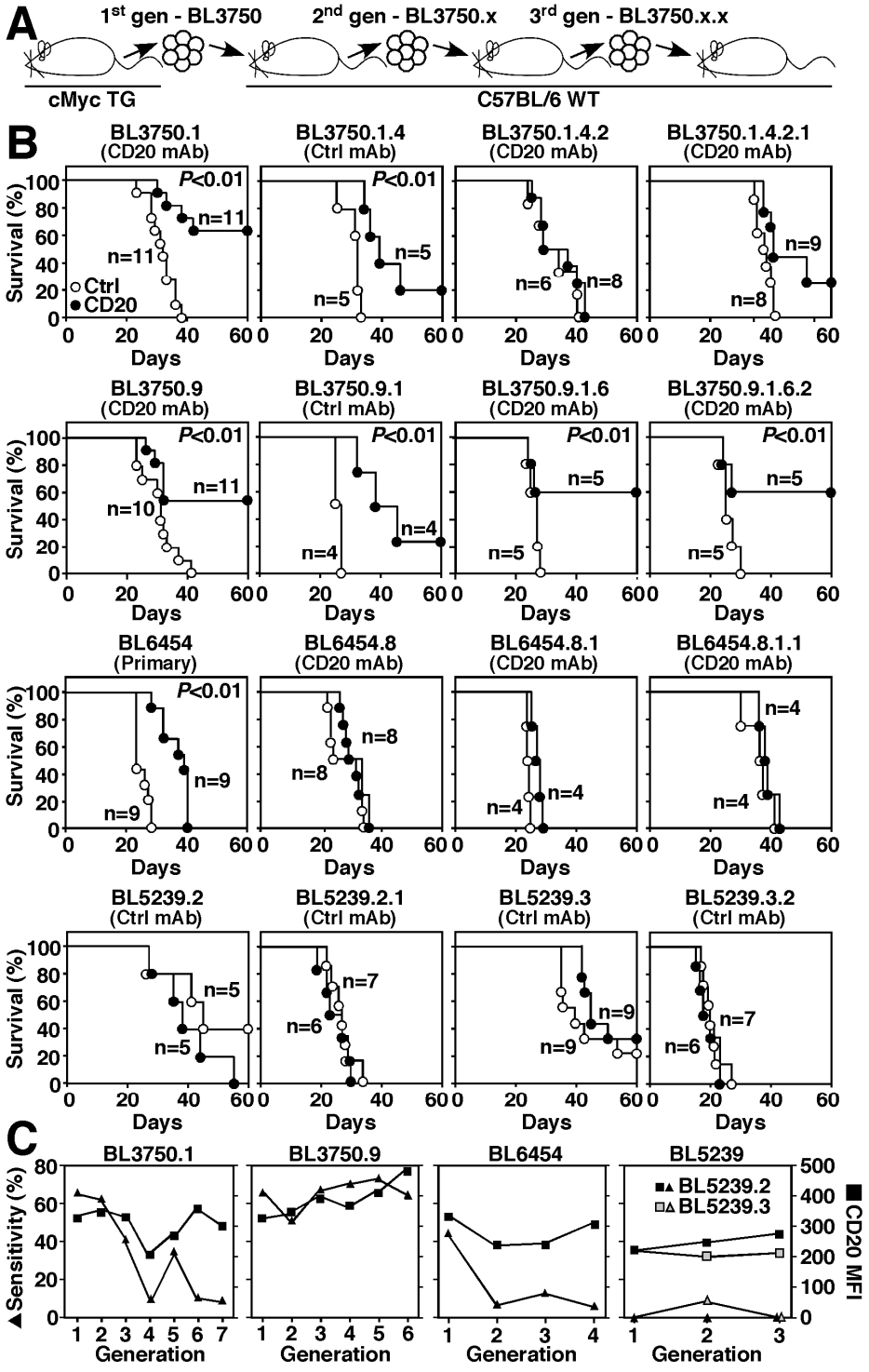

Figure 10. CD20 immunotherapy does not select for treatment-resistant lymphomas.

Figure 10. CD20 immunotherapy does not select for treatment-resistant lymphomas. (A) Method for isolating and naming representative BL3750 lymphoma family members. Primary lymphoma cells were transferred into mice that were then given either CD20 (closed circles) or control (open circles) mAb as in Figs. 7 and 8. Second-generation lymphomas were subsequently collected and adoptively transferred as in Fig. 9. This process was repeated for subsequent generations. (B) Representative changes in BL3750, BL6454, and BL5239 lymphoma family member sensitivities to CD20 immunotherapy during progressive *in vivo* passages. Whether the transferred tumors were primary lymphomas or were isolated from mice treated with either control or CD20 mAb is indicated. Survival plots represent pooled results for 1-3 independent experiments (n = 4-11 total mice per group). Significant cumulative survival differences between groups are indicated. (C) CD20 immunotherapy during progressive *in vivo* passages does not select for CD20-deficient lymphomas. Line graphs compare the sensitivity of representative lymphoma cells to CD20 immunotherapy (closed triangles) versus their CD20 expression levels (closed squares) over 3-7 generations for the lymphoma families shown in (B).

4.2.5. Lymphoma resistance to CD20 immunotherapy is not due to CD20 expression, prior mAb exposure, nor duration *in vivo*

The correlation of lymphoma sensitivity to CD20 immunotherapy with *in vivo* progression was evaluated further using a cohort of twenty-two primary lymphomas and their subsequent generations following *in vivo* passage, which included 167 lymphomas comprising multiple families (Fig. 11). Where tested, members of this lymphoma cohort were mostly resistant to CD20 immunotherapy (red text). CD20-negative lymphomas were never identified, and CD20 mAb resistance had no relation to differences in CD20 expression levels. Lymphomas that were either initially resistant or developed resistance to CD20 immunotherapy maintained treatment resistance through repeated *in vivo* passage. By contrast, some tumors that were initially sensitive to CD20 immunotherapy maintained sensitivity over time (blue text) regardless of prior CD20 (bold text) or control mAb exposure *in vivo* (plain text). Because lymphoma sensitivity to CD20 immunotherapy did not correlate with CD20 expression levels, this extensive lymphoma family tree was used for the unbiased identification of genetic alterations that contribute to CD20 mAb resistance during *in vivo* lymphoma progression.

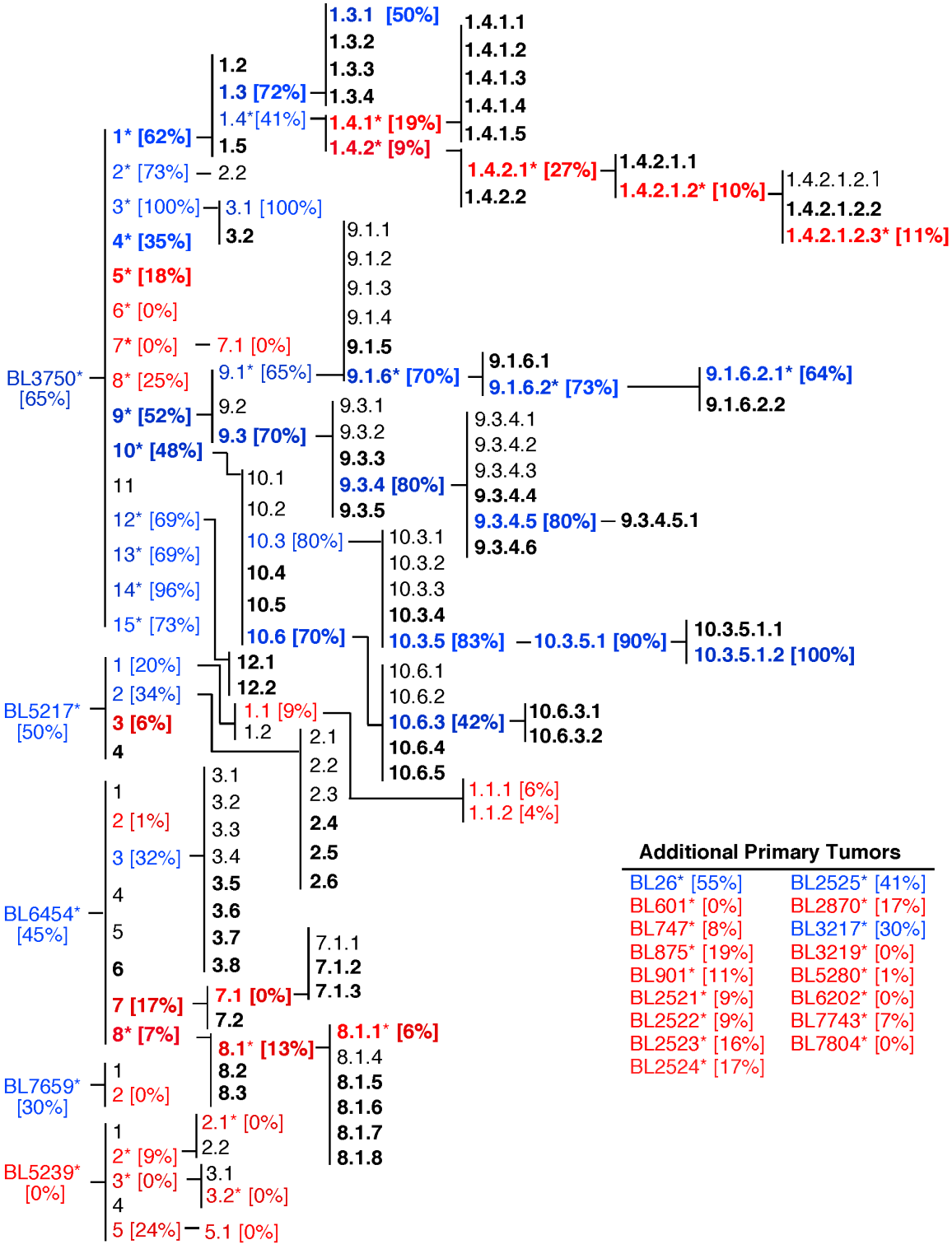

Figure 11. Cumulative family tree for spontaneous primary lymphomas.

Figure 11. Cumulative family tree for spontaneous primary lymphomas. Lymphoma families were evaluated over multiple generations for their sensitivity to CD20 mAb as in Fig. 10. Lymphomas isolated from either CD20 mAb-treated mice (bold text) or control mAb-treated mice (plain text) were either resistant (red) or sensitive (blue) to CD20 immunotherapy. Bracketed numbers indicate lymphoma sensitivity to CD20 immunotherapy. A total of 167 lymphomas have been isolated, including: primary (n = 22); secondary (n = 34); tertiary (n = 45); quaternary (n = 38); quinary (n = 18); senary (n = 7); and septenary (n = 3) generations within families. Asterisks indicate specific lymphomas analyzed as in Figs. 7-12 (n = 53).

4.2.6. Lymphoma galectin-1 expression confers resistance to CD20 mAb therapy

To identify genetic changes associated with CD20 immunotherapy resistance, transcript expression of twenty known immunosuppressive tumor-associated molecules (*48*), including the inhibitory cytokine IL-10 (*17, 159*), was evaluated in ten primary, seven BL3750 secondary, and six late-generation BL3750 family lymphomas (Fig. 11). Of these genes, only galectin-1 (*Lgals1*) expression correlated with lymphoma sensitivity to CD20 immunotherapy (Fig. 12A). In a larger quantitative screen using fifty-three lymphomas (twenty-two primary, seventeen BL3750 secondary, and fourteen late-generation lymphomas), *Lgals1* transcript levels and Gal-1 protein secretion were significantly and inversely correlated with lymphoma sensitivity to CD20 immunotherapy (Fig. 12B-C). Therefore, the contribution of Gal-1 expression to CD20 mAb resistance was examined in mechanistic studies.

Normal and malignant B cells are depleted in mice following MB20-11 treatment by macrophages through FcγR- and Ab-dependent cellular cytotoxicity/phagocytosis mechanisms, which occur independent of complement and cellular immunity (*104, 106, 108*). To evaluate the impact of lymphoma-derived galectin-1 on CD20 mAb-dependent lymphoma clearance *in vivo*,

parental BL3750 lymphoma cells were transfected with either Gal-1 GFP ($BL3750^{Gal1}$) or control GFP ($BL3750^{Ctrl}$) expression plasmids. Genetically stable $BL3750^{Gal1}$ and $BL3750^{Ctrl}$ cells expressing comparable levels of GFP and cell surface CD20 were isolated (Fig. 12D). $BL3750^{Gal1}$ cells secreted 35-fold higher levels of Gal-1 relative to $BL3750^{Ctrl}$ or untransfected BL3750 cells (Fig. 12E), and all cells had equivalent growth rates during *in vitro* cultures. During short-term *in vitro* phagocytosis assays, macrophages readily phagocytosed CD20 mAb-coated $BL3750^{Ctrl}$ tumors, while Gal-1 expression completely inhibited CD20 mAb-dependent phagocytosis (Fig. 12F). Gal-1 expression also abrogated CD19 mAb-dependent phagocytosis, indicating that Gal-1 broadly impairs macrophage-mediated mAb-dependent tumor phagocytosis.

$BL3750^{Ctrl}$ cells remained sensitive to CD20 immunotherapy *in vivo*, while induced Gal-1 expression significantly reduced lymphoma sensitivity to CD20 mAb (Fig. 12G). $BL3750^{Gal1}$ and $BL3750^{Ctrl}$ lymphomas expanded similarly in control mAb-treated littermates, with equivalent median survival rates of 36.5 and 37 days, respectively, while 50% of mice given $BL3750^{Ctrl}$ cells and CD20 mAb survived 60 days (Fig. 12G). $BL3750^{Gal1}$ tumors grew significantly larger in CD20 mAb treated mice than $BL3750^{Ctrl}$ cells, though high serum Gal-1 was observed in littermates bearing either $BL3750^{Ctrl}$ or $BL3750^{Gal1}$ lymphomas. Thus,

Gal-1 expression within the tumor microenvironment by lymphoma cells conferred resistance to CD20 immunotherapy.

4.2.7. Human lymphomas express elevated levels of *LGALS1*

LGALS1 transcript expression patterns among human B cell leukemias and lymphomas was quantified using established databases (*160*). Different B cell subsets purified from non-reactive tonsils expressed relatively low levels of *LGALS1* (Fig. 12I), whereas biopsies or blood samples from patients with either BL, CLL, DLBCL, HCL, or MCL had on average 4.5-fold increased levels of *LGALS1* expression. Biopsies from patients with BL, DLBCL, and HCL expressed the highest levels of *LGALS1* (range 5.7-7.3-fold), while other tumor subtypes expressed modestly elevated *LGALS1* transcripts. Elevated leukemia and lymphoma expression of Gal-1 may therefore inhibit CD20 immunotherapy in humans.

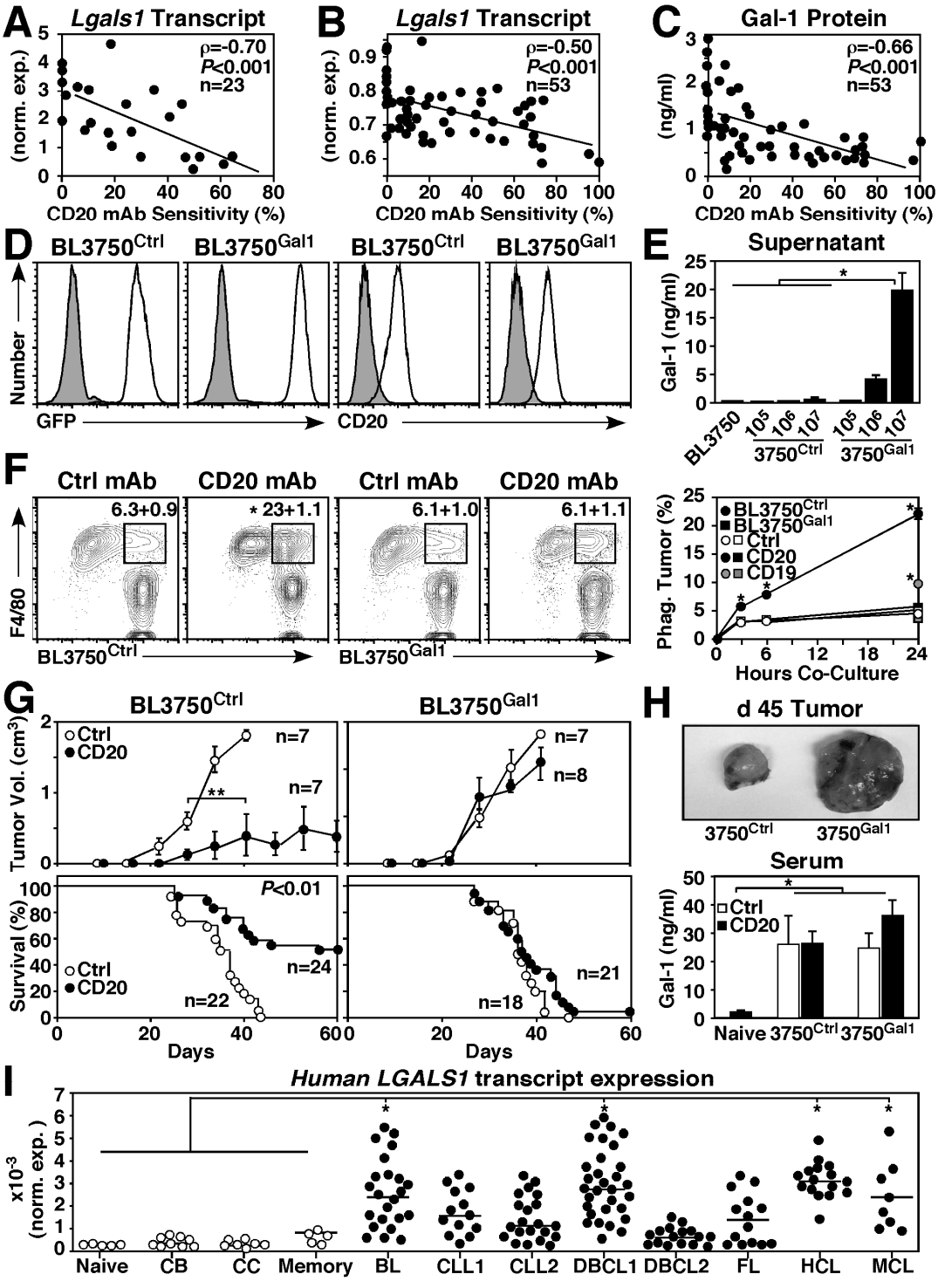

Figure 12. Lymphoma Gal-1 expression confers CD20 mAb resistance.

Figure 12. Lymphoma Gal-1 expression confers CD20 mAb resistance. (A-C) Gal-1 expression inversely correlates with lymphoma sensitivity to CD20 immunotherapy. Scatter plots compare lymphoma (A) normalized and (B) quantitative *Lgals1* transcript expression and (C) Gal-1 secretion relative to CD20 mAb sensitivity. (D) Representative GFP expression and cell surface CD20 expression by BL3750^{Ctrl} or BL3750^{Gal1} cells (open histograms) versus BL3750 cells (left panels, shaded histograms) or isotype-matched control mAb staining (right panels, shaded histograms). (E) Values represent mean (± SEM) Gal-1 secretion by BL3750, BL3750^{Ctrl}, and BL3750^{Gal1} cells (5 experiments). (F) Gal-1 blocks CD20 mAb-dependent phagocytosis of tumor. Peritoneal macrophages were co-cultured for 3, 6, or 24 hours with labelled BL3750^{Ctrl} (circles) or BL3750^{Gal1} cells (squares) previously incubated with control (open shapes), CD20 mAb (closed shapes), or CD19 mAb (gray shapes). Representative contour plots show F4/80 versus labelled BL3750 tumor staining (left and middle panels) with mean phagocytosed tumor frequencies shown for 24 hours and phagocytosed tumor frequencies for 3, 6, and 24 hours from 3 pooled experiments (right panels, n = 6-9 mice per group). (G-H) Gal-1 expression blocks CD20-mediated tumor clearance *in vivo*. Mice given BL3750^{Ctrl} or BL3750^{Gal1} cells were treated with control (open shapes) or CD20 (closed shapes) mAb one day later. Lymphoma

volume (2 experiments, top panels) and mouse survival (2-3 experiments, n = 4-10 mice per group, bottom panels) were monitored for 60 days post-mAb treatment. (H) Representative lymphomas (top panel) and serum Gal-1 (lower panel) was measured in naïve mice (n = 3) and littermates given lymphoma cells 45 days after CD20 mAb treatment (2-3 experiments, 10 mice per group). (I) Human *LGALS1* expression by naïve, centroblast (CB), centrocyte (CC) and memory B cell samples (open circles) in comparison with cells (closed circles) from patients with Burkitt's lymphoma (BL), chronic lymphocytic leukemia [CLL, blood cells (1) or blood $CD19^+$ cells (2)], diffuse large B cell lymphoma [DBCL, lymph node biopsy (1) or node biopsy $CD19^+$ cells (2)], follicular lymphoma (FL), hairy cell leukemia (HCL) or mantle cell lymphoma (MCL). (E-I) Significant differences between sample means are indicated: *, $P < 0.05$; **, $P < 0.01$, ***, $P < 0.001$.

4.3. Conclusions

These collective results demonstrate that spontaneous primary B cell lymphomas can acquire resistance to CD20 immunotherapy through mechanisms independent of CD20 loss. First, 22 spontaneous primary B cell lymphomas were isolated and observed to express varying levels of surface CD20 (Fig. 7). These primary tumors varied significantly in their sensitivity to *in vivo* CD20 mAb therapy, though tumor sensitivity to CD20 mAb therapy did not correlate with CD20 density (Fig. 8). Moreover, the acquisition of primary tumor cell resistance to CD20 immunotherapy during multiple generations of passage occurred regardless of prior exposure to CD20 mAb or control mAb (Fig. 9-11). Thus, low level CD20 expression was sufficient for lymphoma depletion by CD20 mAb, while genetic changes that evolved within some individual lymphomas resulted in intrinsic and acquired resistance to CD20 mAb therapy. The forward genetic screen of CD20 mAb-resistant and -sensitive lymphomas identified Gal-1 as a significant mediator of lymphoma resistance to CD20 immunotherapy (Figs. 12). Gal-1 was elevated in primary lymphomas that were initially resistant to CD20 immunotherapy and further increased in expression in lymphomas that acquired therapy resistance following *in vivo* passage. Gal-1 expression ablated macrophage mAb-dependent phagocytosis of tumor cells during *in vitro* culture

and *in vivo* CD20 mAb-dependent tumor clearance (Fig. 12). Thus, B cell lymphomas develop resistance to mAb immunotherapy through alterations in the tumor transcriptome independent of modifications in target molecule expression. Importantly, this study established a comprehensive tumor library comprised of several families derived from distinct primary lymphomas. This tumor library will be an invaluable tool in the characterization of the global lymphoma genetic network that dictates tumor responsiveness to mAb immunotherapy.

5. Host Genetic Determinants of Antibody-Dependent Cell Depletion *In Vivo*

The following text was modestly adapted from its original manuscript, "Macrophage Mycn Expression Regulates *In Vivo* Antibody-Dependent Cell Depletion," which is currently in submission.

5.1. Introduction

The humoral immune response is a critical component of immunity, as Ab specific for a diverse array of antigens can function as a natural barrier to microorganisms by coating foreign pathogens or cells, often clearing unwanted microorganisms without eliciting significant inflammation. The Ab response also links the innate and adaptive immune systems, as Abs are able to activate several innate immune cell populations, including macrophages, through receptors that bind the Fc portion of different Ab isotypes (FcR). The specificity of Abs for a single antigenic epitope along with their elicitation of innate immunity has made this effector protein an attractive therapeutic option for the treatment of malignancies that express unique or restricted antigens. The chimeric mAb specific for CD20, Rituximab, was the first Ab therapy approved for the treatment of human cancer (*72*), namely Non-Hodgkin lymphoma (NHL). NHL is a diverse group of hematologic malignancies and is the fifth most common

cancer in the United States. Approximately 80-90% of all NHLs are of B cell origin and most express CD20, a B cell-specific surface protein expressed from pre-B cell development until plasma cell differentiation that regulates calcium flux and cell-cycle progression in both human and mouse B cells (*61, 63, 71*). While Rituximab was initially used to treat indolent NHL, its usage has expanded to include treatment of aggressive lymphomas as well as various autoimmune diseases, including rheumatoid arthritis and multiple sclerosis. Despite the widespread practice of treating patients with Rituximab, the mechanisms that regulate CD20 mAb-mediated B cell depletion in humans are still debated. Though CD20 mAb is a primary component of NHL therapy in patients, the initial efficacy of this therapy for NHL patients ranges from 10-60% among different NHL sub-types, despite sustained CD20 expression (*84*). Similarly, many patients with $CD20^+$ NHLs do not respond to retreatment with CD20 mAb upon relapse (*74*). Other than Fc receptor polymorphisms, molecular explanations for these inconsistent and typically insufficient responses remain poorly understood.

In mice, CD20 mAb treatment depletes both endogenous and malignant mouse B cells through a mechanism that requires macrophages and FcγR expression (*104, 106, 108*). Importantly, differences in B cell depletion between B6

and NOD mouse strains have been shown to occur despite comparable levels of CD20 expression, though these differences are in part due to variations in macrophage numbers and FcγR Ab binding between mouse strains (*112*). Thus, variability in B cell depletion among mouse strains can be used to study host-intrinsic factors that lead to effective CD20 mAb-dependent B cell depletion that may be relevant to humans. Further elucidating the specific mechanisms through which macrophages mediate tumor depletion following CD20 immunotherapy could lead to significant improvements in mAb-based therapeutics and expand our understanding of innate mAb-dependent effector mechanisms. Therefore, this study sought to identify the distinct germline components that control the efficacy of host CD20 mAb-dependent B cell and lymphoma depletion.

5.2. Results

5.2.1. Splenic B cell clearance by CD20 mAb is impaired in 129 and NOD mice

CD20 mAb effectively depletes more than 95% of splenic B cells in B6 mice (Fig. 13A, left panels) (*71*), However, low numbers of B cells remain following depletion, despite comparable levels of CD20 expression among depleted and remaining B cells (Fig. 13A, middle and right panels). To determine the variation among mouse strains in CD20 mAb-dependent B cell depletion, B cell numbers

before and following Ab treatment were enumerated in seven of the most common lab mouse strains. While the number of endogenous splenic B cells varied among the lab strains, five of the seven strains depleted >95% splenic B cells within one week of CD20 mAb treatment (Fig. 13B). However, 129 and NOD mice depleted 20-55% fewer splenic B cells following CD20 mAb treatment than B6 mice (Fig. 13B), indicating that B cell depletion by CD20 mAb is impaired in 129 and NOD mice. This effect was not due to differences in B cell CD20 expression levels (Fig. 13A, right panel) or Ab dispersion through the body, as mouse weight did not correlate with the efficiency of B cell depletion (Fig. 13C). There are FcγR polymorphisms between B6, 129, and NOD mice that may contribute to some of the variation observed in CD20 mAb-dependent B cell clearance (Fig. 13D-F). Of note, NOD mice lack the cytoplasmic tail of FcγRI and thus fail to productively signal through this receptor (*112*), which likely explains part of the defect in CD20 mAb-dependent B cell depletion in NOD mice. By contrast, B6 and 129 mice have very similar FcγRs and have nearly identical weights, indicating similar Ab dispersion through the body. Thus, splenic B cell clearance by CD20 mAb *in vivo* is significantly impaired in 129 and NOD mice.

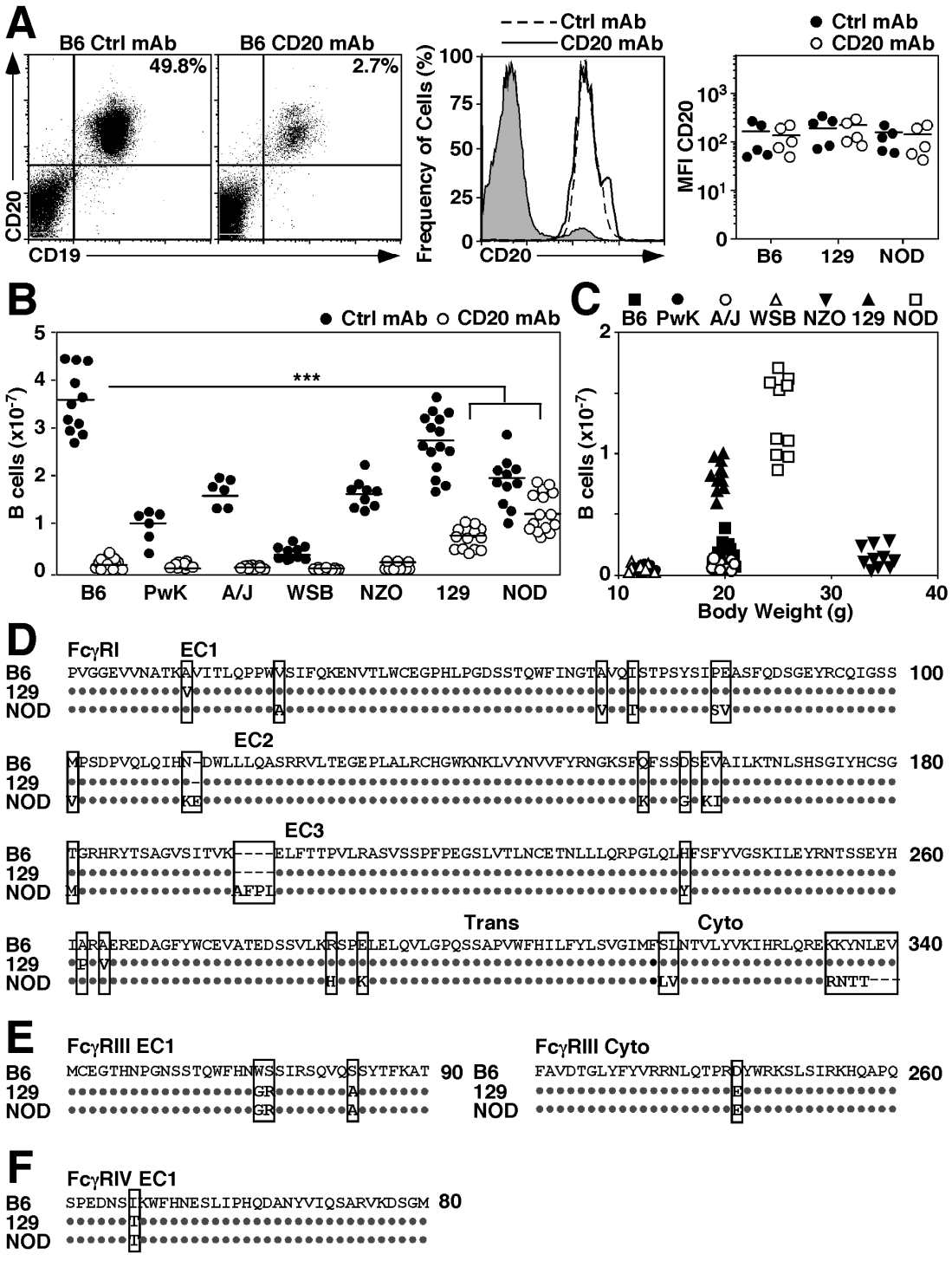

Figure 13. 129 and NOD mice have impaired CD20 mAb-dependent B cell clearance.

Figure 13. 129 and NOD mice have impaired CD20 mAb-dependent B cell clearance. (A) Left panels, representative cell surface expression of CD19 and CD20 is shown for B6 mice treated with either control or CD20 mAb, with gating on single live lymphocytes as identified by forward/side light scatter and dead cell exclusion. Middle panel, histogram shows representative CD20 expression by $CD19^+$ B cells in B6 mice treated with control mAb (dashed line) or CD20 mAb (solid line) relative to isotype control (shaded line). Right panel, CD20 mean fluorescence intensity (MFI) for $CD19^+$ B cells is shown for B6, 129, and NOD mouse strains treated with control (closed circles) or CD20 mAb (open circles). Values represent single mice pooled from 2 experiments. (B-C) Mice on the B6, PWK, A/J, WSB, NZO, 129, and NOD backgrounds were injected with either control (closed circles) or CD20 mAb (open circles) and were examined as in (A). Values represent single mice pooled from 2-4 experiments (n = 6-15 mice per group). Significant differences between sample means are indicated: ***, $P < 0.001$. (C) Values represent single mice from each background that were weighed prior to treatment with CD20 mAb versus the number of splenic B cells remaining following CD20 mAb-dependent depletion as in (A). (D-F) Predicted amino acid sequences of FcγRI (D), FcγRIII (E), and FcγRIV (F) in B6, 129, and NOD mouse strains. Identical residues are indicated by closed circles. Missing

residues are denoted by sequence gaps. Differing residues are boxed. Extracellular domain 1 (EC1), transactivation (Trans), and cytoplasmic (Cyto) domains are shown.

5.2.2. Distinct genetic traits in B6 and 129 mice regulate survival following CD20 immunotherapy of lymphoma

The efficiency of mAb-dependent endogenous B cell depletion could be attributed to differences in both the mAb-dependent immune response as well as responses generated by signaling through CD20 (*61, 71*). To understand the direct contributions of the host response to CD20 mAb-dependent cell depletion, mice were injected with the B cell lymphoma, BL3750, followed by CD20 mAb treatment one day later. The BL3750 lymphoma was derived from a B6 *Eμ-c-myc* transgenic mouse (*108*), which expresses the *c-myc* transgene under the control of the Ig heavy chain enhancer, resulting in the development of immature B cell-like lymphoma by approximately three to five months of age. Importantly, BL3750 retains surface CD20 expression *in vitro* and sensitivity to CD20 mAb therapy *in vivo* over time. B6 and B6 x 129 F1 (F1) mice were injected with BL3750 and then either control or CD20 mAb one day later, and mouse survival was followed for 60 days, as mice that developed tumors died by day 60, and mice that did not develop tumors did not develop tumors after 60 days. A significant difference in survival was observed between B6 and F1 mice following the adoptive transfer of BL3750 and subsequent treatment with control or CD20 mAb therapy one day later (Fig. 14A). The BL3750 tumor grew equally well

within both hosts, as virtually 100% of B6 and F1 animals succumbed to tumor within 37 days of control Ab treatment. Approximately 75% of B6 mice survived tumor transfer following CD20 mAb therapy, though less than 20% of F1 mice treated with CD20 mAb survived (Fig. 14A). Thus, while tumor development and growth rates were comparable between B6 and F1 mice, CD20 mAb-dependent tumor clearance was significantly less efficient in mice on the 129 background. Further, as the B6 background was progressively reintroduced to F1 mice by back-crossing to B6 for one (N1), two (N2), and three generations (N3), mouse survival steadily increased following CD20 mAb treatment to levels comparable to B6 mice (Fig. 14B). However, it is important to note that there were consistently B6 mice that died as well as F1 mice that survived when given CD20 mAb, indicating that there are pro- and anti-survival factors present in both the B6 and 129 backgrounds. Therefore, genetic traits present in both B6 and 129 mice regulate survival following CD20 mAb-mediated tumor depletion.

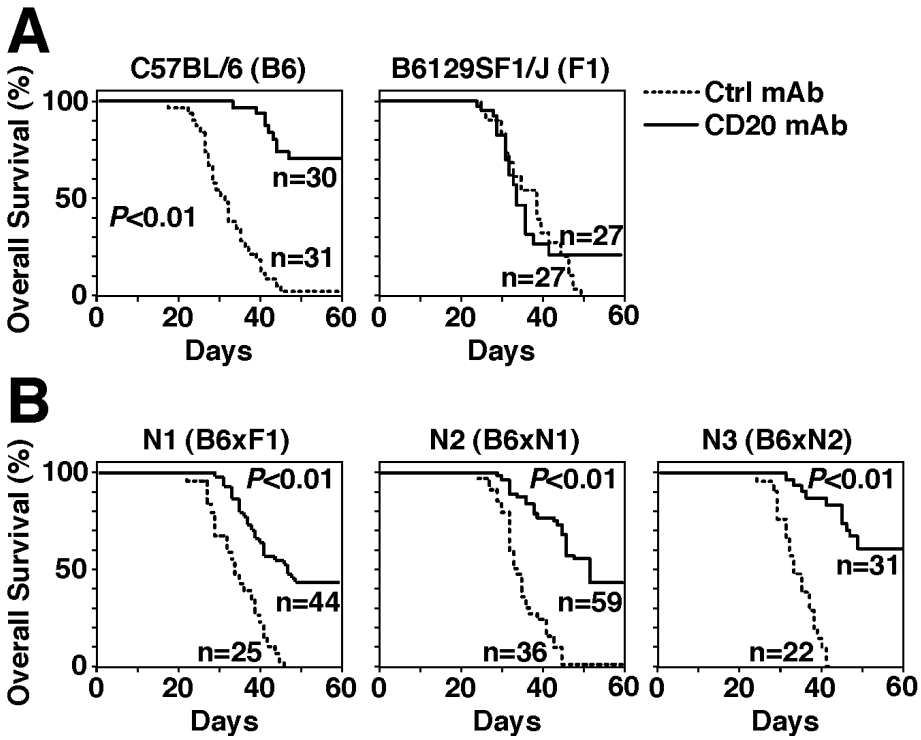

Figure 14. Distinct genetic traits regulate survival following CD20 mAb-mediated tumor depletion.

Figure 14. Distinct genetic traits regulate survival following CD20 mAb-mediated tumor depletion. (A) Survival of B6 mice (left panel) treated with control (*n* = 31, dashed line) or CD20 mAb (*n* = 30, solid line) and B6 x 129 F1 (F1, right panel, dashed line) mice treated with control (*n* = 27, dashed line) or CD20 mAb (*n* = 27, solid line). (B) Survival of N1 mice (B6 x F1, left panel) treated with control (*n* = 25) or CD20 mAb (*n* =4 4), N2 mice (B6 x N1, middle panel) treated with control (*n* = 36) or CD20 mAb (*n* = 59), and N3 mice (B6 x N2, right panel) treated with control (*n* = 22) or CD20 mAb (*n* = 31).

5.2.3. Linkage analysis reveals Chromosome 12 quantitative trait locus that controls lymphoma immunotherapy

Genome-wide linkage analysis was conducted to identify quantitative trait loci (QTL) present in B6 and 129 mice that determine survival following CD20 mAb-dependent lymphoma depletion. This method was used to identify survival regulators present in both B6 and 129 mice in a manner that is not biased by the overall phenotypic model. SNPs from N1 mice treated with CD20 mAb (Fig. 14B, left panel) were sequenced to identify the genotype of each mouse at 377 loci across the mouse genome. The distribution of B6 and F1 genotypes at a given locus was then correlated with the number of days each mouse survived, and an LOD score was used to measure the significance of a given locus. Tail DNA from two independently collected cohorts of N1 animals were sequenced and analyzed separately for loci significantly correlating with the number of days each mouse survived (Fig. 15A). A locus on Chromosome 12 (11.35 Mbp) was identified in both groups of mice in which the genotype distribution strongly correlated with survival. The addition of 105 mice to the original cohorts further confirmed the significance of the Chromosome 12 locus (LOD=5.07), which controlled at least 20% of the variability in survival observed between mouse strains (Fig. 15B), whereas the flanking SNPs at 8.97 and 25.22

Mbp were not significantly associated with survival. Interestingly, the linkage analysis demonstrated that mice with the F1 genotype at the Chromosome 12 locus survived on average 9 days longer than mice with the B6 genotype. This is not surprising, given the unbiased method used to identify survival QTLs and the presence of multiple survival regulators present on both the B6 and 129 backgrounds, as noted earlier (Fig. 14). The Chromosome 12 locus became even more significant with the addition of N2 and N3 mice treated with CD20 mAb, further validating the importance of this locus in survival following CD20 mAb-dependent lymphoma depletion (Fig. 15C). Thus, a locus between 8.97 and 25.22 Mbp on Chromosome 12 regulates lymphoma clearance by CD20 mAb.

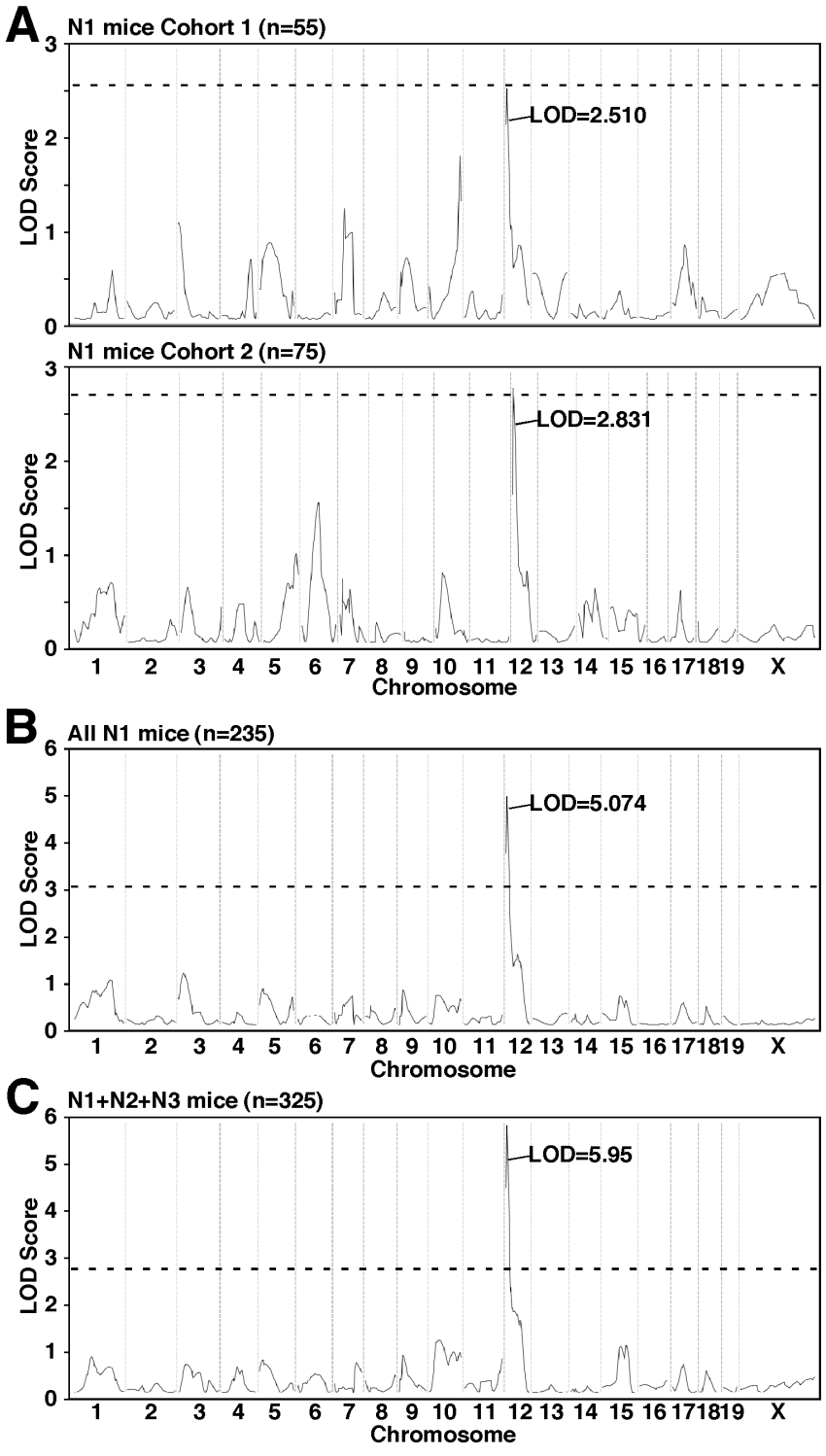

Figure 15. Linkage analysis reveals Chromosome 12 locus that dictates mAb-dependent depletion.

Figure 15. Linkage analysis reveals Chromosome 12 locus that dictates mAb-dependent depletion. (A) Cumulative LOD score maps for the entire mouse genome (Chromosomes 1-19 and X) are shown for two independently collected and analyzed groups of N1 mice, cohort 1 (top panel, $n = 55$) and cohort 2 (bottom panel, $n = 75$). (B-C) Cumulative LOD score maps as in (A) are shown for pooled N1 mice (B, $n = 235$) and pooled N1, N2, and N3 mice (C, $n = 325$). (B) N1 mice and (C) N1 mice combined with N2 mice and N3 mice. (A-C) Genotyped markers are ordered according to chromosomal location versus the individual marker LOD score. Dashed lines indicate significance thresholds: $P < 0.001$.

5.2.4. Chromosome 12 genetic mapping reveals region of genomic concordance

The interval of 8.97-25.22 Mbp on Chromosome 12 contains over 40 genes. To identify the gene that regulates CD20 mAb-dependent lymphoma depletion, the region of genomic concordance, determined from the linkage analysis to be the region where mice that survived to 60 days had the F1 genotype and mice that did not survive to 60 days had the B6 genotype, was determined. SNPs from N1 mice present in the genome-wide analysis cohort (Fig. 15) with genotype cross-overs occurring between 8.97 and 25.22 Mbp on Chromosome 12 (Fig. 16A) were sequenced at 0.5-2.0 Mbp intervals from 8.97-25.22 Mbp. Based on sequencing analysis, 75% of sequenced N1 mice were concordant with the linkage analysis model within the region of 11.5-13.0 Mbp on Chromosome 12 (Fig. 16B), meaning that in the 11.5-13.0 Mbp region, most mice that died prior to 60 days had the B6 genotype and most mice that survived to 60 days had the F1 genotype. The 11.5-13.0 Mbp interval contains two genes, *fam49a* and *mycn*.

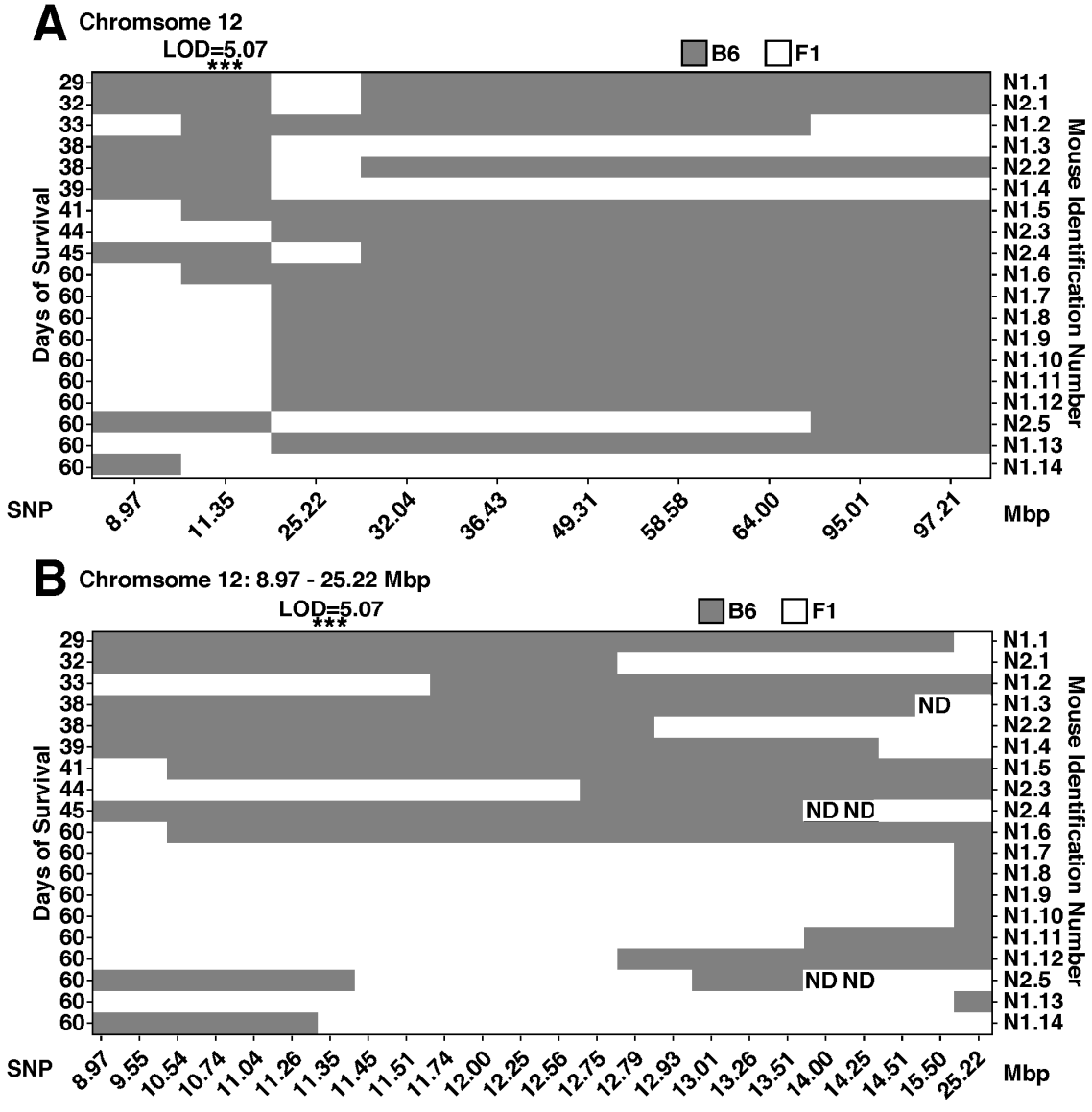

Figure 16. Genetic mapping of Chromosome 12 reveals region of genomic concordance.

Figure 16. Genetic mapping of Chromosome 12 reveals region of genomic concordance. N1 mice from Fig. 15 that had genotype cross-overs flanking the significant SNP on Chromosome 12 were identified (n = 19). (A) The mouse genotype at all SNPs sequenced on Chromosome 12 from Fig. 15 are shown relative to the number of days each mouse survived for N1 mice with genotype cross-overs. Mice are ordered by the number of days each mouse survived and are individually identified by a Mouse Identification Number. Gray boxes indicate B6 genotype, and white boxes indicate F1 genotype. (B) The genotypes of each mouse with cross-overs from (A) from 8.97-25.22 Mbp on Chromosome 12 were determined by sequencing strain-specific SNPs. Mice are ordered and indicated as in (A). Gray boxes indicate B6 genotype, white boxes indicate F1 genotype, and ND indicates no data. (A-B) Significant QTL on Chromosome 12 is indicated as ***, $P < 0.001$.

5.2.5. Macrophage mycn expression regulates mAb-dependent B cell depletion *in vivo*

There are two sequence polymorphisms in the *fam49a* gene untranslated regions between B6 and 129 mice. While there are no sequence polymorphisms between B6 and 129 mice in the *mycn* gene, there is one deletion upstream of the *mycn* locus (9 kb upstream, approximately 100 bp) and two deletions downstream of the *mycn* locus (3 and 5.5 kb downstream, approximately 150 bp each), which may affect the chromosomal stability and accessibility of the *mycn* locus. As macrophages mediate CD20 mAb Ab-dependent depletion in mice (*104, 106, 108*), *fam49a* and *mycn* transcript expression were evaluated in peritoneal macrophages. Expression of *mycn* transcript is significantly elevated in 129 macrophages approximately 3-fold relative to B6 macrophages (2.95$\pm$0.26 fold; Fig. 17A, top left panel and bottom panel). Treatment with Thioglycollate results in an even greater disparity in *mycn* transcript levels between mouse strains (4.99$\pm$0.62 fold; Fig. 17A, top right panel). However, *fam49a* transcript was equivalent between B6 and 129 macrophages both with and without Thioglycollate elicitation. The increased amount of *mycn* in 129 macrophages indicates that higher macrophage *mycn* expression, conferred by changes in

putative *mycn* regulatory regions or accessibility of this locus, may result in enhanced CD20 mAb-dependent B cell depletion.

To confirm that the 129 Chromosome 12 locus that contains *mycn* results in enhanced B cell depletion, consomic mice were bred by back-crossing N1 mice that were heterozygous at the Chromosome 12 QTL to B6 three (N4), four (N5), and five (N6) generations (Fig. 17B). Illumina sequencing revealed that the N5 parent used to breed subsequent N6 mice was B6 homozygous at every sequenced locus other than the significant Chromosome 12 locus (11.5-13 Mbp) based on genome-wide QTL analysis. N4, N5, and N6 offspring that were B6 homozygous across the Chromosome 12 locus had results that were statistically indistinguishable from those of wild-type B6 mice and were thus combined. Consomic mice depleted approximately 30% more B cells than wild-type mice following low-dose CD20 mAb treatment (Fig. 17B). Thus, the 129 Chromosome 12 QTL that contains the *mycn* locus leads to enhanced B cell depletion.

To confirm the role of macrophage mycn expression *in vivo*, mice with macrophages conditionally deficient in mycn were generated by crossing B6 mice with floxed mycn alleles to B6 mice expressing Cre recombinase under the control of the lysozyme M gene ($Lysm^{Cre/+}$ $Mycn^{F/F}$, $Mycn^{-/-}$). At both low and saturating doses of mAb treatment, mice with mycn-deficient macrophages

depleted about 20% fewer B cells than wild-type mice using CD20 mAb (Fig. 17C). Additionally, while consomic mice had approximately 2-fold more resident and Thioglycollate-elicited macrophages, mycn-deficiency resulted in 34-43% fewer peritoneal macrophages without or following Thioglycollate elicitation, respectively (Fig. 17D, left panel). Further, consomic macrophages more rapidly phagocytosed CD20 mAb-coated BL3750 tumors than wild-type mice, with 40% and 20% more phagocytosis occurring during the first three and six hours, respectively, of a short-term *in vitro* phagocytosis assay (Fig. 17E, left panel). Consomic macrophages also phagocytosed approximately 20% more BL3750 tumor cells coated with CD19 mAb in this time frame, indicating that consomic macrophages have enhanced Ab-dependent phagocytosis that is not specific to CD20 mAb. In contrast to consomic macrophages, mycn-deficient macrophages were significantly impaired in their ability to phagocytose CD20 mAb- or CD19 mAb-labeled BL3750 tumors, resulting in 30-50% reductions in tumor phagocytosis (Fig. 17E, right panel). Thus, differential *mycn* expression likely modulates *in vivo* mAb-dependent B cell depletion by elevating macrophage numbers and enhancing Ab-dependent phagocytosis.

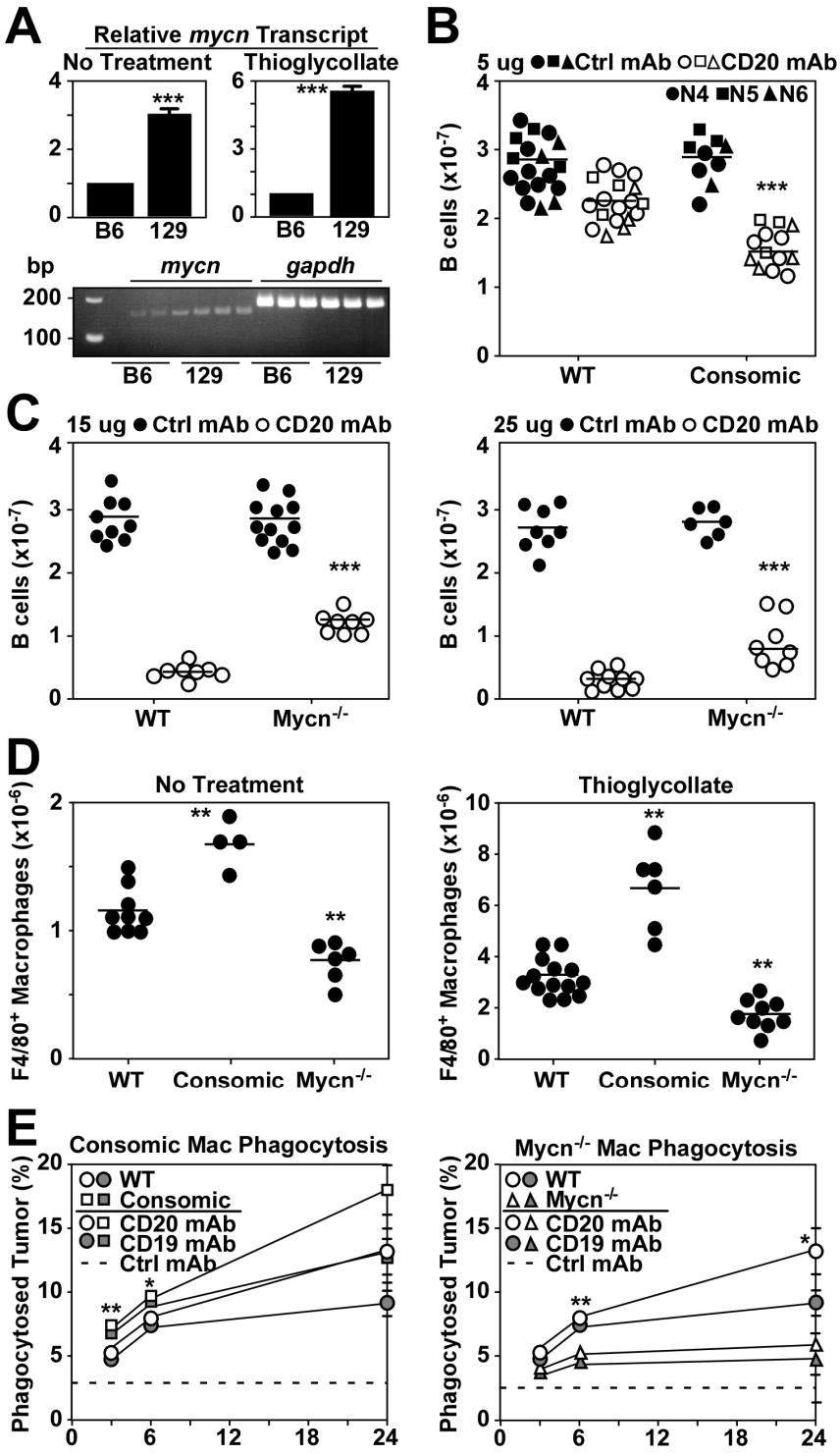

Figure 17. Macrophage mycn expression regulates *in vivo* B cell depletion by CD20 mAb.

Figure 17. Macrophage mycn expression regulates *in vivo* B cell depletion by CD20 mAb. (A) Peritoneal macrophages were collected by lavage from untreated B6 and 129 (No Treatment, top left panel) or mice treated with Thioglycollate (Thioglycollate, top right panel). Values represent fold change relative to *gapdh* and B6 *mycn* transcripts shown pooled from 2 experiments (n = 6 pooled). Transcript expression of *gapdh* and *mycn* was visualized by agarose gel electrophoresis following PCR using cDNA samples and the same program as employed for qPCR (bottom panel). Lane 1, ladder showing 100-200 bp; lanes 3-5, B6 *mycn* transcript; lanes 6-8, 129 *mycn* transcript; lanes 9-11, B6 *gapdh* transcript; lanes 12-14, 129 *gapdh* transcript. (B) Wild-type and consomic Mice were injected with 5 μg control (black shapes) or CD20 mAb (white shapes) and analyzed one week later as in Fig. 13. Values represent single mice pooled from 3-5 experiments (n = 9-18 mice per group). (C) Mice with macrophages conditionally deficient in mycn ($Mycn^{-/-}$) and control wild-type littermates were treated with 15 μg (left panel) or 25 μg (right panel) control (closed circles) or CD20 mAb (open shapes) and were analyzed as in Fig. 13. Values represent single mice pooled from 3 experiments (n = 6-13 mice per group). (D) Peritoneal cells from wild-type, consomic, and $mycn^{-/-}$ mice given either PBS (No Treatment, left panel) or Thioglycollate once four days prior to enumeration. Values

represent single mice pooled from 2-4 experiments (n = 4-14 mice per group). (E) Peritoneal macrophages were co-cultured for 3, 6, or 24 hours with labelled BL3750 cells previously incubated with control (dashed line), CD20 (white shapes), or CD19 mAb (gray shapes). Values represent mean (± SEM) phagocytosed tumor frequencies for 3, 6, and 24 hours from 2-3 pooled experiments (n = 3-7 mice per group). (A-E) Significant differences between sample means are indicated: *, $P < 0.05$; **, $P < 0.01$, ***, $P < 0.001$.

5.2.6. Several polymorphisms in the *mycn* locus exist in mice and humans

The *mycn* locus is polymorphic among common lab strains as well as in humans. B6 and 129 parent mouse strains are largely identical-by-descent in the defined region of genomic concordance (Chromosome 12, 11.5-13 Mbp), though some significant sequence variations occur upstream of this locus, including the deletions described earlier (Fig. 18A). Similarly, all common lab strains exhibit varying levels of sequence variation in the *mycn* locus relative to B6 mice, indicating that this region is polymorphic even among inbred lab mouse strains (Fig. 18B). As with lab mouse strains, humans have a high degree of polymorphisms occurring throughout the *mycn* locus, even in regions of high homology between mouse and human, that range from low to high prevalence in the population (Fig. 18C). Thus, polymorphisms in the *mycn* locus confer differential expression of mycn between B6 and 129 mice, and additional polymorphisms similarly exist in other strains of mice as well as among humans that may result in altered mycn expression and macrophage function.

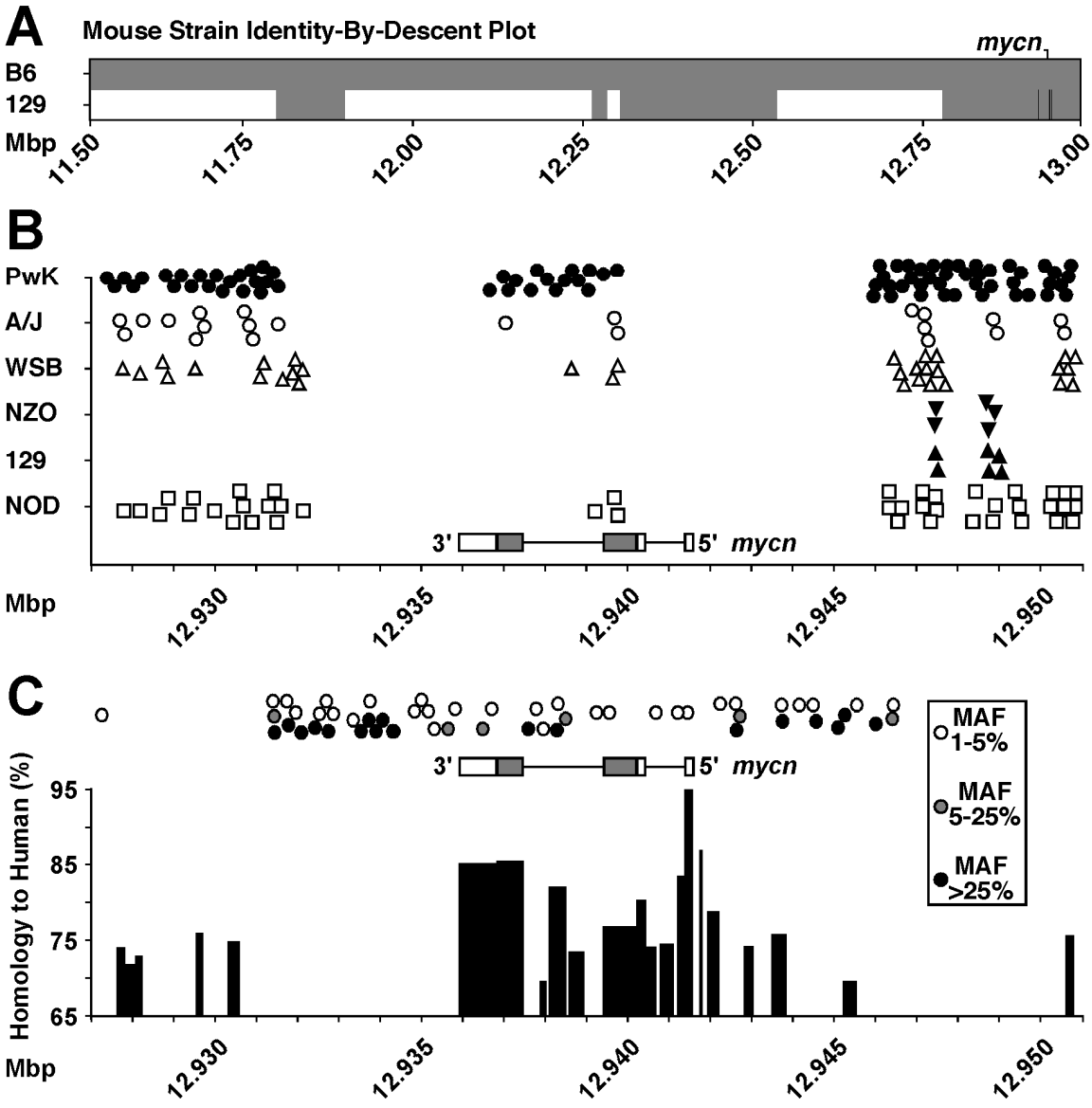

Figure 18. Several polymorphisms exist in the human and mouse *mycn* loci.

Figure 18. Several polymorphisms exist in the human and mouse *mycn* loci. (A) B6 and 129 parent mouse strain identity-by-descent plot in region of genomic concordance identified in Fig. 16. Gray regions indicate genomic locations where parent mice are identical by descent (>99% sequence homology to ancestral gene), and white regions indicate genomic locations where B6 and 129 parents differ significantly by sequence. Black lines indicate deletions in the 129 *mycn* locus relative to the B6 *mycn* locus. (B) Strain polymorphisms exist amongst common lab mice. PWK (closed circles), A/J (open circles), WSB (open triangles), NZO (closed inverted triangles), 129 (closed triangles), and NOD (open squares) strain sequence polymorphisms relative to the B6 mouse strain are shown relative to location on Chromosome 12 and mouse *mycn* gene map. White boxes indicate UTRs, gray boxes indicate coding exons, and lines indicate introns. (C) Sequence homology of the human *mycn* locus (>65% sequence homology) to the mouse *mycn* locus is shown relative to location on mouse Chromosome 12 and mouse *mycn* gene map as described in (B). Circles indicate sites of polymorphisms in the human *mycn* locus. Polymorphism minor allele frequencies (MAF) are indicated by color, where open circles indicate a global MAF of 1-5%, gray circles indicate a global MAF of 5-25%, and black circles indicate a global MAF greater than 25%.

5.3. Conclusions

These collective data demonstrate that host genetic variations in mycn expression in macrophages alter the outcome of Ab-dependent depletion of endogenous and malignant cells. First, variations in CD20 mAb-dependent B cell depletion were noted among several lab mouse strains, where 129 mice had significantly impaired mAb-dependent depletion of endogenous B cells (Fig 13) and primary lymphomas (Fig 14) relative to B6 mice. An unbiased forward genetic screen of mice on a mixed B6 and 129 background revealed that a 1.5 Mbp region of Chromosome 12 that contains *mycn* significantly altered CD20 mAb-dependent lymphoma depletion (Fig. 15-16). Elevated mycn expression enhanced mAb-dependent B cell depletion and lymphoma phagocytosis and correlated with higher macrophage numbers (Fig. 17). Further, several polymorphisms exist in the *mycn* locus among individuals, including several at >25% frequencies in the population, indicating that variations in macrophage mycn expression might affect Ab immunotherapy in humans (Fig. 18). Notably, this study established and validated an unbiased forward genetics approach to identify the totality of factors that influence CD20 mAb therapy *in vivo*.

6. Discussion

The studies described in Chapters 3, 4, and 5 examine the roles of B cells and their humoral immune product, Abs, in the immune system during homeostasis, viral infection, and treatment of malignancy.

6.1. The role of B cells in the Homeostasis and Effector Response of the Cellular Immune System

The data shown in Chapter 3 establish that B cells are required for spleen and lymph node T cell homeostasis and optimal $CD4^+$ and $CD8^+$ T cell responses during acute LCMV infection. Remarkably, short-term mature B cell depletion in both 2- and 4-month-old mice significantly reduced both spleen and lymph node $CD4^+$, $CD8^+$, and Treg cell numbers (Fig. 1). These reductions were most likely due to alterations in T cell homeostasis following B cell depletion, as no overt changes in T cell migration to peripheral organs were observed (Fig. 1). In the absence of B cells, activated $CD44^{hi}CD62L^-$ $CD4^+$ and $CD8^+$ T cell numbers in 2- and 4-month-old mice were more dramatically reduced than naïve $CD44^{lo}CD62L^+$ $CD4^+$ and $CD8^+$ T cell numbers. As a consequence of fewer T cells in B cell-depleted mice, the number of effector CD4+ and CD8+ T cells producing IFN-γ and TNF-α was also significantly decreased (Fig. 2). Importantly, B cell-deficiency during acute LCMV infection led to significant reductions in $CD4^+$ and

$CD8^+$ T cell numbers and the generation of activated, effector, and $CD4^+$ cytokine-producing cells (Figs. 4-5). Virus peptide-specific $CD4^+$ and $CD8^+$ T cell numbers and effector generation as well as $CD4^+$ T cell activation and cytokine production were also dramatically reduced in mice lacking B cells (Fig. 6), while spleen LCMV titers were dramatically increased (Fig. 4C). Thus, B cells were essential for maintaining $CD4^+$ and $CD8^+$ T cell homeostasis and optimal T cell responses during viral infection.

6.1.1. B cells Affect $CD4^+$ T cells More Directly and Profoundly than $CD8^+$ T cells

B cell depletion in 2- and 4-month-old mice had an overall negative effect on both $CD4^+$ and $CD8^+$ T cell homeostasis and function after only two weeks (Fig. 1-2). Chronic B cell depletion over 6-mo in year-old mice similarly resulted in a 50-70% reduction in activated $CD4^+$ and cytokine-producing T cell numbers, but alterations in $CD8^+$ T cell activation were less dramatic (Fig. 3). In complementary studies, acute B cell depletion in mice with otherwise intact immune systems impairs adaptive and autoreactive $CD4^+$ T cell responses to antigen challenge, whereas $CD8^+$ T cell reactivity is less affected (*27*, *36*). B cell depletion also reduces the conversion of naive $CD44^{lo}CD62L^+$ $CD4^+$ T cells to an activated phenotype in response to Listeria challenge, whereas $CD8^+$ T cell

phenotypes are only modestly affected (*27*). A role for B cells in $CD4^+$ T cell priming has also been demonstrated in mice given anti-IgM Ab since birth (*23-26*) and in genetically B cell-deficient μMT mice (*161*). Therapeutic B cell depletion in mice also reduces $CD4^+$ and $CD8^+$ T cell tumor immunity in the B16 melanoma model (*34*). Thereby, depending on mouse age, status of the immune system, and magnitude of the challenge, $CD4^+$ T cell function appears to be more B cell-dependent than $CD8^+$ T cell function.

The importance of CD20 mAb-induced B cell depletion on $CD4^+$, Treg, and $CD8^+$ T cell frequencies or numbers in mice have yielded conflicting results, ranging from increased (*152, 153*), unchanged (*18, 27, 106, 151*) or decreased (*33, 34, 36*). Variability between individual mice was also observed in the current studies, where the numbers of Treg, $CD4^+$, and $CD8^+$ T cells remaining after CD20 or control mAb treatment overlap (Fig. 1B-D). In previous studies, differences between lymphocyte subsets among littermates, measurement of differences in T cell frequencies versus tissue numbers, variability between ages of mice being studied, differences in disease responses to treatments, inherent variability in lymph node sizes between littermates and small sample groups are likely to have obscured differences between CD20 or control mAb-treated groups. The degree of B cell depletion due to the use of different CD20 mAbs and

treatment regimens is also important, as changes in cell numbers and lymphoid tissue architecture are less pronounced when some B cells remain. For example, B cell depletion by CD20 mAb is less effective in NOD mice, due in part to FcγR deficiencies (*112*). CD20 mAb treatment significantly reduces the proliferative capacity of $CD4^+$ and $CD8^+$ T cells within tissues of NOD mice, but does not affect Treg, $CD4^+$, or $CD8^+$ T cell numbers or phenotypes. Others have also demonstrated impaired lymph node T cell activation in congenitally B cell-deficient NOD mice, suggesting a critical need for B cell costimulatory signals (*162*). The timing of evaluation following B cell depletion is also critical (*71*, *106*), as the reductions in total $CD4^+$ and CD8+ T cell numbers one week following CD20 mAb treatment are less significant than those that were observed two weeks after depletion (Fig. 1, ref. (*27*)). The global effects on T cell homeostasis induced by B cell depletion likely change with disease severity and also with age, as was observed for mice chronically depleted of B cells in this study. Nonetheless, reduced numbers of activated and effector cytokine-producing $CD4^+$ T cells are most likely attributable to suboptimal activation in the absence of B cell Ag-presentation in combination with normal T cell turnover (*27*, *33*, *34*, *163*, *164*).

6.1.2. B cell Support is Critical for T cell Function during Viral Infection

There was a specific reduction in Ag-specific effector $CD8^+$ cell development in the absence of B cells (Fig. 6E). Because $CD4^+$ T cells are critical for $CD8^+$ T cell responses to viral infection (*28*), the observed impact of B cell depletion on $CD8^+$ T cell function may be due to B cell-induced alterations in $CD4^+$ T cell expansion, function, and memory maintenance, as shown in this study and elsewhere (*27, 33, 36*). The absence of B cells may thereby also indirectly impact $CD8^+$ T cell memory development, as memory $CD8^+$ T cells derive from the responding Ag-specific effector CD8+ T cell pool (*155*) and there is a reduction in memory $CD8^+$ T cell numbers following LCMV infection in the absence of B cells (*10*). The altered architecture of lymphoid tissues in B cell-depleted mice may also affect T cell responses. In either event, the delayed resolution of viral infection observed in this study may primarily result from reduced T cell homeostasis, resulting in lower numbers of activated and cytokine-producing $CD4^+$ and $CD8^+$ T cells responding to LCMV. Indeed, T cells derived from B cell-deficient mice are unable to develop memory responses sufficient to control persistent viral infection (*30*), and this effect is independent of B cell Ab production (*37, 38*). B cells are also required for optimal $CD4^+$ T cell

memory generation and recall responses upon secondary infection, a process dependent on B cell MHC-II expression (*33, 36*). Total and Ag-specific effector, pre-memory, and T follicular helper $CD4^+$ T cell development T was also significantly inhibited in the current study. Thus, both primary and secondary responses to infection are likely to be significantly affected by B cell depletion.

Acute B cell depletion in mice before LCMV infection resulted in dramatically increased virus titers (Fig. 4C), which is in accordance with previous studies that demonstrated worsened but not protracted LCMV Armstrong infection in B cell-deficient mice (*10, 30*). Similarly, mice depleted of B cells since birth with anti-IgM serum do not develop fully protective T cell immunity to virus-induced tumors (*165, 166*). B cells promote optimal T cell activation and function following immunization (*27, 35*), during viral immunity (*29, 31-33*) and in models of tumor immunity, autoimmunity and graft rejection (*34, 109, 112, 153, 164, 166, 167*). The influence of B cells on both $CD4^+$ and $CD8^+$ T cell activation thus reflects the diverse and multiple known molecular mechanisms through which B cells influence T cell immunity, including B cell contributions to Ag-presentation, costimulatory molecule expression, and cytokine production (*8*). When the immune system develops in the complete absence of B cells in μMT mice, multiple immune system abnormalities have

been identified. The absence of B cells has been shown to impair $CD4^+$ T cell priming in some studies (*24, 25, 35, 38, 168, 169*), whereas others have reported that CD4+ T cell priming is not affected in μMT mice (*11, 170-173*). Additionally, thymocyte and T cell numbers and repertoire are decreased significantly in μMT mice (*10, 174*). Also, because B cells help to organize lymphoid organ architecture, the spleens of μMT mice are smaller in size (*10*), exhibit significant defects within the spleen DC and T cell compartments (*11, 12*), lack follicular dendritic cells and marginal zone and metallophilic macrophages (*13*), have decreased chemokine expression (*12, 13*), and are deficient in Peyer's patch organogenesis and follicular dendritic cell networks (*13, 14*). Dendritic cells in μMT mice also skew immunity towards Th1 responses (*11*). B cell depletion after the establishment and functional maturation of lymphoid tissues as in the current studies may also affect non-lymphoid immune cell populations that influence LCMV clearance. Nonetheless, acute and chronic B cell depletion in the current studies appears to have primarily dampened T cell homeostasis and some cell-mediated immune responses in comparison with the more pleiotropic effects of congenital B cell deficiency or induced B cell depletion after birth.

6.1.3. Implications for Therapeutic B cell Depletion in Humans

B cell depletion reduces the pathogenesis of diverse autoimmune diseases in humans, where the reconstitution of B cells is often accompanied by disease recurrence (*175, 176*). A subset of human T cells has been reported to express CD20 (*177-179*), and a small subset of human T and natural killer cells has been reported to be depleted following CD20 mAb therapy in rheumatoid arthritis patients due to low level CD20 expression (*176, 178*). However, measurable cell surface CD20 expression is widely considered to be B cell-restricted in humans (*180*) as it is in mice (*71, 181*). CD20 mAb treatment in patients with pemphigus decreases autoreactive $CD4^+$ T cell frequencies, while overall T cell numbers are unaffected (*182*). Rituximab reduces both B and T cell numbers in cerebrospinal fluid of multiple sclerosis patients (*183*). Treg cell frequencies are reported to increase following rituximab treatment in patients with lupus or mixed cryoglobulinemia vasculitis (*184-186*). However, Treg cell and $CD4^+$ T cell numbers decreased in parallel following CD20 mAb treatment in the current mouse study (Fig. 1). The complexities of studying humans, particularly in those with disease undergoing therapy, in combination with the difficulties in assessing the extent of tissue B cell depletion, may thereby obfuscate studies of T cell alterations in patients acutely or chronically depleted of B cells. Likewise, B

cell depletion in mice does not result in overt *in vivo* monocyte activation nor does it measurably influence serum cytokines that could in turn modify T cell function (*27*). That B cells are also required for T cell homeostasis in naïve mice and for T cell activation during immune responses to pathogens provides a potential mechanism by which B cell depletion delays and reduces the severity of T cell-mediated autoimmune diseases (*18, 112, 151-153, 187-189*), even though serum Ab levels are not significantly affected by B cell depletion (*105, 150*).

The effects of CD20 mAb treatment on T cell numbers in the current study appears to be a direct consequence of B cell depletion and is likely due to the previously described disruption of lymphoid tissue architecture in the absence of B cells (*103*), consequently impairing cellular immunity. Thereby, the current results suggest a model in which the therapeutic benefits of CD20 mAb treatment in autoimmune patients are, at least in part, due to dysregulated T cell homeostasis and impaired T cell activation, with the potential cost of rendering some patients more susceptible to infections, particularly when given in combination with immunosuppressive drugs (*175*). Indeed, diminished T cell numbers and altered responses may explain rare infections in lymphoma patients receiving rituximab with microorganisms generally associated with T cell immunosuppression such as JC-papovavirus, CMV, or parvovirus B19 (*190*).

Consequently, the impact of efficient B cell depletion on T cell responses observed in the current study urges caution in the broad and prolonged application of B cell depletion therapies in the clinic.

6.1.4. Remaining Questions

This study clearly demonstrated the deleterious effects that B cell depletion has on the primary cellular immune response in mice. A recent study demonstrated that MHC-II-bearing B cells are required during the primary immune response for $CD4^+$ T cells to develop optimal memory to acute LCMV and that $CD4^+$ T cells have a more robust recall response in the presence of B cells, though this latter effect was independent of B cell antigen presentation (*33*). Future studies should therefore evaluate how B cells support T cell immune responses independent of antigen presentation. In this regard, determining whether the depletion of different B cell subsets, including B10 cells, alters cellular immune responses to different pathogens would be important. Further, whether B cell depletion impacts the course and outcome of chronic viral infections, including LCMV Clone-13, hepatitis, or HIV, could have significant implications for treatment of infected individuals with B cell malignancies. Importantly, these data have significant implications for the outcome of vaccination of individuals that have previously been treated with B cell-

depleting therapies and whether B cell depletion after vaccination affects the T cell repertoire. Future studies should evaluate whether B cell depletion at different stages of an immune response (e.g. before and after immunization) differentially impacts the TCR repertoire or T cell effector skewing before and after immunization or an immune response.

6.2. The Role of Lymphoma Genetic Alterations in the Development of Resistance to CD20 Immunotherapy

The results reported in Chapter 4 demonstrate that spontaneous primary B cell lymphomas can acquire resistance to CD20 immunotherapy through mechanisms independent of CD20 loss. Twenty-two spontaneous primary B cell lymphomas examined in this study expressed variable levels of CD20 (Fig. 7) and exhibited a wide spectrum of sensitivity to CD20 immunotherapy *in vivo*, which did not correlate with CD20 density (Fig. 8) nor *in vivo* passage (Figs. 9-10). Moreover, the acquisition of primary tumor cell resistance to CD20 immunotherapy during multiple generations of passage occurred regardless of whether the tumor cells were exposed to CD20 mAb or control mAb (Fig. 11). Therefore, only a low threshold of CD20 expression was required for lymphoma depletion by CD20 mAb, with the evolution of molecular changes other than

CD20 expression within individual lymphomas driving intrinsic and acquired resistance to CD20 mAb therapy.

6.2.1. Galectin-1 in the Tumor Microenvironment Directly Impairs Tumor Immunotherapy

The unbiased screen of CD20 mAb-resistant and -sensitive lymphomas identified Gal-1 as a significant mediator of lymphoma resistance to CD20 immunotherapy (Figs. 12). Indeed, Gal-1 was not only elevated in primary lymphomas that were initially resistant to CD20 immunotherapy, but Gal-1 expression increased as lymphomas acquired therapy resistance following serial *in vivo* passage. Mechanistically, Gal-1 expression directly impaired macrophage mAb-dependent phagocytosis of tumor cells during short-term *in vitro* culture and *in vivo* CD20 mAb-dependent tumor clearance (Fig. 12). Gal-1 belongs to a family of well-conserved carbohydrate-binding proteins that modulate immune responses by inhibiting activation and enhancing cell death both in cell-intrinsic and -extrinsic capacities (*191*). Gal-1 is known to have significant immunosuppressive effects on human and mouse macrophages, T cells, and dendritic cells (*192-197*). Gal-1 binds *N*-acetyllactosamine residues on *N*- and *O*-linked glycans on cell surface glycoproteins, including CD3, CD4, CD7, CD8, CD43, and CD45, and inhibits TCR-dependent T cell activation and proliferation,

leading to T cell apoptosis (*192-195*). Gal-1 expression by melanoma cell lines inhibits T cell-dependent tumor rejection (*198*). Gal-1 also skews human and mouse dendritic cells to an anti-inflammatory phenotype (*197*). Furthermore, Gal-1 exposure attenuates FcγR and MHC-II induction on human and mouse macrophages and inhibits macrophage phagocytosis (*196*). Thus, Gal-1 secreted by lymphoma cells may attach to cell surface carbohydrates through its lectin domain and confer immune privilege within the tumor microenvironment as occurs with other malignancies (*191*). This demonstration of a functional link between Gal-1 expression and lymphoma progression highlights Gal-1 as an important molecular target for manipulation that may have significant implications for enhancing cancer immunotherapy (*198*).

Serum Gal-1 levels increased similarly in mice given BL3750^{Ctrl} or BL3750^{Gal1} cells and both tumors had similar growth rates despite their Gal-1 expression differences (Fig. 12). Elevated serum Gal-1 levels are also associated with lymphoma burden in patients with Hodgkin's lymphoma (*199*). However, CD20 immunotherapy remained effective in mice given BL3750^{Ctrl} tumors, but not in mice given BL3750^{Gal1} cells. Thus, serum Gal-1 is likely to be symptomatic of lymphoma burden, while Gal-1 released within the tumor microenvironment confers lymphoma resistance to CD20 immunotherapy. While Gal-1 is

overexpressed by B lymphoblastic leukemia (*200*), Kaposi's sarcoma (*201*), and classic Hodgkin's lymphoma cells (*202*), serum Gal-1 levels also increase with disease severity in patients with chronic lymphocytic leukemia (*203*), classic Hodgkin's lymphoma (*199*), and prostate tumors (*204*). Although the cellular source of serum Gal-1 is unknown, the current study highlights a novel role for lymphoma-derived Gal-1 in specifically inhibiting CD20 immunotherapy in the tumor microenvironment *in vivo*, with the acquisition of tumor Gal-1 expression likely to have a significant impact on tumor progression during therapy. Thereby, human lymphoma Gal-1 expression may provide a molecular signature for therapy-resistant tumors and drugs that counteract the effects of Gal-1 expression in the tumor microenvironment may enhance lymphoma clearance in response to CD20 immunotherapy.

6.2.2. Lymphoma Resistance to mAb Therapy Develops through Multiple Mechanisms

FcγR polymorphisms and an absence of tumor CD20 expression reduce the efficacy of CD20 immunotherapy (*85, 98-100, 112*). In addition, the incomplete depletion of IL-10-producing regulatory B cells (B10 cells) by CD20 mAb significantly impairs CD20 mAb-dependent lymphoma clearance by inhibiting monocyte activation in mice (*17*), with B10 cells also identified in

humans (*205*). Tumor IL-10 production also inhibits tumor-immunity (*48*), and most chronic lymphocytic leukemias (CLL) retain the functional capacity for IL-10 expression (*159*). Because CD20 mAb-dependent lymphoma depletion relies on FcγR-dependent macrophage functions, it is expected that Gal-1 expression may also impair the function of other CD20 targeted therapeutics for CLL and NHL therapy (Arzerra/Ofatumumab, Genmab; Bexxar/^{131}I-labelled tositumomab/Bexxar, GlaxoSmithKline). Gal-1 may also inhibit other therapies that rely in part on FcγR-dependent macrophage function, such as CD19 mAb for lymphoma (*7, 140*), ERBB2 for breast and gastric cancer treatment (Herceptin/Trastuzumab, Genentech) and EGFR for head and neck squamous cell carcinoma and colorectal cancer therapy (Erbitux/Cetuximab, Bristol-Myers Squibb) (*206*). Thus, the expression of Gal-1 and other immunosuppressive factors within the tumor microenvironment might broadly influence drugs for which the mechanism of action relies on FcγR-dependent macrophage function.

6.2.3. Remaining Questions

The extent of the lymphoma-intrinsic mechanisms that alter mAb therapy remains to be wholly characterized. These studies demonstrate that Gal-1 is an important immunoregulator within what is likely to be a large tumor-intrinsic genetic network that ultimately dictates lymphoma resistance to CD20 immunotherapy. The

contributions of lymphoma Gal-1 expression to CD20 mAb resistance is likely to have been missed previously due to intrinsic genetic differences between both tumors and patients. Lymphoma resistance to CD20 mAb therapy is likely to also be complicated by inherent differences between patient immune responses. This reinforces the value of the current pre-clinical mouse lymphoma model, where lymphoma-intrinsic genetic alterations conferring resistance to single drug therapies can be identified in an unbiased fashion independent of the differential contributions of host genetic heterogeneity and environmental factors inherent to all patient populations. Further interrogation of the mouse lymphoma family tree outlined in this study is likely to identify additional novel immunoregulators that contribute to therapy resistance and the immunologic privilege of tumors. This experimental approach can also be applied to other therapies that rely on FcγR- and monocyte-dependent mechanisms as well as other drugs. Once identified and characterized in mice, these molecular changes can be used to construct lymphoma-intrinsic molecular/genetic networks that may predict the biological outcome of CD20 immunotherapy for human disease. Further, the development of drugs that counteract factors promoting tumor progression may also enhance the *in vivo* efficacy of CD20 mAb and other cancer immunotherapies.

Additionally, a complete understanding of Gal-1 in tumor biology remains to be fully interrogated, including the mechanisms by which Gal-1 expression is induced or enhanced within a tumor. While it is known that activated B cells express Gal-1 (*207*,

208), whether Gal-1 directly promotes malignant transformation or more generally promotes immune privilege (*208*) is not understood. Further, the molecular mechanism by which Gal-1 abrogates macrophage mAb-dependent phagocytosis of lymphoma is not completely known. Other studies have indicated that Gal-1 expression directly reduces macrophage FcγR expression (*196*), but it remains possible that Gal-1 also inhibits CD20 mAb-dependent lymphoma depletion by altering macrophage activation or survival in the tumor microenvironment. How Gal-1 specifically affects macrophage-mediated mAb-dependent phagocytosis could be understood by determining whether macrophages downregulate FcγR expression, die faster, or have altered cytokine expression profiles in the presence of Gal-1. In the present study, Gal-1 did not impair CD20 mAb therapy by masking CD20 from CD20 mAb binding, as staining with the CD20 mAb used to deplete lymphoma cells *in vivo* is unobstructed (Fig. 12). However, Ab Fc glycans are important for FcγR binding (*209*), so it is possible that Gal-1 directly impairs FcγR binding of CD20 mAb by saturating the mAb Fc glycans. Whether Gal-1 blocks or reduces the affinity of FcγRs binding to mAb could be determined by pre-incubating fluorescently-labeled mAb of varying isotypes with Gal-1 and then evaluating whether macrophages are able to bind the fluorescently-labeled mAb through FcγRs as efficiently following exposure to Gal-1. Multiple mAb isotypes would need to be tested, as residue glycosylation varies between isotypes and may thereby be differentially impacted by Gal-1 binding. Additionally, the current study strongly

suggests that therapeutic inhibition of Gal-1 in the tumor microenvironment could significantly improve mAb therapy of lymphomas, particularly of those that are resistant to CD20 mAb treatment. Indeed, to further the clinical applicability of this work, future studies should examine whether the administration of Gal-1-depleting mAbs reverses lymphoma resistance to CD20 mAb *in vivo*. Determining whether Gal-1 expression by human lymphomas directly impedes human macrophage mAb-dependent tumor phagocytosis will be a critical first step in validating this molecule for clinical intervention. Future work should therefore evaluate the feasibility and efficacy of therapeutic Gal-1 intervention during lymphoma mAb therapy.

6.3. The Role of Host Genetic Determinants in Determining the Outcome of Antibody-Dependent Cell Depletion In Vivo

The data presented in Chapter 5 established that variations in host macrophage mycn expression determined the efficacy of CD20 mAb-dependent B cell and lymphoma depletion. Splenic B cell depletion by CD20 mAb was significantly perturbed in 129 and NOD mice but not among several other lab mouse strains relative to B6 mice (Fig 13). Similarly, CD20 mAb-dependent B cell lymphoma depletion was profoundly impaired in B6 x 129 F1 mice, while back-crossing F1 mice to B6 progressively increased survival (Fig 14), indicating that distinct genetic traits present in both the B6 and 129 backgrounds contributed to mAb-dependent cell depletion. Genome-wide quantitative linkage analysis identified a 1.5 Mbp region of Chromosome 12 that significantly affected lymphoma depletion by CD20 mAb (Fig. 15-16). Differential expression of one

gene from this region, mycn, was observed between B6 and 129 macrophages. Elevated mycn expression led to greater numbers of macrophages and enhanced B cell depletion and lymphoma phagocytosis following mAb immunotherapy (Fig. 17). The mouse *mycn* locus contains several sequence polymorphisms among different mouse strains, while several polymorphisms exist in the human *mycn* locus (Fig. 18). Thus, variations in macrophage mycn expression likely also affect Ab immunotherapy in humans. Notably, this study established and validated an unbiased forward genetics approach to identify the totality of lymphoma-derived factors that influence CD20 mAb therapy *in vivo*.

6.3.1. Variations in macrophage mycn expression impact CD20 mAb therapy

Mycn is a basic helix-loop-helix zipper DNA-binding protein and serves as a ubiquitous transcription factors for many genes involved in DNA synthesis, proliferation, and cell cycle progression (*210, 211*). For this reason, mycn and other members of the myc protein family, which also includes c-myc, l-myc and p-myc, are widely studied for their roles as proto-oncogenes. In particular, mycn amplification is present in approximately 20% of all neuroblastomas and its expression is correlated with rapid tumor progression and poor outcome (*212, 213*). During development, mycn is critical for neuronal stem cell development and is required for forebrain, hindbrain, lung, and heart development (*211, 214*). Mycn forms a heterodimer with other basic helix-loop-helix transcript factors and weakly binds to the E-box CACGTG sequence, which can be found in the promoters of a variety of cell cycle- and apoptosis-regulating

genes. Recently, alterations in mycn expression have been shown to dramatically alter chromatin accessibility through differential histone H3 acetylation and methylation, indicating that mycn maintains active euchromatin domains in addition to its activities as a specific transcription factor (*215, 216*). Mycn expression has been observed during embryonic nervous tissue development and in newborn mouse brain, kidney, and intestine and early hematopoietic stem cells. However, mycn expression has not been described in terminally differentiated immune cells. This study therefore characterized a novel role for mycn in macrophage generation and effector function, where enhanced mycn expression poises macrophages for enhanced activation by direct transcription factor activity and/or epigenetic regulation. Intriguingly, modest alterations in mycn expression have significant effects on macrophage numbers and phagocytosis, which at least in part contributed to alterations in CD20 mAb therapy *in vivo* (Fig. 17). That small changes in mycn expression has significant consequences is consistent with previous studies where minor alterations in mycn expression were observed to significantly alter heart and lung tissue development (*214, 217*). There are multiple mechanisms through which alterations in mycn expression could lead to elevated macrophage numbers and activation, including enhanced proliferation and survival of macrophage precursors. The relevance of mycn as a specific transcription factor could be readily evaluated by performing chromatin immunoprecipitation and sequencing assays to determine what mycn binds in macrophages. It is also possible that, because mycn has been implicated

in euchromatin maintenance (*215*, *216*), increased mycn expression results in macrophages that are more transcriptionally poised and thereby more rapidly activated. Whether mycn expression generally leads to enhanced transcriptional accessibility could be determined by comparing global histone acetylation and methylation in wild-type and mycn-deficient macrophages. It is important to note that mycn was not necessary for macrophage phagocytosis of opsonized tumor *in vitro* nor CD20 mAb-dependent B cell depletion *in vivo*, though phagocytosis and *in vivo* depletion were both severely blunted in its absence, indicating that additional mechanisms also regulate macrophage function during mAb therapy.

6.3.2. Host genetic background factors into mAb immunotherapy efficacy

Even though mAb-based therapies have existed for more than 30 years, the mechanisms that regulate the activity and efficiency of many mAbs are still debated. For CD20 mAb, which is a primary component of NHL therapy in most patients, the initial efficacy ranges from 10-60% among different NHL sub-types, despite sustained CD20 expression (*84*), and many patients with $CD20^+$ NHLs do not respond to retreatment upon relapse (*74*). Polymorphisms in the activating FcγRIIa and FcγRIIIa proteins have been correlated with the outcome of B cell and tumor depletion following CD20 mAb treatment patients (*98-100*). Similarly, differences in B cell depletion between B6 and NOD mouse strains have been shown to occur despite comparable levels of CD20 expression due in part to NOD mouse expression of truncated FcγRI and polymorphic

FcγRIII and FcγRIV (*112*). This study elaborated on these earlier findings by demonstrating that differences in mAb-dependent B cell and lymphoma depletion among common lab mouse strains can be used to identify genetic features that predispose individuals to different therapeutic outcomes and further elucidate the mechanism by which different mAb-based therapies function. Indeed, these data demonstrated that expression differences in mycn, which was previously not known to be expressed in macrophages, can dramatically influence mAb-based cell depletion at least in part by controlling macrophage numbers and phagocytosis. Importantly, these studies established a system that uses a whole-genome approach to identify the totality of genes and their respective polymorphic variants that regulate mAb-dependent cell depletion.

6.3.3. Remaining Questions

Much of the host genetic landscape that regulates mAb-dependent cell depletion remains to be characterized. These data demonstrate that mycn, which accounted for at least 20% of the phenotypic variation in this study, is an important component of what is surely a much larger network of genetic elements that cooperatively determine mAb immunotherapy outcome. That a previously unappreciated factor like mycn was identified in this unbiased forward genetic screen and demonstrated to profoundly impact mAb-dependent cell depletion demonstrates the power of this system to detect genetic elements critical for this molecular process. Importantly, this study established a

method and analysis pipeline that can be used to identify the factors driving the remaining 80% of the observed variation in mAb-dependent cell depletion. The genetic elements defined through these methods need not be specific to CD20 mAb therapy and can be applied to other treatments that function through mAb- and macrophage-dependent mechanisms. The defined host-derived network will ultimately have to be considered in tandem with the ongoing tumor-intrinsic molecular processes discussed in Chapter 6.2 to ultimately develop a predictive model that will allow for the identification of patients likely to respond to mAb treatment and to also identify other factors that could be therapeutically manipulated to improve patient outcomes following mAb treatment.

In addition to identifying other factors driving effective cell depletion following mAb therapy, the role of mycn in macrophage development, expansion, and function remains to be fully described. As mycn expression in macrophages was not previously described, it would be important to determine the timing and level of mycn expression in macrophage development and additionally whether this occurs in other immune cell populations. Understanding the relevant genes and regulatory regions that are directly targeted by mycn or are otherwise impacted by altered mycn expression should reveal other genetic elements necessary for macrophage development or function. It is also possible that research into the mechanism by which mycn is induced in macrophages could lead to therapies that enhance mycn expression in macrophages, though this

should be approached with caution as mycn is a known proto-oncogene. Further, defining the mechanism by which mycn expression is altered in 129 mice, likely due to the deletions occurring proximal to the mycn locus, could implicate new factors or mechanisms that regulate mycn expression, which could have significant therapeutic implications.

References

1. R. A. Manz, A. E. Hauser, F. Hiepe, A. Radbruch, Maintenance of serum antibody levels. *Annu. Rev. Immunol.* **23**, 367-386 (2005).

2. C. A. Janeway, Jr., P. Travers, M. Walport, M. J. Shlomchik, *Immunobiology: The Immune System in Health and Disease*. (Garland Science, New York, ed. 5th, 2001).

3. L. Fossati-Jimack, L. Reininger, Y. Chicheportiche, R. Clynes, J. V. Ravetch, T. Honjo, S. Izui, High pathogenic potential of low-affinity autoantibodies in experimental autoimmune hemolytic anemia. *J. Exp. Med.* **190**, 1689-1696 (1999).

4. L. V. Mechetina, A. M. Najakshin, B. Y. Alabyev, N. A. Chikaev, A. V. Taranin, Identification of CD16-2, a novel mouse receptor homologous to CD16/Fc γ RIII. *Immunogenetics* **54**, 463-468 (2002).

5. F. Nimmerjahn, J. V. Ravetch, Fc γ receptors: old friends and new family members. *Immunity* **24**, 19-28 (2006).

6. T. Takai, Roles of Fc receptors in autoimmunity. *Nat. Rev. Immunol.* **2**, 580-592 (2002).

7. T. F. Tedder, A. Baras, Y. Xiu, Fc γ receptor-dependent effector mechanisms regulate CD19 and CD20 antibody immunotherapies for B lymphocyte malignancies and autoimmunity. *Sem. Pathol.* **28**, 351-364 (2006).

8. T. W. LeBien, T. F. Tedder, B-lymphocytes: How they develop and function. *Blood* **112**, 1570-1579 (2008).

9. D. J. DiLillo, M. Horikawa, T. F. Tedder, B-lymphocyte effector functions in health and disease. *Immunol. Res.* **49**, 281-292 (2011).

10. M. S. Asano, R. Ahmed, CD8 T cell memory in B cell-deficient mice. *J. Exp. Med.* **183**, 2165-2174 (1996).

11. V. Moulin, F. Andris, K. Thielemans, C. Maliszewski, J. Urbain, M. Moser, B lymphocytes regulate dendritic cell (DC) function *in vivo*: increased interleukin 12 production by DCs from B cell-deficient mice results in T helper cell type 1 deviation. *J. Exp. Med.* **192**, 475-482 (2000).

12. V. N. Ngo, R. J. Cornall, J. G. Cyster, Splenic T zone development is B cell dependent. *J. Exp. Med.* **194**, 1649-1660 (2001).

13. M. T. Crowley, C. R. Reilly, D. Lo, Influence of lymphocytes on the presence and organization of dendritic cell subsets in the spleen. *J. Immunol.* **163**, 4894-4900 (1999).

14. T. V. Golovkina, M. Shlomchik, L. Hannum, A. Chervonsky, Organogenic role of B lymphocytes in mucosal immunity. *Science* **286**, 1965-1968 (1999).

15. D. P. Harris, L. Haynes, P. C. Sayles, D. K. Duso, S. M. Eaton, N. M. Lepak, L. L. Johnson, S. L. Swain, F. E. Lund, Reciprocal regulation of polarized cytokine production by effector B and T cells. *Nat. Immunol.*, 475-482 (2000).

16. M. Horikawa, E. T. Weimer, D. J. DiLillo, G. M. Venturi, R. Spolski, W. J. Leonard, M. T. Heise, T. F. Tedder, Regulatory B cell (B10 cell) expansion during *Listeria* infection governs innate and cellular immune responses in mice. *J. Immunol.* **190**, 1158-1168 (2013).

17. M. Horikawa, V. Minard-Colin, T. Matsushita, T. F. Tedder, Regulatory B cell production of IL-10 inhibits lymphoma depletion during CD20 immunotherapy in mice. *J. Clin. Invest.* **121**, 4268-4280 (2011).

18. T. Matsushita, K. Yanaba, J.-D. Bouaziz, M. Fujimoto, T. F. Tedder, Regulatory B cells inhibit EAE initiation in mice while other B cells promote disease progression. *J. Clin. Invest.* **118**, 3420-3430 (2008).

19. T. Matsushita, M. Horikawa, Y. Iwata, T. F. Tedder, Regulatory B cells (B10 cells) and regulatory T cells have independent roles in controlling EAE initiation and late-phase immunopathogenesis. *J. Immunol.* **185**, 2240-2252 (2010).

20. A. Yoshizaki, T. Miyagaki, D. J. DiLillo, T. Matsushita, M. Horikawa, E. I. Kountikov, R. Spolski, J. C. Poe, W. J. Leonard, T. F. Tedder, Regulatory B cells control T cell autoimmunity through IL-21-dependent cognate interactions. *Nature* **491**, 264-268 (2012).

21. M. Yang, J. Deng, Y. Liu, K. H. Ko, X. Wang, Z. Jiao, S. Wang, Z. Hua, L. Sun, G. Srivastava, C. S. Lau, X. Cao, L. Lu, IL-10-producing regulatory B10 cells ameliorate collagen-induced arthritis via suppressing Th17 cell generation. *Am. J. Pathol.* **180**, 2375-2385 (2012).

22. D. Maseda, K. M. Candando, S. H. Smith, I. Kalampokis, C. T. Weaver, S. E. Plevy, J. C. Poe, T. F. Tedder, Peritoneal cavity regulatory B cells (B10 cells) modulate IFN-γ^+ $CD4^+$ T cell numbers during colitis development in mice. *J. Immunol.* **191**, 2780-2795 (2013).

23. Y. Ron, P. De Baetselier, J. Gordon, M. Feldman, S. Segal, Defective induction of antigen-reactive proliferating T cells in B cell-deprived mice. *Eur. J. Immunol.* **11**, 964-968 (1981).

24. Y. Ron, J. Sprent, T cell priming *in vivo*: a major role for B cells in presenting antigen to T cells in lymph nodes. *J. Immunol.* **138**, 2848-2856 (1987).

25. C. A. Janeway, Jr., J. Ron, M. E. Katz, The B cell is the initiating antigen-presenting cell in peripheral lymph nodes. *J. Immunol.* **138**, 1051-1055 (1987).

26. E. A. Kurt-Jones, D. Liano, K. A. HayGlass, B. Benacerraf, M. S. Sy, A. K. Abbas, The role of antigen-presenting B cells in T cell priming *in vivo*. Studies of B cell-deficient mice. *J. Immunol.* **140**, 3773-3778 (1988).

27. J. D. Bouaziz, K. Yanaba, G. M. Venturi, Y. Wang, R. M. Tisch, J. C. Poe, T. F. Tedder, Therapeutic B cell depletion impairs adaptive and autoreactive $CD4^+$ T cell activation in mice. *Proc. Natl. Acad. Sci. USA* **104**, 20882-20887 (2007).

28. M. Matloubian, R. J. Concepcion, R. Ahmed, $CD4^+$ T cells are required to sustain $CD8^+$ cytotoxic T-cell responses during chronic viral infection. *J. Virol.* **68**, 8056-8063 (1994).

29. W. Gerhard, K. Mozdzanowska, M. Furchner, G. Washko, K. Maiese, Role of the B-cell response in recovery of mice from primary influenza virus infection. *Immunol. Rev.* **159**, 95-103 (1997).

30. D. Homann, A. Tishon, D. P. Berger, W. O. Weigle, M. G. von Herrath, M. B. Oldstone, Evidence for an underlying CD4 helper and CD8 T-cell defect in B-cell-deficient mice: failure to clear persistent virus infection after adoptive immunotherapy with virus-specific memory cells from μ MT/μ MT mice. *J. Virol.* **72**, 9208-9216 (1998).

31. C. C. Bergmann, C. Ramakrishna, M. Kornacki, S. A. Stohlman, Impaired T cell immunity in B cell-deficient mice following viral central nervous system infection. *J. Immunol.* **167**, 1575-1583 (2001).

32. M. S. Diamond, B. Shrestha, A. Marri, D. Mahan, M. Engle, B cells and antibody play critical roles in the immediate defense of disseminated infection by West Nile encephalitis virus. *J. Virol.* **77**, 2578-2586 (2003).

33. S. B. Mollo, A. J. Zajac, L. E. Harrington, Temporal requirements for B cells in the establishment of CD4 T cell memory. *J. Immunol.* **191**, 6052-6059 (2013).

34. D. J. DiLillo, K. Yanaba, T. F. Tedder, B cells are required for optimal $CD4^+$ and $CD8^+$ T cell tumor immunity: therapeutic B cell depletion enhances B16 melanoma growth in mice. *J. Immunol.* **184**, 4006-4016 (2010).

35. A. Crawford, M. Macleod, T. Schumacher, L. Corlett, D. Gray, Primary T cell expansion and differentiation *in vivo* requires antigen presentation by B cells. *J. Immunol.* **176**, 3498-3506 (2006).

36. I. Misumi, J. K. Whitmire, B Cell depletion curtails $CD4^+$ T cell memory and reduces protection against disseminating virus infection. *J. Immunol.* **192**, 1597-1608 (2014).

37. A. Cerny, S. Sutter, H. Bazin, H. Hengartner, R. M. Zinkernagel, Clearance of lymphocytic choriomeningitis virus in antibody- and B-cell-deprived mice. *J. Virol.* **62**, 1803-1807 (1988).

38. J. K. Whitmire, M. S. Asano, S. M. Kaech, S. Sarkar, L. G. Hannum, M. J. Shlomchik, R. Ahmed, Requirement of B cells for generating $CD4^+$ T cell memory. *J. Immunol.* **182**, 1868-1876 (2009).

39. L. J. Old, E. A. Boyse, Immunology of Experimental Tumors. *Annu. Rev. Med.* **15**, 167-186 (1964).

40. G. Klein, Tumor antigens. *Annu. Rev. Microbiol.* **20**, 223-252 (1966).

41. M. Burnet, Cancer; a biological approach. I. The processes of control. *Br. Med. J.* **1**, 779-786 (1957).

42. M. Burnet, Immunological Factors in the Process of Carcinogenesis. *Br. Med. Bull.* **20**, 154-158 (1964).

43. F. M. Burnet, The concept of immunological surveillance. *Prog. Exp. Tumor Res.* **13**, 1-27 (1970).

44. S. P. Flanagan, 'Nude', a new hairless gene with pleiotropic effects in the mouse. *Genet. Res.* **8**, 295-309 (1966).

45. S. Gillis, N. A. Union, P. E. Baker, K. A. Smith, The *in vitro* generation and sustained culture of nude mouse cytolytic T-lymphocytes. *J. Exp. Med.* **149**, 1460-1476 (1979).

46. S. Ikehara, R. N. Pahwa, G. Fernandes, C. T. Hansen, R. A. Good, Functional T cells in athymic nude mice. *Proc. Natl. Acad. Sci. USA* **81**, 886-888 (1984).

47. G. P. Dunn, A. T. Bruce, H. Ikeda, L. J. Old, R. D. Schreiber, Cancer immunoediting: from immunosurveillance to tumor escape. *Nat. Immunol.* **3**, 991-998 (2002).

48. M. D. Vesely, M. H. Kershaw, R. D. Schreiber, M. J. Smyth, Natural innate and adaptive immunity to cancer. *Annu. Rev. Immunol.* **29**, 235-271 (2011).

49. A. C. Society, "Cancer Facts & Figures 2014," (American Cancer Society, Atlanta, Georgia, 2014).

50. K. C. Anderson, M. P. Bates, B. Slaughenhoupt, G. Pinkus, S. F. Schlossman, L. M. Nadler, Expression of human B cell-associated antigens on leukemias and lymphomas: a model of human B cell differentiation. *Blood* **63**, 1424-1433 (1984).

51. R. Kuppers, Mechanisms of B-cell lymphoma pathogenesis. *Nat. Rev. Cancer* **5**, 251-262 (2005).

52. P. Stashenko, L. M. Nadler, R. Hardy, S. F. Schlossman, Characterization of a human B lymphocyte-specific antigen. *J. Immunol.* **125**, 1678-1685 (1980).

53. P. Stashenko, L. M. Nadler, R. Hardy, S. F. Schlossman, Expression of cell surface markers after human B lymphocyte activation. *Proc. Natl. Acad. Sci. USA* **78**, 3848-3852 (1981).

54. P. Rosenthal, I. J. Rimm, T. Umiel, J. D. Griffin, R. Osathanondh, S. F. Schlossman, E. L. Reinherz, Ontogeny of human hematopoietic cells: analysis using monoclonal antibodies. *J. Immunol.* **131**, 232-237 (1983).

55. L. M. Nadler, K. C. Anderson, G. Marti, M. Bates, E. Park, J. F. Daley, S. F. Schlossman, B4, a human B lymphocyte-associated antigen expressed on normal, mitogen activated, and malignant B lymphocytes. *J. Immunol.* **131**, 244-250 (1983).

56. T. F. Tedder, M. Streuli, S. F. Schlossman, H. Saito, Isolation and structure of a cDNA encoding the B1 (CD20) cell-surface antigen of human B lymphocytes. *Proc. Natl. Acad. Sci. USA* **85**, 208-212 (1988).

57. T. F. Tedder, G. Klejman, C. M. Disteche, D. A. Adler, S. F. Schlossman, H. Saito, Cloning of complementary DNA encoding a new mouse B lymphocyte differentiation antigen, homologous to the human B1 (CD20) antigen and localization of the gene to chromosome 19. *J. Immunol.* **141**, 4388-4394 (1988).

58. T. F. Tedder, G. Klejman, S. F. Schlossman, H. Saito, Structure of the gene encoding the human B lymphocyte differentiation antigen CD20 (B1). *J. Immunol.* **142**, 2560-2568 (1989).

59. T. F. Tedder, S. F. Schlossman, Phosphorylation of the B1 (CD20) cell surface molecule expressed by normal and malignant human B lymphocytes. *J. Biol. Chem.* **263**, 10009-10015 (1988).

60. T. F. Tedder, G. McIntyre, S. F. Schlossman, Heterogeneity in the B1 (CD20) cell surface molecule expressed by human B lymphocytes. *Molec. Immunol.* **25**, 1321-1330 (1988).

61. J. K. Bubien, L.-J. Zhou, P. D. Bell, R. A. Frizzell, T. F. Tedder, Transfection of the CD20 cell surface molecule into ectopic cell types generates a Ca^{++} conductance found constitutively in B lymphocytes. *J. Cell Biol.* **121**, 1121-1132 (1993).

62. T. F. Tedder, C. M. Disteche, E. Louie, D. A. Adler, C. M. Croce, S. F. Schlossman, H. Saito, The gene that encodes the human CD20 (B1) differentiation antigen is located on chromosome 11 near the t(11;14) (q13;q32) translocation site. *J. Immunol.* **142**, 2555-2559 (1989).

63. T. F. Tedder, A. W. Boyd, A. S. Freedman, L. M. Nadler, S. F. Schlossman, The B cell surface molecule B1 is functionally linked with B cell activation and differentiation. *J. Immunol.* **135**, 973-979 (1985).

64. M. A. Valentine, K. E. Meier, S. Rossie, E. A. Clark, Phosphorylation of the CD20 phosphoprotein in resting B lymphocytes: regulation by protein kinase C. *J. Biol. Chem.* **264**, 11282-11287 (1989).

65. M. A. Valentine, K. A. Licciaradi, E. A. Clark, E. G. Krebs, K. E. Meier, Insulin regulates serine/threonine phosphorylation in activated human B lymphocytes. *J. Immunol.* **150**, 96-105 (1993).

66. E. M. Genot, K. E. Meier, K. A. Licciardi, N. G. Ahn, C. H. Uittenbogaart, J. Wietzerbin, E. A. Clark, M. A. Valentine, Phosphorylation of CD20 in cells from a hairy cell leukemia cell line. Evidence for involvement of calcium/calmodulin-dependent protein kinase II. *J. Immunol.* **151**, 71-82 (1993).

67. G. S. Kansas, T. F. Tedder, Transmembrane signals generated through MHC class II, CD19, CD20, CD39, and CD40 antigens induce LFA-1-dependent and independent adhesion in human B cells through a tyrosine kinase-dependent pathway. *J. Immunol.* **147**, 4094-4102 (1991).

68. T. F. Tedder, A. Forsgren, A. W. Boyd, L. M. Nadler, S. F. Schlossman, Antibodies reactive with the B1 molecule inhibit cell cycle progression but not activation of human B lymphocytes. *Eur. J. Immunol.* **16**, 881-887 (1986).

69. J. T. Golay, E. A. Clark, P. C. Beverley, The CD20 (Bp35) antigen is involved in activation of B cells from the G_o to the G_1 phase. *J. Immunol.* **135**, 3795-3801 (1985).

70. J. T. Golay, D. H. Crawford, Pathways of human B-lymphocyte activation blocked by B-cell specific monoclonal antibodies. *Immunology* **62**, 279-284 (1987).

71. J. Uchida, Y. Lee, M. Hasegawa, Y. Liang, A. Bradney, J. A. Oliver, K. Bowen, D. A. Steeber, K. M. Haas, J. C. Poe, T. F. Tedder, Mouse CD20 expression and function. *Int. Immunol.* **16**, 119-129 (2004).

72. D. G. Maloney, L. A. Grillo, D. J. Bodkin, C. A. White, T. M. Liles, I. Royston, C. Varns, J. Rosenberg, R. Levy, IDEC-C2B8: results of a phase I multiple-dose trial in patients with relapsed non-Hodgkin's lymphoma. *J. Clin. Oncol.* **15**, 3266-3274 (1997).

73. M. S. Kaminski, K. R. Zasadny, I. R. Francis, A. W. Milik, C. W. Ross, S. D. Moon, S. M. Crawford, J. M. Burgess, N. A. Petry, G. M. Butchko, S. D. Glenn, R. L.

Wahl, Radioimmunotherapy of B-cell lymphoma with [^{131}I]anti-B1 (anti-CD20) antibody. *N. Engl. J. Med.* **329**, 459-465 (1993).

74. P. McLaughlin, L. A. Grillo, B. K. Link, R. Levy, M. S. Czuczman, M. E. Williams, M. R. Heyman, B. I. Bence, C. A. White, F. Cabanillas, V. Jain, A. D. Ho, J. Lister, K. Wey, D. Shen, B. K. Dallaire, Rituximab chimeric anti-CD20 monoclonal antibody therapy for relapsed indolent lymphoma: half of patients respond to a four-dose treatment program. *J. Clin. Oncol.* **16**, 2825-2833 (1998).

75. P. McLaughlin, C. A. White, A. J. Grillo-Lopez, D. G. Maloney, Clinical status and optimal use of rituximab for B-cell lymphomas. *Oncology* **12**, 1763-1769 (1998).

76. S. V. Onrust, H. M. Lamb, J. A. Balfour, Rituximab. *Drugs* **58**, 79-88 (1999).

77. O. W. Press, J. P. Leonard, B. Coiffier, R. Levy, J. Timmerman, Immunotherapy of Non-Hodgkin's lymphomas. *Hematology* **2001**, 221-240 (2001).

78. L. M. Weiner, Monoclonal antibody therapy of cancer. *Semin. Oncol.* **26**, 43-51 (1999).

79. J. C. W. Edwards, G. Cambridge, Sustained improvement in rheumatoid arthritis following a protocol designed to deplete B lymphocytes. *Rheumatology* **40**, 205-211 (2001).

80. M. J. Leandro, J. C. Edwards, G. Cambridge, Clinical outcome in 22 patients with rheumatoid arthritis treated with B lymphocyte depletion. *Ann. Rheum. Dis.* **61**, 883-888 (2002).

81. M. J. Leandro, J. C. Edwards, G. Cambridge, M. R. Ehrenstein, D. A. Isenberg, An open study of B lymphocyte depletion in systemic lupus erythematosis. *Arthritis Rheum.* **46**, 2673-2677 (2002).

82. G. J. Silverman, S. Weisman, Rituximab therapy and autoimmune disorders: prospects for anti-B cell therapy. *Arthritis Rheum.* **48**, 1484-1492 (2002).

83. T. A. Davis, A. J. Grillo-Lopez, C. A. White, P. McLaughlin, M. S. Czuczman, B. K. Link, D. G. Maloney, R. L. Weaver, J. Rosenberg, R. Levy, Rituximab anti-CD20 monoclonal antibody therapy in non-Hodgkin's lymphoma: safety and efficacy of re-treatment. *J. Clin. Oncol.* **18**, 3135-3143 (2000).

84. A. Grillo-López, Rituximab (Rituxan®/MabThera®): the first decade (1993-2003). *Expert Rev. Anticancer Ther.* **3**, 767-779 (2003).

85. M. R. Smith, Rituximab (monoclonal anti-CD20 antibody): mechanisms of action and resistance. *Oncogene* **22**, 7359-7368 (2003).

86. A. Demidem, T. Lam, S. Alas, K. Hariharan, H. Hanna, B. Bonavida, Chimeric anti-CD20 antibody (IDEC-C2B8) monoclonal antibody sensitizes a B cell lymphoma cell line to cell killing by cytotoxic drugs. *Cancer Biother. Radiopharm.* **12**, 177-186 (1997).

87. D. Shan, J. A. Ledbetter, O. W. Press, Apoptosis of malignant human B cells by ligation of CD20 with monoclonal antibodies. *Blood* **91**, 1644-1652 (1998).

88. J. Golay, M. Lazzari, V. Facchinetti, S. Bernasconi, G. Borleri, T. Barbui, A. Rambaldi, M. Introna, CD20 levels determine the *in vitro* susceptibility to rituximab and complement of B-cell chronic lymphocytic leukemia: further regulation by CD55 and CD59. *Blood* **98**, 3383-3389 (2001).

89. M. E. Reff, K. Carner, K. S. Chambers, P. C. Chinn, J. E. Leonard, R. Raab, R. A. Newman, N. Hanna, Depletion of B cells *in vivo* by a chimeric mouse human monoclonal antibody to CD20. *Blood* **83**, 435-445 (1994).

90. R. A. Clynes, T. L. Towers, L. G. Presta, J. V. Ravetch, Inhibitory Fc receptors modulate *in vivo* cytotoxicity against tumor targets. *Nat. Med.* **6**, 443-446 (2000).

91. D. G. Maloney, A. J. Grillo-L'opez, C. A. White, D. Bodkin, R. J. Schilder, J. A. Neidhart, N. Janakiraman, K. A. Foon, T. M. Liles, B. K. Dallaire, K. Wey, I. Royston, T. Davis, R. Levy, IDEC-C2B8 (Rituximab) anti-CD20 monoclonal antibody therapy in patients with relapsed low-grade non-Hodgkin's lymphoma. *Blood* **90**, 2188-2195 (1997).

92. B. Bellosillo, N. Villamor, A. López-Guillermo, S. Marcé, J. Esteve, E. Campo, D. Colomer, E. Montserrat, Complement-mediated cell death induced by rituximab in B-cell lymphoproliferative disorders is mediated *in vitro* by caspase-independent mechanism involving the generation of reactive oxygen species. *Blood* **98**, 2771-2777 (2001).

93. M. S. Cragg, M. S. M., H. T. Chan, B. P. Morgan, A. V. Falatov, P. W. Johnson, R. R. French, M. J. Glennie, Complement-mediated lysis by anti-CD20 mAb correlates with segregation into lipid rafts. *Blood* **101**, 1045-1052 (2003).

94. N. Di Gaetano, E. Cittera, R. Nota, A. Vecchi, V. Grieco, E. Scanziani, M. Botto, M. Introna, J. Golay, Complement activation determines the therapeutic activity of Rituximab *in vivo*. *J. Immunol.* **171**, 1581-1587 (2003).

95. L. E. van der Kolk, A. J. Grillo-López, J. W. Baars, C. E. Hack, M. H. J. van Oers, Complement activation plays a key role in the side-effects of rituximab treatment. *Br. J. Hematol.* **115**, 807-811 (2001).

96. W.-K. Weng, R. Levy, Expression of complement inhibitors CD46, CD55, and CD59 on tumor cells does not predict clinical outcome after rituximab treatment in follicular non-Hodgkin lymphoma. *Blood* **98**, 1352-1357 (2001).

97. D. Herlyn, H. Koprowski, IgG2a monoclonal antibodies inhibit human tumor growth through interaction with effector cells. *Proc. Natl. Acad. Sci. USA* **79**, 4761-4765 (1982).

98. G. Cartron, L. Dacheux, G. Salles, P. Solal-Celigny, P. Bardos, P. Colombat, H. Watier, Therapeutic activity of humanized anti-CD20 monoclonal antibody and polymorphism in IgG Fc receptor Fc γ RIIIa gene. *Blood* **99**, 754-758 (2002).

99. W.-K. Weng, R. Levy, Two immunoglobulin G fragment C receptor polymorphisms independently predict response to rituximab in patients with follicular lymphoma. *J. Clin. Oncol.* **21**, 3940-3947 (2003).

100. D. H. Kim, H. D. Jung, J. G. Kim, J. J. Lee, D. H. Yang, Y. H. Park, Y. R. Do, H. J. Shin, M. K. Kim, M. S. Hyun, S. K. Sohn, FCGR3A gene polymorphisms may correlate with response to frontline R-CHOP therapy for diffuse large B-cell lymphoma. *Blood* **108**, 2720-2725 (2006).

101. S. Camilleri-Broet, N. Mounier, A. Delmer, J. Briere, O. Casasnovas, L. Cassard, P. Gaulard, B. Christian, B. Coiffier, C. Sautes-Fridman, Fc γ RIIB expression in diffuse large B-cell lymphomas does not alter the response to CHOP+rituximab (R-CHOP). *Leukemia* **18**, 2038-2040 (2004).

102. J. Westermann, R. Pabst, Lymphocyte subsets in the blood: a diagnostic window on the lymphoid system? *Immunol. Today* **11**, 406-410 (1991).

103. Y. Hamaguchi, J. Uchida, D. W. Cain, G. M. Venturi, J. C. Poe, K. M. Haas, T. F. Tedder, The peritoneal cavity provides a protective niche for B1 and conventional B lymphocytes during anti-CD20 immunotherapy in mice. *J. Immunol.* **174**, 4389-4399 (2005).

104. Y. Hamaguchi, Y. Xiu, K. Komura, F. Nimmerjahn, T. F. Tedder, Antibody isotype-specific engagement of Fc γ receptors regulates B lymphocyte depletion during CD20 immunotherapy. *J. Exp. Med.* **203**, 743-753 (2006).

105. D. J. DiLillo, Y. Hamaguchi, Y. Ueda, K. Yang, J. Uchida, K. M. Haas, G. Kelsoe, T. F. Tedder, Maintenance of long-lived plasma cells and serological memory despite mature and memory B cell depletion during CD20 immunotherapy in mice. *J. Immunol.* **180**, 361-371 (2008).

106. J. Uchida, Y. Hamaguchi, J. A. Oliver, J. V. Ravetch, J. C. Poe, K. M. Haas, T. F. Tedder, The innate mononuclear phagocyte network depletes B lymphocytes through Fc receptor-dependent mechanisms during anti-CD20 antibody immunotherapy. *J. Exp. Med.* **199**, 1659-1669 (2004).

107. D. G. Maloney, T. M. Liles, D. K. Czerwinski, C. Waldichuk, J. Rosenberg, A. Grillo-Lopez, R. Levy, Phase I clinical trial using escalating single-dose infusion of chimeric anti-CD20 monoclonal antobody (IDEC-C2B8) in patients with recurrent B-cell lymphoma. *Blood* **84**, 2457-2466 (1994).

108. V. Minard-Colin, Y. Xiu, J. C. Poe, M. Horikawa, Y. Hamaguchi, K. M. Haas, T. F. Tedder, Lymphoma depletion during CD20 immunotherapy in mice is mediated by macrophage Fc γ RI, Fc γ RIII, and Fc γ RIV. *Blood* **112**, 1205-1213 (2008).

109. D. J. DiLillo, R. Griffiths, S. V. Seshan, C. M. Magro, P. Ruiz, T. M. Coffman, T. F. Tedder, B lymphocytes differentially influence acute and chronic allograft rejection in mice. *J. Immunol.* **186**, 2643-2654 (2011).

110. F. Montalvao, Z. Garcia, S. Celli, B. Breart, J. Deguine, N. Van Rooijen, P. Bousso, The mechanism of anti-CD20-mediated B cell depletion revealed by intravital imaging. *J. Clin. Invest.* **123**, 5098-5103 (2013).

111. N. Gul, L. Babes, K. Siegmund, R. Korthouwer, M. Bogels, R. Braster, G. Vidarsson, T. L. ten Hagen, P. Kubes, M. van Egmond, Macrophages eliminate circulating tumor cells after monoclonal antibody therapy. *J. Clin. Invest.* **124**, 812-823 (2014).

112. Y. Xiu, C. P. Wong, Y. Hamaguchi, Y. Wang, S. Pop, R. M. Tisch, T. F. Tedder, B lymphocyte depletion by CD20 monoclonal antibody prevents diabetes in NOD mice despite isotype-specific differences in Fc γ R effector functions. *J. Immunol.* **180**, 2863-2875 (2008).

113. T. F. Tedder, C. M. Isaacs, Isolation of cDNAs encoding the CD19 antigen of human and mouse B lymphocytes. A new member of the immunoglobulin superfamily. *J. Immunol.* **143**, 712-717 (1989).

114. S. Sato, N. Ono, D. A. Steeber, D. S. Pisetsky, T. F. Tedder, CD19 regulates B lymphocyte signaling thresholds critical for the development of B-1 lineage cells and autoimmunity. *J. Immunol.* **157**, 4371-4378 (1996).

115. L.-J. Zhou, D. C. Ord, A. L. Hughes, T. F. Tedder, Structure and domain organization of the CD19 antigen of human, mouse, and guinea pig B lymphocytes. Conservation of the extensive cytoplasmic domain. *J. Immunol.* **147**, 1424-1432 (1991).

116. M. Fujimoto, Y. Fujimoto, J. C. Poe, P. J. Jansen, C. A. Lowell, A. L. DeFranco, T. F. Tedder, CD19 regulates Src-family protein tyrosine kinase activation in B lymphocytes through processive amplification. *Immunity* **13**, 47-57 (2000).

117. L. E. Bradbury, G. S. Kansas, S. Levy, R. L. Evans, T. F. Tedder, The CD19/CD21 signal transducing complex of human B lymphocytes includes the target of antiproliferative antibody-1 and Leu-13 molecules. *J. Immunol.* **149**, 2841-2850 (1992).

118. L. E. Bradbury, V. S. Goldmacher, T. F. Tedder, The CD19 signal transduction complex of B lymphocytes: deletion of the CD19 cytoplasmic domain alters signal transduction but not complex formation with TAPA-1 and Leu-13. *J. Immunol.* **151**, 2915-2927 (1993).

119. S. Sato, P. J. Jansen, T. F. Tedder, CD19 and CD22 expression reciprocally regulates tyrosine phosphorylation of Vav protein during B lymphocyte signaling. *Proc. Natl. Acad. Sci. USA* **94**, 13158-13162 (1997).

120. S. Sato, A. S. Miller, M. C. Howard, T. F. Tedder, Regulation of B lymphocyte development and activation by the CD19/CD21/CD81/Leu 13 complex requires the cytoplasmic domain of CD19. *J. Immunol.* **159**, 3278-3287 (1997).

121. L.-J. Zhou, H. M. Smith, T. J. Waldschmidt, R. Schwarting, J. Daley, T. F. Tedder, Tissue-specific expression of the human CD19 gene in transgenic mice inhibits antigen-independent B lymphocyte development. *Mol. Cell. Biol.* **14**, 3884-3894 (1994).

122. P. Engel, L.-J. Zhou, D. C. Ord, S. Sato, B. Koller, T. F. Tedder, Abnormal B lymphocyte development, activation, and differentiation in mice that lack or overexpress the CD19 signal transduction molecule. *Immunity* **3**, 39-50 (1995).

123. S. Sato, D. A. Steeber, T. F. Tedder, The CD19 signal transduction molecule is a response regulator of B-lymphocyte differentiation. *Proc. Natl. Acad. Sci. USA* **92**, 11558-11562 (1995).

124. S. Sato, D. A. Steeber, P. J. Jansen, T. F. Tedder, CD19 expression levels regulate B lymphocyte development: human CD19 restores normal function in mice lacking endogenous CD19. *J. Immunol.* **158**, 4662-4669 (1997).

125. A. Pezzutto, B. Dorken, P. S. Rabinovitch, J. A. Ledbetter, G. Moldenhauer, E. A. Clark, CD19 monoclonal antibody HD37 inhibits anti-immunoglobulin-induced B cell activation and proliferation. *J. Immunol.* **138**, 2793-2799 (1987).

126. R. H. Carter, D. A. Tuveson, D. J. Park, S. G. Rhee, D. T. Fearon, The CD19 complex of B lymphocytes. Activation of phospholipase C by a protein tyrosine kinase-dependent pathway that can be enhanced by the membrane IgM complex. *J. Immunol.* **147**, 3663-3671 (1991).

127. M. Fujimoto, J. C. Poe, P. J. Jansen, S. Sato, T. F. Tedder, CD19 amplifies B lymphocyte signal transduction by regulating Src-family protein tyrosine kinase activation. *J. Immunol.* **162**, 7088-7094 (1999).

128. M. Fujimoto, J. C. Poe, M. Hasegawa, T. F. Tedder, CD19 amplification of B lymphocyte Ca^{2+} responses: a role for Lyn sequestration in extinguishing negative regulation. *J. Biol. Chem.* **276**, 44820-44827 (2001).

129. F. M. Uckun, W. Jaszcz, J. L. Ambrus, A. S. Fauci, K. Gajl-Peczalska, C. W. Song, M. R. Wick, D. E. Myers, K. Waddick, J. A. Ledbetter, Detailed studies on expression and function of CD19 surface determinant by using B43 monoclonal antibody and the clinical potential of anti-CD19 immunotoxins. *Blood* **71**, 13-29 (1988).

130. M. L. Grossbard, A. S. Freedman, J. Ritz, F. Coral, V. S. Goldmacher, L. Eliseo, N. Spector, K. Dear, J. M. Lambert, W. A. Blattler, J. M. Taylor, L. M. Nadler, Serotherapy of B-cell neoplasms with anti-B4-blocked ricin: a phase I trial of daily bolus infusion. *Blood* **79**, 576-585 (1992).

131. M. L. Grossbard, O. W. Press, F. R. Appelbaum, I. D. Bernstein, L. M. Nadler, Monoclonal antibody-based therapies of leukemia and lymphoma. *Blood* **80**, 863-878 (1992).

132. M. L. Grossbard, P. Fidias, J. Kinsella, J. O'Toole, J. M. Lambert, W. A. Blattler, D. Esseltine, G. Braman, L. M. Nadler, K. C. Anderson, Anti-B4-blocked ricin: a phase II trial of 7 day continuous infusion in patients with multiple myeloma. *Br. J. Hematol.* **102**, 509-515 (1998).

133. M. L. Grossbard, P. S. Multani, A. S. Freedman, S. O'Day, J. G. Gribben, C. Rhuda, D. Neuberg, L. M. Nadler, A phase II study of adjuvant therapy with anti-B4-blocked ricin after autologous bone marrow transplantation for patients with relapsed B-cell non-Hodgkin's lymphoma. *Clin. Cancer Res.* **5**, 2392-2398 (1999).

134. G. A. Pietersz, L. Wenjun, V. R. Sutton, J. Burgess, I. F. McKenzie, H. Zola, J. A. Trapani, *In vitro* and *in vivo* antitumor activity of a chimeric anti-CD19 antibody. *Cancer Immunol. Immunother.* **41**, 53-60 (1995).

135. W. M. J. Vuist, F. v. Buitenen, M. A. de Rie, A. Hekman, P. Rumke, C. J. M. Melief, Potentiation by interleukin 2 of Burkitt's lymphoma therapy with anti-pan B (anti-CD19) monoclonal antibodies in a mouse xenotransplantation model. *Cancer Res.* **49**, 3783-3788 (1989).

136. W. M. J. Vuist, F. v. Buitenen, A. Hekman, C. J. M. Melief, Two distinct mechanisms of antitumor activity mediated by the combination of interleukin 2 and monoclonal antibodies. *Cancer Res.* **50**, 5767-5772 (1990).

137. M.-A. Ghetie, L. J. Picker, J. A. Richardson, K. Tucker, J. W. Uhr, E. S. Vitetta, Anti-CD19 inhibits the growth of human B-cell tumor lines *in vitro* and of Daudi cells in SCID mice by inducing cell cycle arrest. *Blood* **83**, 1329-1336 (1994).

138. H. M. Horton, M. J. Bernett, E. Pong, M. Peipp, S. Karki, S. Y. Chu, J. O. Richards, I. Vostiar, P. F. Joyce, R. Repp, J. R. Desjarlais, E. A. Zhukovsky, Potent *in vitro*

and *in vivo* activity of an Fc-engineered anti-CD19 monoclonal antibody against lymphoma and leukemia. *Cancer Res.* **68**, 8049-8057 (2008).

139. J. Zalevsky, I. W. Leung, S. Karki, S. Y. Chu, E. A. Zhukovsky, J. R. Desjarlais, D. F. Carmichael, C. E. Lawrence, The impact of Fc engineering on an anti-CD19 antibody: increased Fc γ receptor affinity enhances B-cell clearing in nonhuman primates. *Blood* **113**, 3735-3743 (2009).

140. N. Yazawa, Y. Hamaguchi, J. C. Poe, T. F. Tedder, Immunotherapy using unconjugated CD19 monoclonal antibodies in animal models for B lymphocyte malignancies and autoimmune disease. *Proc. Natl. Acad. Sci. USA* **102**, 15178-15183 (2005).

141. S. Gallagher, Y. Wang, C. Groves, T. Tedder, A. J. Coyle, R. Herbst, Macrophages are required for anti-CD19 mAb mediated B cell depletion in mice. *J. Immunol.* **182**, 50.16 (2009).

142. H. Pircher, K. Burki, R. Lang, H. Hengartner, R. M. Zinkernagel, Tolerance induction in double specific T-cell receptor transgenic mice varies with antigen. *Nature* **342**, 559-561 (1989).

143. R. Ahmed, A. Salmi, L. D. Butler, J. M. Chiller, M. B. Oldstone, Selection of genetic variants of lymphocytic choriomeningitis virus in spleens of persistently infected mice. Role in suppression of cytotoxic T lymphocyte response and viral persistence. *J. Exp. Med.* **160**, 521-540 (1984).

144. D. A. Spandidos, J. Paul, Transfer of human globin genes to erythroleukemic mouse cells. *EMBO J.* **1**, 15-20 (1982).

145. D. A. Steeber, P. Engel, A. S. Miller, M. P. Sheetz, T. F. Tedder, Ligation of L-selectin through conserved regions within the lectin domain activates signal transduction pathways and integrin function in human, mouse, and rat leukocytes. *J. Immunol.* **159**, 952-963 (1997).

146. K. Murali-Krishna, J. D. Altman, M. Suresh, D. J. D. Sourdive, A. J. Zajac, J. D. Miller, J. Slansky, R. Ahmed, Counting antigen-specific CD8 T cells: a reevaluation of bystander activation during viral infection. *Immunity* **8**, 177-187 (1998).

147. N. Matsushita, S. A. Pilon-Thomas, L. M. Martin, A. I. Riker, Comparative methodologies of regulatory T cell depletion in a murine melanoma model. *J. Immunol. Methods.* **333**, 167-179 (2008).

148. M. M. McCausland, S. Crotty, Quantitative PCR technique for detecting lymphocytic choriomeningitis virus *in vivo*. *J. Virol. Methods* **147**, 167-176 (2008).

149. J. M. Lykken, D. J. DiLillo, E. T. Weimer, S. Roser-Page, M. T. Heise, J. M. Grayson, M. N. Weitzmann, T. F. Tedder, Acute and chronic B cell depletion disrupts CD4+ and CD8+ T cell homeostasis and expansion during acute viral infection in mice. *J. Immunol.* **193**, 746-756 (2014).

150. M. C. Levesque, E. W. St. Clair, B cell-directed therapies for autoimmune disease and correlates of disease response and relapse. *J. Allergy Clin. Immunol.* **121**, 13-21 (2008).

151. M. Hasegawa, Y. Hamaguchi, K. Yanaba, J.-D. Bouaziz, J. Uchida, M. Fujimoto, T. Matsushita, Y. Matsushita, M. Horikawa, K. Komura, K. Takehara, S. Sato, T. F. Tedder, B-lymphocyte depletion reduces skin fibrosis and autoimmunity in the tight-skin mouse model for systemic sclerosis. *Am. J. Pathol.* **169**, 954-966 (2006).

152. A. Ahuja, J. Shupe, R. Dunn, M. Kashgarian, M. R. Kehry, M. J. Shlomchik, Depletion of B cells in murine lupus: efficacy and resistance. *J. Immunol.* **179**, 3351-3361 (2007).

153. C. Y. Hu, D. Rodriguez-Pinto, W. Du, A. Ahuja, O. Henegariu, F. S. Wong, M. J. Shlomchik, L. Wen, Treatment with CD20-specific antibody prevents and reverses autoimmune diabetes in mice. *J. Clin. Invest.* **117**, 3857-3867 (2007).

154. A. Gallimore, A. Glithero, A. Godkin, A. C. Tissot, A. Pluckthun, T. Elliott, H. Hengartner, R. Zinkernagel, Induction and exhaustion of lymphocytic choriomeningitis virus-specific cytotoxic T lymphocytes visualized using soluble tetrameric major histocompatibility complex class I-peptide complexes. *J. Exp. Med.* **187**, 1383-1393 (1998).

155. S. Sarkar, V. Kalia, W. N. Haining, B. T. Konieczny, S. Subramaniam, R. Ahmed, Functional and genomic profiling of effector CD8 T cell subsets with distinct memory fates. *J. Exp. Med.* **205**, 625-640 (2008).

156. G. Cartron, H. Watier, J. Golay, P. Solal-Celigny, From the bench to the bedside: ways to improve rituximab efficacy. *Blood* **104**, 2635-2642 (2004).

157. J. M. Adams, A. W. Harris, C. A. Pinkert, L. M. Corcoran, W. S. Alexander, S. Cory, R. D. Palmiter, R. L. Brinster, The *c-myc* oncogene driven by immunoglobulin enhancers induces lymphoid malignancy in transgenic mice. *Nature* **318**, 533-538 (1985).

158. A. W. Harris, C. A. Pinkert, M. Crawford, W. Y. Langdon, R. L. Brinster, J. M. Adams, The E μ-*myc* transgenic mouse. A model for high-incidence spontaneous lymphoma and leukemia of early B cells. *J. Exp. Med.* **167**, 353-371 (1988).

159. D. J. DiLillo, J. B. Weinberg, A. Yoshizaki, M. Horikawa, J. M. Bryant, Y. Iwata, T. Matsushita, K. M. Matta, Y. Chen, G. M. Venturi, G. Russo, J. P. Gockerman, J. O. Moore, L. F. Diehl, A. D. Volkheimer, D. R. Friedman, M. C. Lanasa, T. F. Tedder, Chronic lymphocytic leukemia and regulatory B cells share IL-10 competence and immunosuppressive function. *Leukemia* **27**, 170-182 (2012).

160. K. Basso, L. Arcangelo, E. Tiacci, R. Benedetti, A. Pulsoni, R. Foa, F. Di Raimondo, A. Ambrosetti, A. Califano, U. Klein, R. Dalla Favera, B. Falini, Gene expression profiling of hairy cell leukemia reveals a phenotype related to memory B cells with altered expression of chemokine and adhesion receptors. *J. Exp. Med.* **199**, 59-68 (2008).

161. D. Kitamura, J. Roes, R. Kuhn, K. Rajewsky, A B cell-deficient mouse by targeted disruption of the membrane exon of the immunoglobulin μ chain gene. *Nature* **350**, 423-426 (1991).

162. S. A. W. Greeley, D. J. Moore, H. Noorchashm, L. E. Noto, S. Y. Rostami, A. Schlachterman, H. K. Song, B. Koeberlein, C. F. Barker, A. Naji, Impaired activation of islet-reactive CD4 T cells in pancreatic lymph nodes of B cell-deficient nonobese diabetic mice. *J. Immunol.* **167**, 4351-4357 (2001).

163. P. J. Linton, B. Bautista, E. Biederman, E. S. Bradley, J. Harbertson, R. M. Kondrack, R. C. Padrick, L. M. Bradley, Costimulation via OX40L expressed by B cells is sufficient to determine the extent of primary CD4 cell expansion and Th2 cytokine secretion *in vivo*. *J. Exp. Med.* **197**, 875-883 (2003).

164. S. K. O'Neill, Y. Cao, K. M. Hamel, P. D. Doodes, G. Hutas, A. Finnegan, Expression of CD80/86 on B cells is essential for autoreactive T cell activation and the development of arthritis. *J. Immunol.* **179**, 5109-5116 (2007).

165. J. Gordon, H. T. Holden, S. Segal, M. Feldman, Anti-tumor immunity in B-lymphocyte-deprived mice. III. Immunity to primary Moloney sarcoma virus-induced tumors. *Int. J. Cancer* **29**, 351-357 (1982).

166. K. R. Schultz, J. P. Klarnet, R. S. Gieni, K. T. HayGlass, P. D. Greenberg, The role of B cells for *in vivo* T cell responses to a Friend virus-induced leukemia. *Science* **249**, 921-923 (1990).

167. C. M. Coughlin, B. A. Vance, S. A. Grupp, R. H. Vonderheide, RNA-transfected CD40-activated B cells induce functional T-cell responses against viral and tumor antigen targets: implications for pediatric immunotherapy. *Blood* **103**, 2046-2054 (2004).

168. Y. Liu, Y. Wu, L. Ramarathinam, Y. Guo, D. Huszar, M. Trounstine, M. Zhao, Gene-targeted B-deficient mice reveal a critical role for B cells in the CD4 T cell response. *Int. Immunol.* **7**, 1353-1362 (1995).

169. P. J. Linton, J. Harbertson, L. M. Bradley, A critical role for B cells in the development of memory CD4 cells. *J. Immunol.* **165**, 5558-5565 (2000).

170. M. M. Epstein, F. Di Rosa, D. Jankovic, A. Sher, P. Matzinger, Successful T cell priming in B cell-deficient mice. *J. Exp. Med.* **182**, 915-922 (1995).

171. H. Shen, J. K. Whitmire, X. Fan, D. J. Shedlock, S. M. Kaech, R. Ahmed, A specific role for B cells in the generation of CD8 T cell memory by recombinant *Listeria monocytogenes*. *J. Immunol.* **170**, 1443-1451 (2003).

172. O. Lassila, O. Vainio, P. Matzinger, Can B cells turn on virgin T cells? *Nature* **334**, 253-255 (1988).

173. F. Ronchese, B. Hausmann, B lymphocytes *in vivo* fail to prime naive T cells but can stimulate antigen-experienced T lymphocytes. *J. Exp. Med.* **177**, 679-690 (1993).

174. C. Joao, B. M. Ogle, C. Gay-Rabinstein, J. L. Platt, M. Cascalho, B cell-dependent TCR diversification. *J. Immunol.* **172**, 4709-4716 (2004).

175. J. C. Edwards, L. Szczepanski, J. Szechinski, A. Filipowicz-Sosnowska, P. Emery, D. R. Close, R. M. Stevens, T. Shaw, Efficacy of B-cell-targeted therapy with rituximab in patients with rheumatoid arthritis. *N. Engl. J. Med.* **350**, 2572-2581 (2004).

176. M. J. Leandro, G. Cambridge, M. R. Ehrenstein, J. C. Edwards, Reconstitution of peripheral blood B cells after depletion with rituximab in patients with rheumatoid arthritis. *Arthritis Rheum.* **54**, 613-620 (2006).

177. L. Quintanilla-Martinez, F. Preffer, D. Rubin, J. A. Ferry, N. L. Harris, $CD20^+$ T-cell lymphoma. Neoplastic transformation of a normal T-cell subset. *Am. J. Clin. Pathol.* **102**, 483-489 (1994).

178. L. E. Hultin, M. A. Hausner, P. M. Hultin, J. V. Giorgi, CD20 (pan-B cell) antigen is expressed at a low level on a subpopulation of human T lymphocytes. *Cytometry* **14**, 196-204 (1993).

179. K. M. Algino, R. W. Thomason, D. E. King, M. M. Montiel, F. E. Craig, CD20 (pan-B cell antigen) expression on bone marrow-derived T cells. *Am. J. Clin. Pathol.* **106**, 78-81 (1996).

180. L.-J. Zhou, T. F. Tedder, in *Leukocyte Typing V. White Cell Differentiation Antigens,* S. F. Schlossman, L. Boumsell, W. Gilks, J. M. Harlan, T. Kishimoto, C. Morimoto, J. Ritz, S. Shaw, R. Silverstein, T. Springer, T. F. Tedder, R. F. Todd, Eds. (Oxford University Press, Oxford, 1995), vol. 1, pp. 511-514.

181. Q. Gong, Q. Ou, S. Ye, W. P. Lee, J. Cornelius, L. Diehl, W. Y. Lin, Z. Hu, Y. Lu, Y. Chen, Y. Wu, Y. G. Meng, P. Gribling, Z. Lin, K. Nguyen, T. Tran, Y. Zhang, H. Rosen, F. Martin, A. C. Chan, Importance of cellular microenvironment and circulatory dynamics in B cell immunotherapy. *J. Immunol.* **174**, 817-826 (2005).

182. R. Eming, A. Nagel, S. Wolff-Franke, E. Podstawa, D. Debus, M. Hertl, Rituximab exerts a dual effect in pemphigus vulgaris. *J. Invest. Dermatol.* **128**, 2850-2858 (2008).

183. A. H. Cross, J. L. Stark, J. Lauber, M. J. Ramsbottom, J. A. Lyons, Rituximab reduces B cells and T cells in cerebrospinal fluid of multiple sclerosis patients. *J. Neuroimmunol.* **180**, 63-70 (2006).

184. T. Vallerskog, I. Gunnarsson, M. Widhe, A. Risselada, L. Klareskog, R. van Vollenhoven, V. Malmstrom, C. Trollmo, Treatment with rituximab affects both the cellular and the humoral arm of the immune system in patients with SLE. *Clin. Immunol.* **122**, 62-74 (2007).

185. M. Vigna-Perez, B. Hernandez-Castro, O. Paredes-Saharopulos, D. Portales-Perez, L. Baranda, C. Abud-Mendoza, R. Gonzalez-Amaro, Clinical and immunological effects of Rituximab in patients with lupus nephritis refractory to conventional therapy: a pilot study. *Arthritis. Res. Ther.* **8**, R83-91 (2006).

186. D. Saadoun, M. Rosenzwajg, D. Landau, J. C. Piette, D. Klatzmann, P. Cacoub, Restoration of peripheral immune homeostasis after rituximab in mixed cryoglobulinemia vasculitis. *Immunobio.* **111**, 5334-5341 (2008).

187. K. Yanaba, Y. Hamaguchi, G. M. Venturi, D. A. Steeber, E. W. St.Clair, T. F. Tedder, B cell depletion delays collagen-induced arthritis in mice: arthritis induction requires synergy between humoral and cell-mediated immunity. *J. Immunol.* **179**, 1369-1380 (2007).

188. K. Hamel, P. Doodes, Y. Cao, Y. Wang, J. Martinson, R. Dunn, M. R. Kehry, B. Farkas, A. Finnegan, Suppression of proteoglycan-induced arthritis by anti-CD20 B cell depletion therapy is mediated by reduction in autoantibodies and $CD4^+$ T cell reactivity. *J. Immunol.* **180**, 4994-5003 (2008).

189. R. Eisenberg, D. Albert, B-cell targeted therapies in rheumatoid arthritis and systemic lupus erythematosus. *Nat. Clin. Pract. Rheumatol.* **2**, 20-27 (2006).

190. S. L. Goldberg, A. L. Pecora, R. S. Alter, M. S. Kroll, S. D. Rowley, S. E. Waintraub, K. Imrit, R. A. Preti, Unusual viral infections (progressive multifocal leukoencephalopathy and cytomegalovirus disease) after high-dose chemotherapy with autologous blood stem cell rescue and peritransplantation rituximab. *Blood* **99**, 1486-1488 (2002).

191. G. A. Rabinovich, M. A. Toscano, Turning 'sweet' on immunity: galectin-glycan interactions in immune tolerance and inflammation. *Nat. Rev. Immunol.* **9**, 338-352 (2009).

192. N. L. Perillo, K. E. Pace, J. J. Seilhamer, L. G. Baum, Apoptosis of T cells mediated by galectin-1. *Nature* **378**, 736-739 (1995).

193. G. N. R. Vespa, L. A. Lewis, K. R. Kozak, M. Moran, J. T. Nguyen, L. G. Baum, M. C. Miceli, Galectin-1 specifically modulates TCR signals to enhance TCR apoptosis but inhibit IL-2 production and proliferation. *J. Immunol.* **162**, 799-806 (1999).

194. K. E. Pace, C. Lee, P. L. Stewart, L. G. Baum, Restricted receptor segregation into membrane microdomains occurs on human T cells during apoptosis induced by galectin-1. *J. Immunol.* **163**, 3801-3811 (1999).

195. K. E. Pace, H. P. Hahn, M. Pang, J. T. Nguyen, L. G. Baum, Cutting edge: CD7 delivers a pro-apoptotic signal during galectin-1-induced T cell death. *J. Immunol.* **165**, 2331-2334 (2000).

196. P. Barrionuevo, M. Beigier-Bompadre, J. M. Ilarregui, M. A. Toscano, G. A. Bianco, M. A. Isturiz, G. A. Rabinovich, A novel function for galectin-1 at the crossroad of innate and adaptive immunity: galectin-1 regulates monocyte/macrophage physiology through a nonapoptotic ERK-dependent pathway. *J. Immunol.* **178**, 436-445 (2007).

197. J. M. Ilarregui, D. O. Croci, G. A. Bianco, M. A. Toscano, M. Salatino, M. E. Vermeulen, J. R. Geffner, G. A. Rabinovich, Tolerogenic signals delivered by dendritic cells to T cells through a galectin-1-driven immunoregulatory circuit involving interleukin 27 and interleukin 10. *Nat. Immunol.* **10**, 981-991 (2009).

198. N. Rubinstein, M. Alvarez, N. W. Zwirner, M. Toscano, J. M. Ilarregui, A. Bravo, J. Mordoh, L. Fainboim, O. L. Podhajcer, G. A. Rabinovich, Targeted inhibition of galectin-1 gene expression in tumor cells results in heightened T cell-mediated rejection: A potential mechanism of tumor-immune privilege. *Cancer Cell* **5**, 241-251 (2004).

199. J. Ouyang, A. Plütschow, E. Pogge von Strandmann, K. S. Reiners, S. Ponader, G. A. Rabinovich, D. Neuberg, A. Engert, M. A. Shipp, Galectin-1 serum levels reflect tumor burden and adverse clinical features in classical Hodgkin lymphoma. *Blood* **121**, 3431-3433 (2013).

200. P. Juszczynski, S. J. Rodig, J. Ouyang, E. O'Donnell, K. Takeyama, W. Mlynarski, K. Mycko, T. Szczepanski, A. Gaworczyk, A. Krivtsov, J. Faber, A. U. Sinha, G. A. Rabinovich, S. A. Armstrong, J. L. Kutok, M. A. Shipp, MLL-rearranged B lymphoblastic leukemias selectively express the immunoregulatory carbohydrate-binding protein galectin-1. *Clin. Cancer Res.* **16**, 2122-2130 (2010).

201. D. O. Croci, M. Salatino, N. Rubinstein, J. P. Cerliani, L. E. Cavallin, H. J. Leung, J. Ouyang, J. M. Ilarregui, M. A. Toscano, C. I. Domaica, M. C. Croci, M. A. Shipp, E. A. Mesri, A. Albini, G. A. Rabinovich, Disrupting galectin-1 interactions with N-glycans suppresses hypoxia-driven angiogenesis and tumorigenesis in Kaposi's sarcoma. *J. Exp. Med.* **209**, 1985-2000 (2012).

202. P. Juszczynski, J. Ouyang, S. Monti, S. J. Rodig, K. Takeyama, J. Abramson, W. Chen, J. L. Kutok, G. A. Rabinovich, M. A. Shipp, The AP1-dependent secretion of galectin-1 by Reed Sternberg cells fosters immune privilege in classical Hodgkin lymphoma. *Proc. Natl. Acad. Sci. USA* **104**, 13134-13139 (2007).

203. D. O. Croci, P. E. Morande, S. Dergan-Dylon, M. Borge, M. A. Toscano, J. C. Stupirski, R. F. Bezares, J. S. Avalos, M. Narbaitz, R. Gamberale, G. A. Rabinovich, M. Giordano, Nurse-like cells control the activity of chronic lymphocytic leukemia B cells via galectin-1. *Leukemia* **27**, 1413-1416 (2013).

204. D. J. Laderach, L. D. Gentilini, L. Giribaldi, V. C. Delgado, L. Nugnes, D. O. Croci, N. A. Nakouzi, P. Sacca, G. Casas, O. Mazza, M. A. Shipp, E. Vazquez, A. Chauchereau, J. L. Kutok, S. J. Rodig, M. T. Elola, D. Compagno, G. A. Rabinovich, A unique galectin signature in human prostate cancer progression suggests galectin-1 as a key target for treatment of advanced disease. *Cancer Res.* **73**, 86-96 (2013).

205. Y. Iwata, T. Matsushita, M. Horikawa, D. J. DiLillo, K. Yanaba, G. M. Venturi, P. M. Szabolcs, S. H. Bernstein, C. M. Magro, A. D. Williams, R. P. Hall, E. W. St.Clair, T. F. Tedder, Characterization of a rare IL-10-competent B cell subset in humans that parallels mouse regulatory B10 cells. *Blood* **117**, 530-541 (2011).

206. A. M. Scott, J. D. Wolchok, L. J. Old, Antibody therapy of cancer. *Nat. Rev. Cancer* **12**, 278-287 (2012).

207. C. Blaser, M. Kaufmann, C. Muller, C. Zimmermann, V. Wells, L. Mallucci, H. Pircher, Beta-galactoside-binding protein secreted by activated T cells inhibits antigen-induced proliferation of T cells. *Eur. J. Immunol.* **28**, 2311-2319 (1998).

208. E. Zuniga, G. A. Rabinovich, M. M. Iglesias, A. Gruppi, Regulated expression of galectin-1 during B-cell activation and implications for T-cell apoptosis. *J. Leukoc. Biol.* **70**, 73-79 (2001).

209. J. Lu, J. Chu, Z. Zou, N. B. Hamacher, M. W. Rixon, P. D. Sun, Structure of Fc γ RI in complex with Fc reveals the importance of glycan recognition for high-affinity IgG binding. *Proc. Natl. Acad. Sci. USA* **112**, 833-838 (2015).

210. W. Lutz, M. Stohr, J. Schurmann, A. Wenzel, A. Lohr, M. Schwab, Conditional expression of N-myc in human neuroblastoma cells increases expression of alpha-prothymosin and ornithine decarboxylase and accelerates progression into S-phase early after mitogenic stimulation of quiescent cells. *Oncogene* **13**, 803-812 (1996).

211. P. S. Knoepfler, P. F. Cheng, R. N. Eisenman, N-myc is essential during neurogenesis for the rapid expansion of progenitor cell populations and the inhibition of neuronal differentiation. *Genes Dev.* **16**, 2699-2712 (2002).

212. G. M. Brodeur, R. C. Seeger, M. Schwab, H. E. Varmus, J. M. Bishop, Amplification of N-myc in untreated human neuroblastomas correlates with advanced disease stage. *Science* **224**, 1121-1124 (1984).

213. G. M. Brodeur, Neuroblastoma: biological insights into a clinical enigma. *Nat. Rev. Cancer* **3**, 203-216 (2003).

214. T. Okubo, P. S. Knoepfler, R. N. Eisenman, B. L. Hogan, Nmyc plays an essential role during lung development as a dosage-sensitive regulator of progenitor cell proliferation and differentiation. *Development* **132**, 1363-1374 (2005).

215. P. S. Knoepfler, X. Y. Zhang, P. F. Cheng, P. R. Gafken, S. B. McMahon, R. N. Eisenman, Myc influences global chromatin structure. *EMBO J.* **25**, 2723-2734 (2006).

216. R. Cotterman, V. X. Jin, S. R. Krig, J. M. Lemen, A. Wey, P. J. Farnham, P. S. Knoepfler, N-Myc regulates a widespread euchromatic program in the human genome partially independent of its role as a classical transcription factor. *Cancer Res.* **68**, 9654-9662 (2008).

217. C. B. Moens, B. R. Stanton, L. F. Parada, J. Rossant, Defects in heart and lung development in compound heterozygotes for two different targeted mutations at the N-myc locus. *Development* **119**, 485-499 (1993).

Biography

I was born on Langley Air Force Base in Virginia on February 15th, 1986 to Drs. James and Jean Bryant, and I have a younger sister named Jessica. I graduated from Hampton Roads Academy in Newport News, Virginia on May 22nd, 2004. I then moved to Harrisonburg, Virginia to study biology and management science at James Madison University and graduated cum laude with a Bachelor of Science on May 3rd, 2008. After graduating from James Madison University, I moved to Durham, North Carolina to study immunology at Duke University. I spent the next few years studying B cell biology with Dr. Thomas F. Tedder.

I have published or submitted for publication the following manuscripts:

1. Lykken JM, Horikawa M, Minard-Colin V, Xiu Y, Keum S, Marchuk DA, Poe JC, and Tedder TF. Macrophage Mycn Expression Regulates *in vivo* B cell and Lymphoma Clearance by CD20 mAb. In submission.

2. Lykken JM*, Horikawa M*, Minard-Colin V*, Kamata M, Miyagaki T, Poe JC, and Tedder TF. Galectin-1 expression confers lymphoma resistance to CD20 immunotherapy. In submission. *co-first authorship

3. Lykken JM, Dilillo DJ, Weimer ET, Roser-Page S, Heise MT, Grayson JM, Weitzmann MN, and Tedder TF. Acute and chronic B cell depletion disrupts CD4+ and CD8+ T cell homeostasis and expansion during acute viral infection in mice. Journal of Immunology 193(2): 746-756, 2014.

4. Candando KM*, Lykken JM*, and Tedder TF. B10 cell regulation of health and disease. Immunological Reviews 259(1): 259-272, 2014. *co-first authorship

5. Poe JC, Kountikov EI, Lykken JM, Natarajan A, Marchuk DA, and Tedder TF. EndoU is a novel regulator of AICD during peripheral B cell selection. Journal of Experimental Medicine 211(1): 57-69, 2014.

6. DiLillo DJ, Weinberg JB, Yoshizaki A, Horikawa M, Bryant JM, Iwata Y, Matsushita T, Matta KM, Chen Y, Venturi GM, Russo G, Gockerman JP, Moore JO, Diehl LF, Volkheimer AD, Friedman DR, Lanasa MC, Hall RP, and Tedder TF. Chronic lymphocytic leukemia and regulatory cells share IL-10 competence and immunosuppressive function. Leukemia 27(1): 170-182, 2013.

7. Maseda D, Smith SH, DiLillo DJ, Bryant JM, Candando KM, Weaver CT, and Tedder TF. Regulatory B10 cells differentiate into antibody-secreting cells after transient IL-10 production *in vivo*. Journal of Immunology 188(3): 1036-1048, 2012.

I received the following fellowships and academic honors while at Duke University:

1. RIKEN Center for Integrative Medical Sciences Summer Program and International Symposium on Immunology Chosen Participant and Presenter, RIKEN Institute, Yokohama, Japan (June 2015)

2. Duke Basic Science Day Chosen Participant, Duke University, Durham, NC (October 2013)

3. D. Bernard Amos Research Lecture Poster Session Award Winner, Duke University, Durham, NC (May 2013)

4. 98th Annual Meeting of the American Association of Immunologists Chosen Participant, San Francisco, CA (May 2011)

5. Conference Travel Fellowship Award Recipient, Duke University, Durham, NC (April 2011)

6. 97th Annual Meeting of the American Association of Immunologists Chosen Participant, Baltimore, MD (May 2010)

7. Conference Travel Fellowship Award Recipient, Duke University, Durham, NC (April 2010)

8. NIH Ruth L. Kirschstein National Research Service (T32) Award Recipient, Duke University, Durham, NC (September 2008 – August 2010)

I defended my dissertation on April 3rd, 2015 with the faculty of the Duke University Department of Immunology. I am married to my husband Erik, who is also a graduate student in the Department of Immunology at Duke University, and we currently reside in Durham, North Carolina with our dog, Molly.